

Predictive Models For Falls-Risk Assessment in Older People, Using Markerless Motion Capture

S Maudsley-Barton

PhD 2020

Predictive Models For Falls-Risk Assessment in Older People, Using Markerless Motion Capture

Sean Maudsley-Barton

A thesis submitted in partial fulfilment of the requirements of Manchester Metropolitan University for the degree of Doctor of Philosophy

Department of Computing and
Mathematics
Manchester Metropolitan University

2020

This thesis is dedicated to Flora, Hannah and Beatrix

Acknowledgements

I would like to extend my gratitude to the many people who made this work possible. My supervisors Dr Moi Hoon Yap, Dr Anthony Bukowski and Prof. Jamie McPhee, for provided constant encouragement and advice, throughout. I am also grateful to the Department of Computing and Mathematics at, who funded my studentship.

This work would not have been possible if not for the kindness of the wider staff of Manchester Metropolitan University who were free with their time and advice. In particular, I would like to thank Dr Chesney Craig for her help with data collection, Dr Richard Mills, who's help with biomechanics was invaluable and Dr Connah Kendrick for all types of practical support, as well as his friendship.

I have also been fortunate in working in a Lab with amazing fellow students, I have enjoyed enlightening conversations with all of them: Manu Goyal, Jireh Jam, Guido Ascenso, Jhan Alarifi, Xulu Yao and Chuin Hong Yap.

Looking further afield, this work would not have been possible without the help of many private individuals and several u3a groups. In particular, I would like to thank the Hale, St. Helens and Up Holland u3a groups, for their continued support.

Finally, I would like to thank the constant support of my entire family during my studies. Special thanks go to my immediate family, Flora, Hannah and Beatrix who have lived through my PhD every step of the way. This has been particularly true during Lockdown and on into the new normal of COVID-19, were the distinction between work and home life has completely broken down.

Abstract

Falling in old age contributes to considerable misery for many people. Currently, there is a lack of practical, low cost and objective methods for identifying those at risk of falls. This thesis aims to address this need.

The majority of the literature related to falls risk and balance impairment uses force plates to quantify postural sway. The use of such devices in a clinical setting is rare, mainly due to cost. However, some force-plate-based commercial products have been created, e.g. the Balance Master. To align the research in this thesis to both the literature and existing methods of assessing postural sway, a method is proposed which can generate sway metrics from the output of a low-cost markerless motion capture device (Kinect V2). Good agreement was found between the proposed method and the output of the Balance Master.

A key reason for the lack of research into falls-risk using markerless motion capture, is the lack of an appropriate dataset. To address this issue, a dataset of clinical movements, recorded using markerless motion capture, was created. Named KINECAL, It contains the recordings of 90 participants, labelled by age and falls-risk. The data provided includes depth images, 3D joint positions, sway metrics and socioeconomic and health meta data.

Many studies have noted that postural sway increases with age and conflate age-related changes with falls risk. However, if one examines sub-populations of older people, such as master athletes, It is clear that this is not necessarily true. The structure of KINECAL allows for the examination of age-related factors and falls-risk factors simultaneously. In addition, it includes labels of falls history, clinical impairment and comprehensive metadata.

KINECAL was used to identify sway metrics most closely associated with falls risk, as distinct from the ageing process. Using the identified metrics, a model was developed that can identify those who would be classified as impaired by a range of clinical tests.

Finally, a model is proposed, which can predict fallers by placing individuals on a scale of physical impairment. An autoencoder was used to model, healthy adult sit-to-stand movements. Using an anomaly detection approach, an individuals level of impairment can be plotted relative to this healthy standard. Using this model, the existence of two older populations (one with a high falls risk and one with a low falls risk) is demonstrated.

Contents

List of Abbreviations	xvii
1 Introduction	2
1.1 Ageing and Frailty	3
1.1.1 What is an injurious Fall?	6
1.2 Identifying Those at Risk of Falls	7
1.2.1 Assessment by a Clinician	8
1.3 Motivation	9
1.4 Problem Statement	10
1.5 Aim and Objectives	11
1.6 Contributions	11
1.7 Thesis Organisation	13
2 Literature Review	14
2.1 Introduction	14
2.2 What is Balance?	14
2.2.1 Posturography	17
2.2.2 Postural Sway Metrics	20
2.3 Postural Sway, Ageing, and Falls	20
2.4 Criticism of Sway Measured by Force Plates	21
2.5 Motion Capture	22
2.5.1 Origins	22
2.5.2 Marker-based Motion Capture	23
2.5.3 Markerless Motion Capture	23
2.6 Issues with Kinect	24
2.7 Comparison, Between Kinect and Marker-based Systems	25
2.8 Kinect and Human Action Recognition	26
2.9 Gait Assessment	26

2.10	Falls Detection	36
2.11	Rehabilitation	37
2.12	Assessment of Balance and falls-risk	38
2.13	Working with Skeletal Data	39
2.14	Automatic Feature Extraction and Representational Models	41
2.14.1	Automatic Feature Selection	41
2.14.2	Representational Models	42
2.14.3	Autoencoders	43
2.15	Clinical Datasets	44
2.16	Machine Learning	44
2.16.1	Types of Machine Learning	44
2.16.2	Machine Learning Algorithms	45
2.16.3	Statistical Machine Learning Models	48
2.16.4	Neural Networks - reborn	50
2.16.5	Recurrent Neural Networks (RNN)	52
2.16.6	Autoencoders	55
2.17	Conclusion	56
3	Techniques and Methods	58
3.1	Introduction	58
3.2	Joints and Skeletons	58
3.2.1	The Human Body	59
3.3	Working with Kinect skeletons	59
3.3.1	Filtering	59
3.3.2	Pose Normalisation	60
3.3.3	General Method for Calculating CoM	60
3.3.4	Centre of Mass from Force Plate Data	61
3.3.5	Centre of Mass from Kinect Data	61
3.4	Conclusion	61
4	Preliminary Research	62
4.1	Introduction	62
4.2	A Method to Distinguishing Young from Older, in the KD3a Dataset	63
4.2.1	Pose Normalisation	64
4.2.2	Feature Encoding	64
4.2.3	K-mean Clustering	67

4.2.4	Motion Representation	67
4.2.5	Model Training	68
4.3	Results	68
4.4	Discussion	69
4.5	Conclusion	70
5	A New Process to Measure Postural Sway, Using a Kinect Depth Camera	72
5.1	Introduction	72
5.2	Methods	73
5.2.1	Participants	73
5.2.2	Procedure	74
5.2.3	Experimental Setup	75
5.2.4	Recording of CoM path	76
5.2.5	Creation of CoM Time Series	79
5.2.6	Calculation of Sway	80
5.2.7	Data Exclusions	80
5.2.8	A priori Sample Size Calculation	80
5.2.9	Statistical Tools	81
5.3	Results	82
5.3.1	Repeatability	82
5.3.2	Agreement of Postural Sway Measurement	83
5.3.3	Implications of the Increased Disagreement	87
5.4	Discussion	88
5.4.1	Limitations, Considerations and Future Work	91
5.5	Conclusion	91
6	KINECAL: A Dataset of Clinically Significant Movements	93
6.1	Introduction	93
6.2	Clinically Significant Movements	95
6.3	Participants	97
6.4	Dataset Labelling	98
6.4.1	Self-reported Labels	98
6.4.2	Single and Multiple Fallers	99
6.4.3	Clinical labelling	100
6.4.3.1	Thresholds of Clinical-Impairment	101
6.5	Methods	103

6.5.1	Experimental Setup	103
6.5.2	Data recording	103
6.5.3	Signal Processing	104
6.5.4	Estimation of CoM	105
6.6	Generation of sway metrics	106
6.6.1	Sway Metric - Time Series	106
6.6.2	Calculation of Sway Metrics	108
6.7	Questionnaire	112
6.8	Open Source Code	112
6.9	Conclusion	113
7	An Investigation of Sway Metrics Associated With Falls	114
7.1	Introduction	114
7.2	Sway Metrics Identification	116
7.2.1	Sway Metrics	116
7.2.2	Participant groups	117
7.2.3	Outlier Detection	117
7.2.4	Assessment of Significant Difference, Between Participant Groups	117
7.2.5	Age-related Sway Metrics	119
7.2.5.1	Grouping of Participants	119
7.2.5.2	Results	120
7.2.6	Falls-Risk related Sway Metrics	121
7.2.6.1	Grouping of Participants	121
7.3	Machine Learning Methods	124
7.3.1	Sliding Window	124
7.3.2	Monte Carlo Cross-Validation and Rebalancing	124
7.3.3	Experiments	126
7.4	Results	126
7.5	Discussion	127
7.6	Conclusion	130
8	Quantification of Falls-Risk, Based on a Representational Model	131
8.1	Introduction	131
8.2	Participants	133
8.3	Methods	134
8.3.1	Skeletal Preprocessing	134

8.3.2	Calculation of Joint Angles	134
8.3.3	Segmentation of Repetitions	135
8.3.4	Resampling and Padding	135
8.3.5	Autoencoder	136
8.3.6	Distance Metrics and Scoring	137
8.3.7	Training and Cross-validation	141
8.3.8	Calculation of Metrics	143
8.3.9	Calculation of Threshold	143
8.4	Results	144
8.5	Discussion	146
8.6	Conclusion and Future Work	150
9	Conclusion	151
9.1	Introduction	151
9.2	Summary or work	152
9.3	Limitations	154
9.4	Future Work	154
9.5	Closing Comments	156
	Appendices	157
A		158
A.1	SPPB Scoring Sheet	158
B		167
B.1	Motor Unit Study Questionnaire: MMU	167
	Bibliography	188

List of Figures

1.1	Walston’s cycle of frailty. Recreated from J. Walston, Sci. Aging Knowl. Environ. 2004, pe4 (2004)	4
1.2	CSHA frailty index. Recreated from K. Rockwood, “A global clinical measure of fitness and frailty in elderly people,” Can. Med. Assoc. J., vol. 173, no. 5, pp. 489–495, Aug. 2005.	5
1.3	Thesis Organisation	13
2.1	CoP in relation to the BoS. the CoP is marked by a black dot This figure shows three possible BoS (shaded grey), and the associated CoP (shown as a black dot). The first two are narrow stances, quiet standing and semi-tandem, repetitively. The third is a wide version of quiet standing (feet shoulder width apart).	15
2.2	Balance for different objects. This figure shows a simple triangle and 3 vertebrate bodies, with the CoM shown as a red point, and the LoG shown as a red line. It is easy to see why the triangle resting on its long-side is inherently more stable than the one resting on its point. By applying this intuition to the vertebrate bodies you get an appreciation of how the upright, human body, on the far right, is less stable than the ape and dog pictured to the left of it.	16
2.3	SMART Balance Master: The SMART Balance Master, is one of the few devices used in the clinical assessment of balance. However, it widescale adoption is restricted by its size and cost.	18

2.4	Elements of the SOT. (1) eyes open, platform fixed (used as a baseline); (2) eyes closed to remove visual input; (3) eyes open with moving surround, to create sensory conflict between visual input (simulating a moving room) and vestibular inputs (a stable room); (4) eyes open and the platform support rotating freely to disrupt somatosensory and proprioceptive feedback from the feet and ankles; (5) eyes closed and the platform support rotating freely; and (6) eyes open with moving surround and the platform support rotating freely	19
2.5	Single inverted pendulum. This is the standard model of sway when using a force plate. The CoM of the body is modelled as a point mass m on top of a stick with length l . u , marks the location of the effective ground reaction force, and x marks the point where the LoG touches the ground.	22
2.6	Typical VICON setup: VICON uses an array of infrared cameras, pointing inwards, to create a capture volume. Reflective markers are attached to a human body, to mark key anatomical features which are to be tracked, eg bone ends. . .	23
2.7	Kinect V2. Kinect is equipped with both an RGB video camera and a depth camera. It can output a 25 joint skeleton, without the need for makers.	24
2.8	Diagram of skeletons generated by Kinect. This figure details the 25 joints of the Kinect skeleton model	25
2.9	Gait cycle: A. Step length and stride length characteristics. B phases of the gait cycle (reproduced from [218])	27
2.10	Sub-phases of gait: this figure show the sup-phases of gait, in relation to a single stride (reproduced from [231])	28
2.11	Kinematics of gait: this figure show the normal movement of the foot(ankle), knee, hip and pelvis throughout the gait cycle toe-off is marked with a solid vertical line (reproduced from [218])	30
2.12	Gait features, extracted from Kinect: By tracking the vertical component of the CoM, estimated form the Kinect depth stream. step length, step time, and gait speed were calculated (reproduced from [60])	31

2.13	A comparison spatio-temporal and kinematic variables during the gait cycle, between the output of a Kinect camera and a 3DMA motion capture system (reproduced from [152]) Results are shown for conformable and fast paced walking. The validity column shows agreement between devices. The reliability columns show the reliability of each device, between days . . .	33
2.14	A comparison kinematic and spatio-temporal variables during the walking gait cycle, between Kinect and SMART-DX 7000 (BTS Italy) motion capture system (reproduced from [64]) There is good agreement in Spatio-temporal measures between the two devices, along with Hip and knee ROM. However, ankle joints are less well tracked.	34
2.15	Linear separation by SVM	50
2.16	RNN: conceptually an RNN is just a feed forward network which at each time step can take in new information and a memory of the past outputs, X_t is the input plus h_t , the output of the previous step. Reproduced from [173]	53
2.17	LSTM cell: The structure of an LSTM cell, is a MLP in its own right. Multiple layers of LSTM cells can learn complex time-series relationships, without the issues of exploding or vanishing gradients. Recreated from commons.wikimedia.org.	54
2.18	GRU: Similar to an LSTM unit but the the cell state and the hided states are merged, as are the forget gate and input gate. Recreated from commons.wikimedia.org.	54
2.19	Autoencoder: The layers of an autoencoder are arranged to allow for the encoding and decoding of an input. The original input is used as an error signal in training.Recreated from commons.wikimedia.org	55
3.1	Kinect coordinate system: Z axis projects from the depth camera, with x and y orthogonal to it his image is recreated from here.	58

3.2	Body planes: The planes of the body, are Sagittal, which bisects the body left to right; Coronal (Also know as Frontal), which bisects the body, front to back and Transverse, which bisects the body head to tail. This image is adapted from an open-sourced figure.	59
4.1	Data processing pipeline: this pipeline was used to extract features from the K3Da dataset.	64
4.2	A diagram of the relationship between, an individual, being recorded and the Microsoft Kinect camera. The salient joints are shown. The <i>BodyLeanAngle</i> , is the angle between <i>SPINE_MID</i> and <i>NECK</i> joints. The <i>TorsoAngle</i> , is the angle between <i>SPINE_BASE</i> and <i>NECK</i> joints. The Centre of Mass (CoM) is calculated as the euclidean average of the <i>HIP_LEFT</i> , <i>HIP_RIGHT</i> and <i>SPINE_MID</i> joints (modified, from [124])	65
4.3	The age profile of KD3a: The graph shows the polarised nature of the kD3a dataset, while this is perfect of looking at age related changes, it makes identify those at risk of falls difficult	70
5.1	Setup of Balance Master and Kinect V2, Depth Camera.	76
5.2	Diagram of sway angle calculation used by the Balance Master [204].	77
5.3	The pipeline of the Skel recorder.	78
5.4	Kinect V2 Skeleton, the joints used to estimate CoM and the CoM position, are labelled.	79
5.5	Correlation of postural sway derived from the SMART Balance Master and Kinect depth camera. The line of equality is shown (continuous line) as well as the linear regression (dotted line).	84
5.6	Bland-Altman plot of the SMART Balance Master vs the Proposed Pipeline’s estimates of postural sway. Bold horizontal line indicates the mean, dashed horizontal lines indicate two standard deviations from the mean. The shaded areas represent associated confidence intervals. The figures marked a-f represent the six conditions of the SOT test.	86

6.1	Kinect point-of-view This figure is of a young participant in quiet stance. (a) is an RGB image, (b) is a depth image, (c) is the 25 joint skeleton, created by Kinect. <i>Permission was obtained from the person in the frame for their image to be used.</i>	104
6.2	Kinect V2 Skeleton, the joints used to estimate CoM and the CoM position, are labelled.	106
6.3	95% Confidence Ellipse and CoM path: This figure compares CoM paths and associated 95% Confidence Ellipses of a person labelled Healthy-Adult (SPPB25) to someone labelled Clinically-Impaired (SPPB201), Standing Quietly. Column (a) shows a tight view. Column (b) shows the 95% Confidence Ellipses plotted on the same scale.	108
7.1	A flowchart of the bootstrap process. 1) The dataset was split into unimpaired and impaired groups; 2) Outliers in the unimpaired group were removed (using the same outlier detection method as used to identify candidate metrics); 3) Train and Test subsets were created, split on Participant ID (PART_ID) and records assigned to each subset randomly, such that in every iteration a new set is drawn, without replacement. However, no participant was present in both Train and Test subsets; 4) Random re-sampling with replacement was used to create bootstraps of the original data and normalised (using the normalize method of sci-kit learn [225] ; 5) The bootstraps were rebalanced using SMOTE-ENN [126]; 6) The model was trained; 7) The test set was used to obtain result metrics, for that iteration and these results where stored; 8) This process continued for 10,000 iterations; and 9) At the end of 10,000 iterations, mean values for all results and 95% confidence intervals were displayed.	125
7.2	Confusion matrices produced from training a Gaussian Naive Bayes Model: The best separation is seen when using clinical labels. Confusion is seen in the models when using falls history as a label	127

7.3	ROC curves for models. The AUC increases from top left to bottom right, the greatest overlap, seen between the those labelled clinically impaired vs Healthy-Adults	128
8.1	Knee Angle: Example of knee angle in the Sagittal plane. The angles in the other two planes are calculate in the same way. .	135
8.2	Joint angle for a single rep: Illustration of the changes in joint angles over a single rep for Healthy-Adult (left) and Clinical-Impaired (right).	136
8.3	Autoencoder: representation of autoencoder architecture. It consists of a three layer encoding and a 3-layer decoder. The latent representation is 4 LSTM units. The input time series was 200 frames by 16 channels, this was also the demotions of the reconstructed output	138
8.4	Reconstruction of STS-5 movement: This figure shows the reconstruction of STS-5 movements carried out by (a) a member of the Healthy-Adult group and (b) a member of the Clinically-Impaired group. Movement (a) was part of the validation set, movement (b) was part of the test set. The Autoencoder is able to recreate movement (a) with high faithfulness, and so the reconstruction error, (expressed as Euclidean Distance) is low. The autoencoder struggles to recreate movement (b) because it comes from a different distribution, the reconstruction error is 5.5 times larger for this movement, indicating it lies far away from the training distribution. The time series, shown here have been normalised to aid recognition. <i>Note, the first 30 and last 30 frames, of the reconstructed time series, are clipped before the distance is calculated, these early frames often contain encoding errors and so do not truly reflect the reconstruction.</i>	139
8.5	Graph of Train vs Validation loss: these graphs show how the validation set loss (to the right) matches the train set loss (to the left) in terms of MSE, very well throughout the training process. This demonstrates the similarity between the two set of healthy individuals.	141

8.6	A flowchart of the cross validation process. 1) The dataset was split into Train and Test sets. The train being a single class Healthy-Adults ; 2) 5 folds were created to for cross validation, each fold contained a train and validation set; 3) A model was trained, using the ith fold (nominally 1000 epocs); 4) Early sopping was used to prevent overfitting; 5) The trained model was used to reconstruct the movement from the Test set ; 6) Each member of the test set was scored; 7) The best threshold to identify impairment was calculated; 8) The metrics were calculated and stored; 9) the process continues for 5 iterations; 10) The mean metrics were calculated and scored; 11) The graph, showing separation were displayed	142
8.7	Separation of individuals by impairment: this graph represents the score derived from the autoencoder, One marker denotes a single participant. The most impaired are shown furthest away from the normal threshold. The normal threshold is indicated by the blue line. Key NF : Non-Fallers, FHs : Self-reported-Fallers_s, FHm : Self-reported-Fallers_m, Clin-Imp : Clinically-Impaired	144
8.8	ROC curve for the proposed model: the ROC curve shows the trade of between different cut off levels for the threshold of normal. a score of 0.991 was found to give the best separation, with a Specificity of 0.88 95% CI (± 0.22) and a Sensitivity of 0.68 95% CI (± 0.21).	145
8.9	Regression of age vs impairment: this graph shows two distinct populations, Unimpaired (blue) and impaired (orange), One marker denotes a single participant. The Unimpaired group have scores that are similar to those found in the Healthy-Adult group, over a wide range of ages. The scores for the Impaired group decline with age. As the score goes down the falls-risk increases.	146

List of Tables

1.1	Table of common clinical tests: the table provides a list of common clinical test and a short description. Relevant references are included	9
2.1	Interpretation of Balance Master results, and their relation to different balance conditions, reproduced from the Balance Master Clinical Interpretation Guide [204]	20
2.2	Results from [60]: The results show % difference between gait metrics derived from the smart carpet and the Kinect, assuming the smart carpet to be the ground truth	32
4.1	Movements used in this work, along with the rationale for inclusion	63
4.2	The features used in this study	65
4.3	A comparison of the different machine models: All three machine models were able to separated the extracted features	69
5.1	Table of participants: The table provides a breakdown of Age, Sex, Weight, BMI and Age Class: Young (20-30 years), Middle Age (31-59 years) and Older (>60 years)	74
5.2	Table of Exclusions	80
5.3	A priori power calculations G*Power was used to calculate the sample size required for 95% power. The data came from an initial study, used to ensure the placement of the Kinect camera was correct.	81
5.4	Repeatability of each method, Balance Master (BM) and the Proposed Pipeline (PP), has measured by the Standard Deviation (SD) and Repeatability Coefficient (CR).	82

5.5	Pearson correlation coefficient between the two methods: The Pearson correlation coefficient demonstrates a high correlation between the two methods	83
5.6	The normality of the difference between the two methods given by D’Agostio-Pearson tests for normality.	85
5.7	The normality of the difference between the two methods given by D’Agostio-Pearson tests for normality.	85
5.8	A summary of the agreement of postural sway derived from the two methods: Balance Master (BM) and the Proposed Pipeline (PP). The mean, standard deviation (in brackets) - within each method, mean standard deviation (in brackets) - between the methods (bias), the 95% Confidence Interval (CI) and Limits of Agreement (LOA) and the significance of the t-test are shown. Eyes open conditions show no significant difference between methods, shaded in grey	87
6.1	A comparison of datasets: Comparing KINECAL to previous datasets that contain clinically significant movements, the advantages of KINICAL can clearly be seen.	95
6.2	A description of each movement in the dataset, and how they were explained to the participants.	96
6.3	Grouping of Self-reported Labels: This table shows the split between the different groups, in terms of mean age, total numbers and gender split. A description of each group is also included.	99
6.4	Grouped Sub-labelling of Self-reported-Fallers : This table shows the split between the different single (_s) and multiple fallers (_m), in terms of mean age, total numbers and gender split. A description of each group is also included.	100
6.5	Details of the Clinically-Impaired group: Details of, mean age, total numbers and gender split. A description of this group is also included.	100
6.6	SPPB classification	101
6.7	TUG classification	102

6.8	Truncated Table of Sway Metics: This table provides a truncated view of the sway metric data, comparing just two participants over a selection of metrics, for quite standing, eyes open. <i>Note: Group HA:Healthy-Adult, FHm: Self-reported-Multiple-Faller, Sex 0:Male, 1:Female, Self-Rep: Self-Reported-Faller, Clin-imp: Clinically-Impaired.</i>	111
7.1	Table of sway metrics: This table details the sway metrics from the KINECAL dataset. RD refers to the Resultant Distance, AP Anterior-posterior and ML Medio-lateral directions, details of how these metrics were calculated can be found in section 6.6	116
7.2	Participant groups used in this investigation: The groups shown here are the standard groups of participants from the KINECAL dataset, along with a description of the criteria for inclusion.	117
7.3	Participant groups used: The groups described here were used in the identification of metrics useful in falls-risk assessment. The numbers shown here were after outliers had been removed. Each participant belonged to only one group.	119
7.4	Results of analysis of the difference in sway metrics, between different groupings:. The shading of the background signifies the degree of significance (light grey = $p < 0.05$, dark grey = $p < 0.001$).	121
7.5	Participant groups used: The groups described here were used in the identification of metrics useful in falls-risk assessment. The numbers shown here were after outliers had been removed. Each participant belonged to only one group. In this investigation, group membership was exclusive, and one participant does not appear in more than one group.	122
7.6	Results of analysis of the difference in sway metrics between levels of impairment: The shading of the background signifies the degree of significance (light to dark grey $p < 0.05$, $p < 0.01$, $p < 0.001$). The final column gives a grouping for the metrics.	122

7.7	The mean results after rounds of 10,000 bootstrapping: The results show the mean value and the 95% CI	126
8.1	Participant Groups: This table shows the split between the different groups used in this trial. The groups are exclusive and no participant belongs to more than one group	133
8.2	Table of metrics: summation of 5-fold cross validation the mean values are shown with standard deviation in brackets and 95% confidence interval below.	145
9.1	Table of objectives and outputs	152

List of Abbreviations

ANFIS	Adaptive Neuro-Fuzzy Inference System
ANN	Artificial Neural Network
AP	Anterior-posterior
AREA-CE	95% Confidence Area
BMI	Body Mass Index
BoS	Base of support
CNN	Convolutional Neural Networks
CoM	Centre of Mass
CoP	Centre of Pressure
DTW	Dynamic Time Warping
EC	eyes closed
EO	eyes open
FoG	Freeze of Gait
GNB	Gaussian Naive Bayes
GRU	Gated Recurrent Unit
HAR	Human Action Recognition
HMM	Hidden Markov Model
HSMM	Hidden Semi-Markov Model
K-NN	K-Nearest Neighbours

LoG	Line of Gravity
LSTM	Long Short Term Memory
MART	Multiple Additive Regression Trees
MDIST	Mean distance of the RD time series
MDIST_AP	Mean distance of the AP time series
MDIST_ML	Mean distance of the ML time series
MFREQ	Mean frequency of the RD time series
MFREQ_AP	Mean frequency of the AP time series
MFREQ_ML	Mean frequency of the ML time series
ML	Medio-lateral
MLP	Multilayer Perceptron
MoCap	Motion capture
MVELO	Mean velocity of the RD time series
MVELO_AP	Mean velocity of the AP time series
NNS	Nearest Neighbour Search
PCA	Principal Component Analysis
RDIST	RMS distance of the RD time series
RDIST_AP	RMS distance of the AP time series
RDIST_ML	RMS distance of the ML time series
reps	repetitions
RGB+D	Red Green Blue + Depth
RNN	Recursive Neural Network
SI	Superior-inferior
SOT	Sensory Organisation Test
SPPB	Short Physical Performance Battery
STS-5	Five times sit-to-stand
SVM	Support Vector Machine
TBCM	Total Body Centre of Mass
TOTEX	Total excursions of the RD time series
TOTEX_AP	Total excursions of the AP time series

TOTEX_ML	Mean velocity of the ML time series
TOTEX_ML	Total excursions of the ML time series
TUG	Timed Up and Go
ULS	Unilateral Stance

Publications

1. **Maudsley-Barton, S.**, McPhee, J., Bukowski, A., Leightley, D. and Yap, M.H., 2017, October. A comparative study of the clinical use of motion analysis from kinect skeleton data. In 2017 IEEE International Conference on Systems, Man, and Cybernetics (SMC) (pp. 2808-2813). IEEE.
2. **Maudsley-Barton, S.**, Hoon Yap, M., Bukowski, A., Mills, R. and McPhee, J., 2020. A new process to measure postural sway using a Kinect depth camera during a Sensory Organisation Test. Plos one, 15(2), p.e0227485.

Chapter 1

Introduction

The effect of ageing on the motor control system means coordination patterns change with age. Intern, this can lead to a propensity to lose balance, resulting in a fall. Deaths due to complications after a fall are the most common cause of death for those aged over 65 [260, 49], with one study suggesting that a further 30% of people die within 12 months after a major fall. [238]. Less significant falls may result in fractures (the most common being wrist, arm, ankle and hip) and/or head injuries, both have the possibility to change lives.[168]. Even trivial falls can lead to a loss of confidence and reduce social mobility, both of which could well spark the cycle of frailty 1.1

By the age of 65, 1/3 of people fall once a year. By the age of 80, this has turned into 1/2. [242]. The estimated population of over 65s living in the UK in 2021 is around 9.7 million. The estimate for over 85s is 1.7 million. [175]. In addition to the personal cost, health providers bear huge monetary cost [229]. In 2011 the cost to the NHS and the wider economy (due to absence and reduced productivity) was estimated to be £2 billion every year. [226].

There are many potential causes for falls: slippery floors, poor vision, long term health conditions like heart disease, Parkinson's disease and dementia, to name but a few. However, one of the most tractable factors that can greatly affect the likelihood of a fall is a deterioration in muscle tone, and balance [150]. Several studies have shown that with appropriate intervention, such as balance and strength training, functional movement can be improved, leading to fewer falls in the future [102, 81, 214, 62]. For most people, this requires the intervention of a trained specialist. In the UK, the most common way to access such a specialist is a referral by a GP to a falls clinic, following the report of a fall. However, even a single fall could be the beginning of the cycle of frailty,

discussed in section 1.1. Currently, there is no low-cost and easy-to-use device that could be used to screen those at risk of falls. The main focus of this thesis is to bring such a device, a step, closer to reality.

1.1 Ageing and Frailty

Ageing produces bodily changes, related to a reduction in the bodies ability to repair [251]. These changes can be detected at many scales. **At a molecular level:** cumulative damage caused by many processes including oxidative stress, which is a particular issue for brain and nerve tissues [243]. A reduction in the effectiveness of DNA repair pathways [224], along with a reduction in the size of telomeres, essential to DNA replication and cell division [6]. **At the cell level** the effect of molecular damage produces noticeable changes in cells. For instance, changes in gene expression can induce cells to secrete inflammatory cytokines (chemicals associated with inflammation) [31]. At the sub-cellular level, damage can also be seen in cell organelles, Rygie et al. showed the effect of damaged mitochondria on ageing [208]. **At the level of the body** the effect of these underlying changes give rise to the classic phenotypes of frailty, degradation of eyesight, loss of proprioception [65], metabolic conditions (e.g. insulin resistance and diabetes), muscle weakness (Sarcopenia), heart disease, changes in bone density (osteoporosis), joint issues, slower walking speeds, and the tendency to fall. Intern, these conditions can induce **Behavioural changes** a notable lessening of movement [183] and lessening of social interaction [168, 188]. Over time one issue can exacerbate another. Walston arranged these phenotypes into a cycle of frailty shown in Figure 1.1. Rockwood [202] also developed a frailty index using the phenotypic changes shown in Figure 1.2.

Looking at both definitions of frailty, sarcopenia is a key element [150], and one that has been identified both in the initiation of the cycle of frailty and a major cause of balance impairment, leading to falls (Figure 1.1). The outwards signs of sarcopenia are a reduction in muscle mass and associated contractile strength. The underlying cause is primarily due to the loss of alpha motor neurons. This results in motor unit pools (MU) receiving a weaker signal, hence a less powerful contraction in the associated muscle [54]. More general neurological damage, which presents as dis-coordination, has also been implicated in the development of frailty and increased falls-risk. Nerve damage

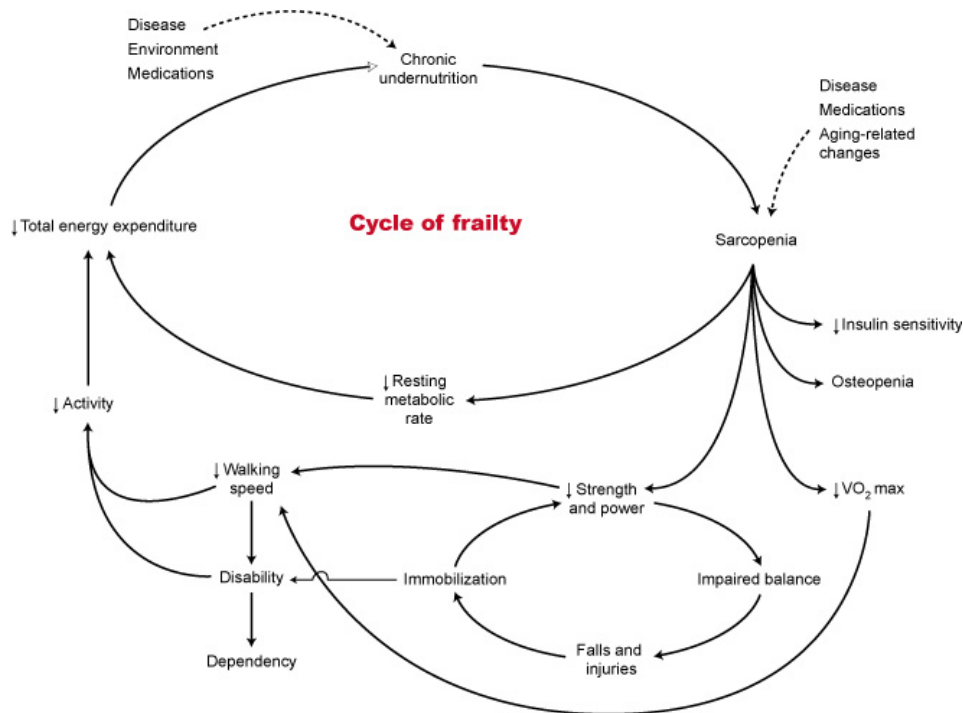


Figure 1.1: **Walston's cycle of frailty.** Recreated from J. Walston, *Sci. Aging Knowl. Environ.* 2004, pe4 (2004)

can be exacerbated by inflammation, insulin resistance and inactivity, adding fuel to the cycle of frailty [252, 117]. This process begins in middle age and becomes significant by age 70 [203].

These findings correlate well with the tendency for falls to become a problem in those over the age of 65. Although neurological decline is inevitable and irreversible, regular exercise can help to maintain or even improve muscle function, and bodily coordination [99, 179]. This is why master athletes are so well studied. Master athletes are individuals over the age of 30, but many of whom are aged over 80, who still take part in athletic competition. In spite of demanding regimes of training and competition, the risk of an adverse event during these activities was found to be no higher than it was for younger athletes [72]. While they are seen as functionally fitter, when compared to those, of a similar age who do not compete in sporting events, the effects of ageing are still detectable [52, 154]. McPhee et al. [150] suggested that the protective effects of regular exercise are universal, and not limited to elite athletes.

Therefore, a distinction must be drawn between evidence of ageing and evidence of functional decline if one seeks to identify those at risk of injury from everyday activities. Mouel et al. [159] proposed an in-silico model that

Appendix 1: List of variables used by the Canadian Study of Health and Aging to construct the 70-item CSHA Frailty Index		
• Changes in everyday activities	• Mood problems	• Seizures, partial complex
• Head and neck problems	• Feeling sad, blue, depressed	• Seizures, generalized
• Poor muscle tone in neck	• History of depressed mood	• Syncope or blackouts
• Bradykinesia, facial	• Tiredness all the time	• Headache
• Problems getting dressed	• Depression (clinical impression)	• Cerebrovascular problems
• Problems with bathing	• Sleep changes	• History of stroke
• Problems carrying out personal grooming	• Restlessness	• History of diabetes mellitus
• Urinary incontinence	• Memory changes	• Arterial hypertension
• Toileting problems	• Short-term memory impairment	• Peripheral pulses
• Bulk difficulties	• Long-term memory impairment	• Cardiac problems
• Rectal problems	• Changes in general mental functioning	• Myocardial infarction
• Gastrointestinal problems	• Onset of cognitive symptoms	• Arrhythmia
• Problems cooking	• Clouding or delirium	• Congestive heart failure
• Sucking problems	• Paranoid features	• Lung problems
• Problems going out alone	• History relevant to cognitive impairment or loss	• Respiratory problems
• Impaired mobility	• Family history relevant to cognitive impairment or loss	• History of thyroid disease
• Musculoskeletal problems	• Impaired vibration	• Thyroid problems
• Bradykinesia of the limbs	• Tremor at rest	• Skin problems
• Poor muscle tone in limbs	• Postural tremor	• Malignant disease
• Poor limb coordination	• Intention tremor	• Breast problems
• Poor coordination, trunk	• History of Parkinson's disease	• Abdominal problems
• Poor standing posture	• Family history of degenerative disease	• Presence of snout reflex
• Irregular gait pattern		• Presence of the palmomental reflex
• Falls		• Other medical history

Figure 1.2: **CSHA frailty index.** Recreated from K. Rockwood, “A global clinical measure of fitness and frailty in elderly people,” *Can. Med. Assoc. J.*, vol. 173, no. 5, pp. 489–495, Aug. 2005.

suggests that by modulating ankle joint stiffness while standing quietly, older individuals could compensate for a reduction in neural feedback. This mechanism is also seen in younger people when asked to adopt more challenging stances, such as standing on a narrow support. In the model, an increasing ankle stiffness only produced an increase in stability when the reaction time is reduced by 30-40ms (the same range as is seen in age-related changes). Conversely, a combination of quick feedback and stiffened ankle joints produced an increase in sway due to overcompensation.

Many studies have shown that ageing has a delaying effect on the Anticipatory Postural Adjustments (APAs) and subsequent compensatory postural adjustments (CPAs) [266, 181, 165], the result is larger CoM displacement, for older people, compared to young adults [109]. To counter this excessive displacement, older people can be seen to adopt a hip strategy [20], while also decoupling the head and hip segments, this allows them to recruit extra degrees of freedom in the stabilisation task. Younger people, with less innate sway, predominantly use an ankle strategy, in which movements of the hips and head are couples. This results in young peoples sway being more closely

related to the single inverted pendulum model, which predominates in posturography. However, if the visual input is removed from the elderly subject (by asking them to close their eyes), the time for APAs and CPAs further increases, and coupling returns between head and hips, resulting in increased sway [166].

From the examples above, it is clear that human balance is complex and constantly evolving. While ageing and balance is well studied, identifying coordination patterns and associated sway metrics that are more associated with fallers vs the overall process of ageing is an under-researched area. However, it is one that is key to better identify those at risk of falls in old age.

1.1.1 What is an injurious Fall?

Berg and Cassells [14] define an injurious fall as follows: “A fall is an unintentional event that results in the person coming to rest on the ground or another lower level.” They also suggest that falls have three phases:

1. **The initial event displaces the bodies CoM, outside of its Base of support (BoS)** - This event involves **extrinsic** factors (e.g. hazards in the environment) and **intrinsic factors** (e.g. muscle weakness, worn joints, slowing of reflexes)
2. **The failure of the bodies systems that maintain upright posture, to detect the displacement of the CoM, in time to correct it** - The main factors here are **intrinsic** (e.g. loss of proprioception, slowed reflexes, bad eyesight, muscle weakness, medication, cognition, health problems)
3. **Impact the body comes in contact with the environment, at speed (usually the ground)** - Resulting in the transmission of force into the bodies tissue and organs. - The main factors are **extrinsic**, the potential for injury relates to the magnitude and direction of the force experienced by the body.

From this short list it is clear that injurious falls are a mixture of extrinsic and intrinsic factors. NICE [168] suggest a multifactorial approach to falls risk assessment. looking at the following elements

- cognitive impairment

- continence problems
- footwear that is unsuitable or missing
- health problems that may increase their risk of falling
- medication
- syncope syndrome
- visual impairment.
- falls history, including causes and consequences (such as injury and fear of falling)
- postural instability, mobility problems and/or balance problems

It is clear that one maps neatly on to the other, and many factors can affect the cause and severity of a fall. In the UK, there is a network of falls clinics which take a multi-functional approach to reducing the likelihood of future falls, for those who have had one or more falls in the past.

1.2 Identifying Those at Risk of Falls

Given the complexity of injurious falls, it is perhaps surprising that the most common form of screening for falls risk, and the one recommended by NICE, is to ask the question “Have you fallen in the last 12 months” or more formally **“Have you had any fall including a slip or trip in which you lost your balance and landed on the floor or ground or lower level in the past 12 months?”**. This is the standard question used when collecting falls history [258]. Possible answers are [**None, One, Two, Three, Four or more**]

This question assumes that the person has already fallen. As discussed above, a single fall could have severe and lasting consequences. It is in this situation where an inexpensive and objective test to preemptively identify people at risk of falls could make a significant impact at both the personal and state level.

1.2.1 Assessment by a Clinician

Clinical assessments are carried out by observing an individual, carrying out a proscribed set of movements and then rating them, on a predefined scale. Pre-established cutoffs are used to categorise the level of impairment. While these cutoffs are well-established, results can vary from assessor to assessor and location to location [221]. In addition clinical assessments can be time-consuming and so soak up many hours in a clinicians day.

Many clinical assessments exist, Table 1.1 provides a list of the most commonly used for the assessment of the purely physical signs of impairment. However, as discussed in section 1.1.1. It should be acknowledged that an holistic approach should be taken to falls-risk assessment. Additional cognitive and psychological factors can greatly affect the likelihood of a fall. In particularly frail older people, the inability to walk and talk at the same time can be predictive of falls [140]. This is an example of dual-tasking, where an individuals ability to complete a physical task is affected by their brain attending to other tasks. This example is at the extreme end of this phenomenon. However, the incorporation of dual-tasking into clinical tests can provide insights for less impaired populations. Shumway-Cook et al. [220] examined the postural sway of aged-matched fallers and non-fallers while dual-tasking, in this case, quite standing while carrying out a sentence completion task. They demonstrated that both fallers and non-fallers show a significant increase in postural sway. However, fallers showed a greater increase in sway, the difference being predictive of falls-risk. Dual-task assessments have become a popular option when considering the contribution of cognition to balance, Muir-Hunter and Wittwer [161] provides an excellent review of their application to falls-risk.

The psychological components of falls-risk should also not be overlooked, key is the fear of falling. The fear of falling can affect both fallers and non-fallers. Ironically, the fear of falling can initiate behaviours that make falls more likely, such as the avoidance of physical activity and social isolation. Vellas et al. [245] suggested that this issue should be specifically addressed in rehabilitation programs. The Falls Efficacy Scale-International (FES-I) [82] is a well-validated scale for assessing the fear of falling in older adults and has become the de facto questioner for this type of assessment.

Table 1.1: **Table of common clinical tests:** the table provides a list of common clinical test and a short description. Relevant references are included

Test	Description
Short Physical Performance Battery (SPPB) [85]	SPPB is a well validated test for impairment. The test is made up of several movements : Quiet standing, eyes open (EO) and eyes closed (EC) Semi-tandem stance, Tandem stance, 3m walk and 5x sit to stand (STS-5).
Five times sit-to-stand (STS-5) [256]	The STS-5 is a well validated test with applications in falls-risk. It can provide a good indicator of muscle strength and general coordination.
3m Walk [247]	The 3m walk is the basis of many instrumented and non-instrumented gait assessments. It is a simple means of assessing dynamic balance.
Timed Up and Go (TUG) [147, 219]	TUG combines elements of STS-5 and 3m walk into a single test.
Unilateral Stance (ULS) [24]	Standing on one leg is an easy to administer means of increasing anyone's postural sway. Maximum stand time has been used as a predictor of falls-risk.

1.3 Motivation

In research, the instrumented assessment of balance is well established. Most commonly, this is achieved through the tracking of the **Centre of Pressure (CoP)** and **CoM** calculated from the ground reaction forces at the surface of a force plate. The work of Nashner et al. [167] lead to the establishment of the discipline of Posturography and the creation of the device which has become synonymous with it, the Balance Master. The Balance Master uses twin force plates to measure both static (quiet standing) and dynamic (in reaction to a perturbation) postural sway [204]. As well as outputting raw data, it has inbuilt software that can provide clinical measures such as the equilibrium score (ES) and comparisons against the general population. However, its size and cost are prohibitive for widescale clinical use, which certainly puts it out of the range of possibilities for a family doctor.

An alternative to using force plates is to use one of the many clinical test [84, 86, 187, 147, 24, 22]. This is the standard approach during the initial appointment at a falls clinic. On the whole, these clinical tests relate to the timing of a set of proscribed physical movements which are then scored against a predefined scale. While this type of approach is able to identify those with high levels of impairment, it is prone to variation in scoring, from assessor to assessor [221].

The most complete description of an individuals balance can be achieved through motion capture. This technique uses reflective beads and an array of

infrared cameras to capture the intricacies of human movement. However, it requires a long period of set up and a dedicated space, i.e. a motion capture lab. This makes motion capture impractical for regular assessments, especially for the most vulnerable of people.

In 2011 Microsoft released the first version of their human-action-based games controller, Kinect. This was superseded by version 2 in 2014 (the version used to collect data for this thesis) and version 3 in 2019. Version 3, the azure Kinect, marks the official transition of Kinect from a games controller to a device intended to be used for research, development and ultimately incorporation into commercial products. From the start, researchers leapt on the Kinect as a means of tracking human movement without the need for a lengthy setup. Human action recognition (HAR) has made great strides in recent years, utilising the plentiful data which has been created using Kinect. Unfortunately, datasets of clinically relevant movements are not as numerous. At the time of starting this research, an extensive search revealed only one, the K3Da dataset, and that lacks the labelling necessary to progress this field.

The knock-on effect of this lack of data is a lack of research into the practical use of such devices for automated balance assessment and falls-risk. This is not to say that there has been no research into the instrumented identification of fallers. However, the majority of instrumented falls assessment relates to the use of expensive force plates conducted in lab conditions. Burns et al. [28] in their paper, "The direct costs of fatal and non-fatal falls among older adults" concluded *Widely implementing evidence-based interventions for fall prevention is essential to decrease the incidence and healthcare costs associated with these injuries*. However, currently, there is a lack of practical and objective methods of screening for fallers in the general population.

1.4 Problem Statement

Falls are a huge problem for older people worldwide. A fall can lead to a multiplicity of consequence and may be indicative of deeper issues, including frailty. These issues can be addressed by targeted rehabilitation. However, access to this type of treatment is only provided after the report of a fall. Currently, there is no practical screening for this issue, due to the cost of equipment or man-power required, for the widescale use of clinical tests. A system that

utilises low-cost markerless motion capture could provide the answer. Interpretation of such data can provide a range of traditional, well-recognised metrics along with the ability to provide more advanced methods of assessing the early signs of impairment. This would allow for early referrals and prophylactic treatment regimes. In addition, such a system could be used to track the progress of recovery.

1.5 Aim and Objectives

The aim of this research is to create a predictive model for the objective assessment of falls-risk in old age. To achieve this, the following objectives were set out:

1. To develop a method to track CoM and calculate traditional postural sway metrics from the output of a Kinect, then compare the proposed method to the output of a device used in clinical practice
2. To create a new dataset of movements, widely used in clinical tests, using markerless motion capture, i.e. a Kinect V2 camera
3. To disambiguate sway metrics associated with age-related changes and those related to the impairment
4. To develop a method to quantify impairment using deep learning and the captured data

1.6 Contributions

1. *A new process to measure postural sway using a Kinect depth camera* (Chapter 5). The output of the proposed method and the output of the Balance Master were compared and found to be in good agreement.
2. *KINECAL: A dataset of clinically significant movements* (KINECAL, Chapter 6), This dataset addresses a major stumbling block in this area of research, and which will aid research into the clinical use of depth cameras for falls-risk and physical impairment.

3. *An investigation of sway metrics associated with falls* (Chapter 7). The question of which sway metrics are the most appropriate to identify fallers is still an open question. In this chapter, this question is examined. In addition, a machine model is also discussed, which could be used as a screen to identify those who would be classed as impaired by clinical tests.
4. *Quantification of physical impairment, based on a representational model* (Chapter 8). An anomaly detection approach was taken to quantifying impairment. By using an autoencoder to model normal movement, a scoring system was developed, which uses distance-from-normal as an indication of impairment.

1.7 Thesis Organisation

Figure 1.3 presents an overview of the thesis organisation. The details of each chapter are follows:

1. Chapter 1-5: Introductory chapters, set this thesis in context, they provide background, previous work descriptions of the common methods used and the motivation of this work. In addition, they detail some preliminary work which became the inspiration for the work in this thesis.
2. Chapters 6-9: Contribution chapters, detail the contributions made in this thesis.
3. Chapter 10: Conclusion, provides a summary of this thesis and the direction of future work.

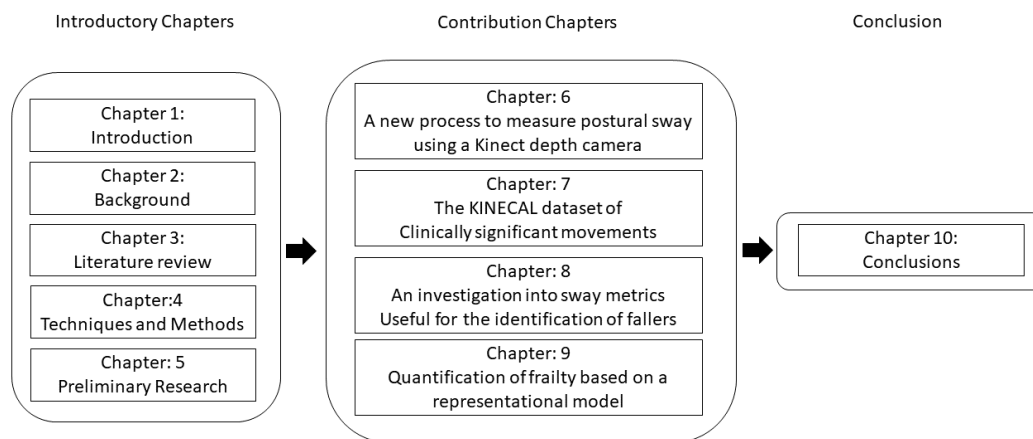


Figure 1.3: Thesis Organisation

Chapter 2

Literature Review

2.1 Introduction

This chapter places this thesis in context. It explains the background to balance assessment, their importance and application. It also describes the current methods for balance assessment, their use and their limitations. It then goes on to discuss the application of machine learning to the assessment of balance and human movement. The chapter concludes with a discussion of common types of machine learning algorithms.

2.2 What is Balance?

Any object has a **CoM**, seen as the point in the body where the mass of the object acts. If an object is uniform in density, this point is the geometric centre of the object. Let us consider a toy see-saw, consisting of a plastic plank and a rotary bearing, attached to a frame, exactly halfway along the plank's length. Assuming one has a perfect see-saw, when in the horizontal position, the force on both sides is equal, and so one can say the see-saw is balanced. If a force is applied to one end alone, the see-saw will rotate around its CoM. In this case, this is true because the bearing is constraining the plastic plank, but it would also be true if the plank was removed from the bearing and, holding one end, it was thrown, through the air, using a flicking motion. The plank would rotate around its CoM. What is true for the toy, is also true for other bodies that have mass, including human bodies. A gymnast executing a floor routine

is exploiting this fact to great effect. Whenever they flip or rotate in the air, they are rotating around their CoM.

Now let us consider a human body that is at rest and balanced, upright and standing on the ground. The body is balanced because all of the forces applied to it even out as described by Newton's third law [172]. Gravity exerts a downward force, and the ground resists with equal, but opposite force. This is known as the ground reaction force. The ground reaction force is experienced by any part of the body touching the ground, for example, the feet (another example could be one foot and the base of a walking stick). Summing these forces identifies the CoP. The CoP is distinct from the BoS, which is the area described by the outside edge of the weight-bearing elements touching the ground. Figure 2.1 demonstrates the relationship between BoS and CoP.



Figure 2.1: **CoP in relation to the BoS. the CoP is marked by a black dot** This figure shows three possible BoS (shaded grey), and the associated CoP (shown as a black dot). The first two are narrow stances, quiet standing and semi-tandem, repetitively. The third is a wide version of quiet standing (feet shoulder width apart).

Gravity acts on the CoM, in a line which can be described as the **Line of Gravity (LoG)**. If the LoG of an object falls outside the BoS, that object will tend to rotate until it finds a more stable attitude. Therefore, the wider the BoS, the more inherently stable the object. Generally, CoM is thought of as acting directly, and the LoG is ignored. Figure 2.5 shows the relationship between LoG, CoM and CoP.

Looking at the triangles in Figure 2.2 it is easy to understand the relationship between BoS, CoM and Balance. You can almost sense the tendency for the first triangle to rotate to adopt the attitude of the second one. This is because only a small perturbational force would be required to unbalance it. However, a significantly higher force would be required to make the second triangle rotate, because of its larger BoS.

If one applies this intuition to the vertebrate animals on the right. It is clear that the dog and the ape, who use four points of contact, have a bigger BoS than the human using just two. i.e. their CoM is less likely to fall outside the BoS. Hence humans are more likely to fall, even when standing still.

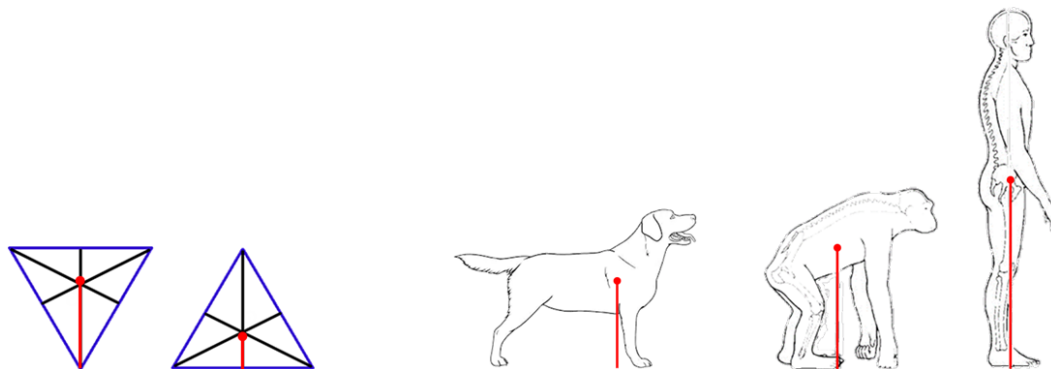


Figure 2.2: **Balance for different objects.** This figure shows a simple triangle and 3 vertebrate bodies, with the CoM shown as a red point, and the LoG shown as a red line. It is easy to see why the triangle resting on its long-side is inherently more stable than the one resting on its point. By applying this intuition to the vertebrate bodies you get an appreciation of how the upright, human body, on the far right, is less stable than the ape and dog pictured to the left of it.

Although this model explains the principles, it is slightly disingenuous. Vertebrate animals are not uniform objects, and are certainly not inanimate. They are complex entities that move in any number of ways to achieve their day-to-day goals. Movement is achieved using a skeleton of interconnected joints, on to which is attached many different types of tissue, muscles, tendons, ligaments and assorted connective tissues. All controlled by conscious and unconscious control systems which process information from sense organs, connected through the nervous system. This means that the CoP and CoM is in constant flux, even when standing still, often called quiet standing. In order to keep the CoM within the BoS, the system described above, known as the motor control system, is always adjusting. This is the essence of balance in animals.

As discussed, due to the upright stance adopted by humans, balance is a particular issue for us. The human skeleton has more than 100 degrees of freedom [68]. This provides incredible flexibility and redundancy. Consequently, there are many ways to achieve a particular movement. You may have experienced this multiplicity of options when you have sustained a minor muscular

injury. Your body adapts its coordination patterns to enable you to still move around, albeit in a sum-what awkward fashion [128]. The inbuilt redundancy of the human body was first studied by Nikolai Bernstein in his pioneering work in motor control and motor learning in the 1920's [16], and gave rise to the phrase "Bernstein's problem". Bernstein's answer was the motor control system is able to dynamically constrain certain degrees of freedom, although this constraining must be learned. The work of Karl Newell [171], explains how these constraints can be learned and goes some way to explaining differences between those who play sport recreationally and elite athletes. You might reasonably expect that no two individuals would move in quite the same way when trying to achieve a particular goal. However, studies have shown stereotypical patterns of muscle activation, and limb movements for a given task [103].

2.2.1 Posturography

An alternative to Clinical assessment is the use of posturography. Posturography provides an objective measurement of an individual's postural control. I.e. a balance assessment, based on the movement of the body's CoP and or CoM, measured by using force plates [92]. Posturography has become the standard for assessing balance impairments and has been widely applied to the assessment of vestibular problems, Parkinson's disease, ageing and the relation of ageing to falls prediction.

Force plates use the ground reaction force, discussed in section 2.2, to locate and track the CoP. The CoP is either used directly or used to calculate the position of the CoM. Several methods have been proposed to estimate CoM from CoP [270, 264, 158, 204]

If the CoM is perturbed, for instance, by standing on a compliant surface or pivoting platform [265], the CoM can move more easily and so will tend to move more frequently to the edge of the BoS. To regain balance, the body moves the CoP ahead of the CoM, which counteracts the perturbation and brings the CoM back towards the centre of the BoS. This requires the coordination of the CNS and muscles, based on input from many senses. Key among these are three systems. The visual (information taken in through the eyes), vestibular (information taken in through the semicircular canals in the inner ear) and proprioceptive feedback from the joint, muscles, tendons and

ligaments, especially from the lower body (hips, knees, ankles and feet). The amount of correction, required to remain balance can be quantified as postural sway.



Figure 2.3: **SMART Balance Master:** The SMART Balance Master, is one of the few devices used in the clinical assessment of balance. However, it widescale adoption is restricted by its size and cost.

The device which has become synonymous with posturography, the Balance Master (shown in Figure 2.4, was developed directly from the work of [167]. It automates the process of identifying which sense is contributing most to an individuals balance, using the [Sensory Organisation Test \(SOT\)](#) [204]. There are six components to SOT, pictured in Figure 2.4, are as follows:

1. Eyes open, platform fixed, used as a baseline, visual, vestibular, and somatosensory inputs are available
2. Eyes closed, to remove visual input
3. Eyes open with moving surround, to create sensory conflict between visual input and both somatosensory and vestibular inputs
4. Eyes open and moving support, to disrupt somatosensory and proprioceptive feedback from the feet and ankles
5. Eyes closed and with moving support, combining inaccurate somatosensory input combined with no visual input

6. Eyes open with moving surround and platform, providing inaccurate visual and somatosensory input

As the test progress, they become steadily more challenging to balance. Table 2.1 provides an interpretation of SOT results.







		VISUAL CONDITION		
		FIXED	EYES CLOSED	SWAY-REFERENCED
SUPPORT CONDITION	FIXED	1 	2 	3 
	SWAY-REFERENCED	4 	5 	6 

Figure 2.4: **Elements of the SOT.** (1) eyes open, platform fixed (used as a baseline); (2) eyes closed to remove visual input; (3) eyes open with moving surround, to create sensory conflict between visual input (simulating a moving room) and vestibular inputs (a stable room); (4) eyes open and the platform support rotating freely to disrupt somatosensory and proprioceptive feedback from the feet and ankles; (5) eyes closed and the platform support rotating freely; and (6) eyes open with moving surround and the platform support rotating freely

Balance Master outputs

The balance master provides the following outputs

- Raw
 - CoM [Anterior-posterior \(AP\)](#) and [Medio-lateral \(ML\)](#) displacement

- CoM Path
- Equilibrium Score
 - Stability of an individual, in the AP direction, vs a normative score, expressed as an inverse percentage, 100 indicates perfect stability
- Strategy Score
 - contributions of hip and ankle strategies 100 = all ankle 0 = all hips)

Table 2.1: Interpretation of Balance Master results, and their relation to different balance conditions, reproduced from the Balance Master Clinical Interpretation Guide [204]

Pattern	Over reliant (dependent) upon:	Problem SOT conditions:
Vestibular Dysfunction	Visual and Somatosensory	SOT 5, 6
Visual and Vestibular Dysfunction	Somatosensory	SOT 4, 5, 6
Somatosensory and Vestibular Dysfunction	Vision	SOT 2, 3, 5, 6
Visual Preference	Vision	SOT 3, 6
Vestibular Dysfunction and Visual Preference	Vision	SOT 3, 5, 6
“Across the Board”	No sensory system	SOT 1, 2, 3, 4, 5, 6

2.2.2 Postural Sway Metrics

Postural sway is a widely used measure of stability [137]. Many papers have demonstrated the connection between increased postural sway and fall risk, in both neurological disease [201] and age-related decline [87]. Over the years, researchers have used many measures to assess postural sway. The most straightforward and intuitive measure of sway is the displacement of the CoM from the mean position, in the ML and AP direction. Summing these small displacements together gives the CoM path [36, 186, 87]. Both of these measures are used by the Balance Master.

In addition to these primary measures, secondary measures, such as RMS of distance, frequency, and elliptical area, can be derived [190, 189, 148, 209]. The calculation of these metrics is covered in Chapter 6.

2.3 Postural Sway, Ageing, and Falls

The majority of studies looking at the change in postural sway with age, conclude that on the whole, sway increases with age. Since increased sway is

related to an increase in falls likelihood, as the CoM is less well controlled. Therefore, it is logical to say that ageing and falls likelihood are so intimately connected that one is a proxy for the other. Yet as discussed earlier, falls likelihood can be reduced through appropriate training, and elderly athletes seem to naturally adapt to the limitations imposed by ageing. Some studies have pointed to particular sway metrics that are associated with age, e.g. Prieto et al. [189], suggested that CoM frequency and velocity increase with age. Hageman et al. [87] suggested an association between path length and age. Others, e.g. Piirtola and Pertti in their review paper [185] drew the connection between falls likelihood, elliptical sway area and various measures of ML sway. In chapter 7, a study of classical sway metrics was undertaken, cross-referencing age and falls-risk. It was found that, while these factors are connected, sway area (equation 6.12) and mean CoM distance (equation 6.6), are more associated with falls-risk.

2.4 Criticism of Sway Measured by Force Plates

The model of postural sway used for force plates is the single, inverted pendulum model. This assumes that the human body is rigid, with a single pivot at the ankle, shown in Figure 2.5. For quiet standing, this model holds up. However, for more challenging stances, this model brakes down. Winter, in his review on human balance [265] noted that the human body pivots about the ankle (the ankle strategy) in quiet stance and about both hip and ankle in reaction to a perturbation (the hip strategy), such as standing on a pivoting platform, or compliant surface.

Cretual et al. [48] suggested the single pendulum model should be used with caution to estimate CoM during more challenging conditions. Lafond et al. [118] also found error in this method of calculating CoM for more difficult poses, and Yeung et al. [269] demonstrated that Kinect performed better when recording more challenging balance tasks compared with force plates. Benda et al. [11] demonstrated that the accuracy of CoM estimated from CoP reduces with increased dynamics.

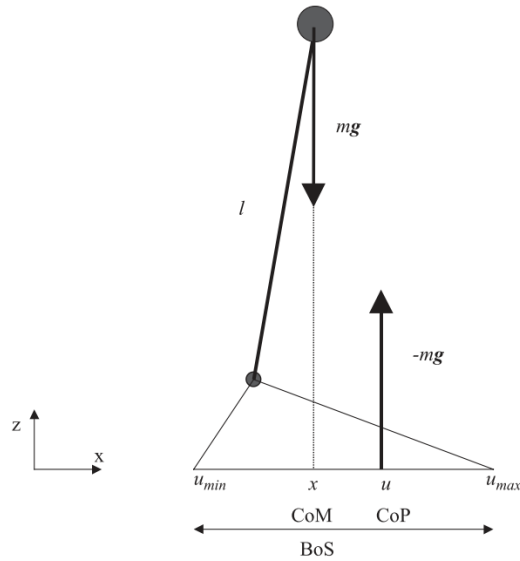


Figure 2.5: **Single inverted pendulum.** This is the standard model of sway when using a force plate. The CoM of the body is modelled as a point mass m on top of a stick with length l . u , marks the location of the effective ground reaction force, and x marks the point where the LoG touches the ground.

2.5 Motion Capture

Many of the issues associated with estimates of CoM, by force plate, can be overcome by the use of Motion Capture. But motion capture can do more than estimate CoM. It can fully describe the actions of a jointed body through space and time.

2.5.1 Origins

[Motion capture \(MoCap\)](#) began in the 1960s with the work of Lee Harrison [90]. Harrison created a motion capture suit that could be used to interpret an actor's movements. The suit used potentiometers at each human joint to encode the movement. A program called the bone generator interpreted these signals and produced a stick figure of the movement. The system was called ANIMAC. Using ANIMAC, Harrison created several short demos, for which he received an Emmy award in 1972 [35]. At the same time Harrison was picking up his Emmy, the psychophysicist, Gunnar Johansson was demonstrating that people can recognise a wide range of human motions, even if only the joints of an actor are highlighted[105]. Johansson's insights led directly to the large

multi-camera, marker-based motion capture systems, now regarded as the gold standard for mocap.

2.5.2 Marker-based Motion Capture

Marker-based motion capture is provided by several vendors, but the most well recognised is VICON, who originated the central ideas of this type of MoCap. The system consists of an array of infrared cameras pointing inwards. This constitutes the capture volume. Reflective beads are attached to key locations on the body, typically bone-ends (in a similar way to which Johansson marked up his subjects). The markers can be tracked in 3D space anywhere inside the capture volume. Software, included in the system (Nexus) is used to record the movements. In addition, the software is able to calculate joint angles, velocities, and accelerations. Figure 2.6 shows a diagram of a typical setup.

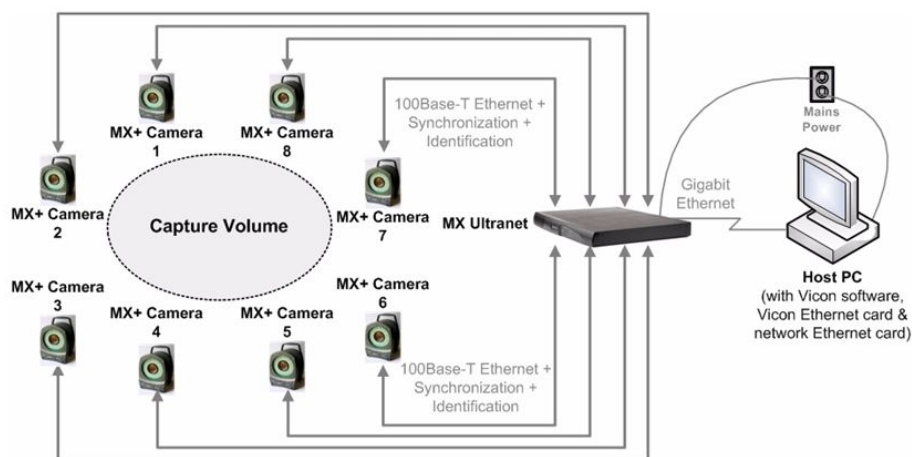


Figure 2.6: **Typical VICON setup:** VICON uses an array of infrared cameras, pointing inwards, to create a capture volume. Reflective markers are attached to a human body, to mark key anatomical features which are to be tracked, eg bone ends.

2.5.3 Markerless Motion Capture

Kinect, popularised markerless motion capture, originally designed as a game controller, the research community was quick to recognise its potential. Shotton et al. [216] took an object recognition approach to segment the human

body. Essentially converting the pose recognition problem to a per-pixel segmentation problem, using a deep random forest as the classifier. In training, they generated thousands of synthetic depth images of all types of body shape to ensure the algorithm is robust in most situations. The output of this model is a 25-joint-skeleton (for Kinect V2) that is widely regarded as being close to the output of a marker-based system [178, 42, 268, 71, 164].

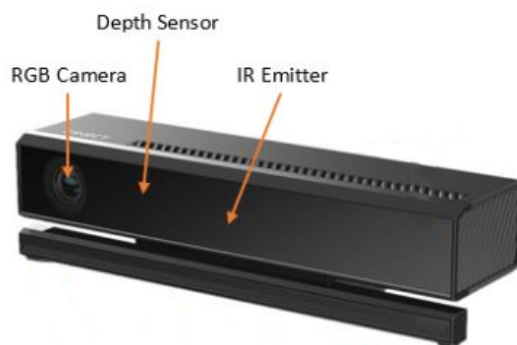


Figure 2.7: **Kinect V2**. Kinect is equipped with both an RGB video camera and a depth camera. It can output a 25 joint skeleton, without the need for makers.

Kinect is a hybrid camera, able to record 2D RGB video and 3D depth videos, both at 30 fps, shown in Figure 2.7. The depth camera is a pixel-wise range finding device that uses the time of flight (TOF) of an infra-red (IR) beam to estimate the distance from the camera to objects within its field of view (512 x 424 px). As well as RGB and depth videos, Kinect V2 outputs a 25-joint-skeleton, created from the model discussed above [216]. The joints are named as shown in Figure 2.8

2.6 Issues with Kinect

The downside of using a single camera is the issue of occlusions. Several studies have addressed this issue by using multiple Kinect cameras [74, 163]. However, this reduces the portability of Kinect-based solutions, as multiple cameras need to be installed on a semi-permanent basis, and they require more space than setups that use just one camera. Also, custom software must be written to synchronise the outputs [44]. Hence, most studies use a single camera. Although, it should be noted that the latest version of the

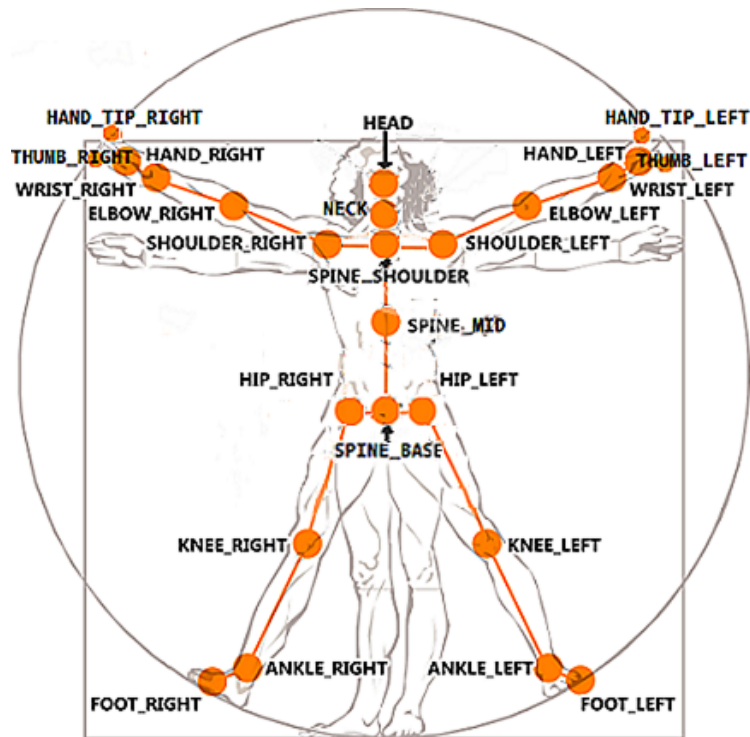


Figure 2.8: **Diagram of skeletons generated by Kinect.** This figure details the 25 joints of the Kinect skeleton model

Kinect camera (Azure Kinect) has the ability to create arrays of cameras as an intrinsic function, so this area of research might see some renewed interest.

The use of a single camera also creates issues with tracking accuracy. Skeleton joints that are close to 0° from the centre of the depth sensor are very well tracked. Joints that are away from this axis are tracked less well.

The Kinect estimates joint positions using a random forest model. If a Kinect camera comes across a pose that is very different from the ones it was trained on, it can become confused. This is evident in the tracking of crossed arms during sit to stand.

2.7 Comparison, Between Kinect and Marker-based Systems

Several studies have compared the tracking of clinical movements between Kinect and VICON [41, 71, 178, 32]. They conclude that Kinect has potential use in a clinical setting while pointing to the issues discussed in 2.6. However, these insights have not translated into practical applications. In addition, the

majority of research considers young and older groups, but not populations of older fallers.

2.8 Kinect and Human Action Recognition

Perhaps the most common use of Kinect in research is in [Human Action Recognition \(HAR\)](#). HAR has been an area of research for many years. Before the advent of inexpensive depth cameras, HAR relied on RGB images. The predominant method for tracking human movement was through the analysis of spatio-temporal volumes [267, 271]. By identifying elements that move relative to a static background, motion silhouettes can be extracted. However, these methods are badly affected by changes in light intensity, between frames. Depth images do not suffer such issues as they are invariant to lighting conditions. Kinect V1 was introduced in 2011, followed by Kinect V2 in 2014 and Kinect V3 in 2020. In short order, after the initial release, many HAR datasets were recorded and made available. Firman et al. [66] detailed 44 HAR datasets, recorded using Kinect. NTU RGB+D [211] was listed as the largest, containing 4 million frames of data, collected from 40 distinct subjects carrying out 60 different movements. The same group (ROSE lab at the Nanyang Technological University, Singapore) updated the dataset in 2019 to contain 120 action classes [135]. These datasets have now become the standard for benchmarking new methods of HAR [113, 254, 212, 227]. Unfortunately, there has not been a similar proliferation in clinical datasets. That said, Kinect's use, in relation to health applications, has been explored. These applications include gait assessment, detection of falls, rehabilitation, and falls-risk assessment. The next section of this thesis will explore these one-by-one.

2.9 Gait Assessment

Healthy human gait has a symmetrical, alternating gait pattern of stance and swing phases, with a phase lag of 0.5. This phase lag means that as one limb reaches the midpoint of its cycle, the other limb is beginning its own cycle, shown in Figure 2.9A. One gait cycle is, generally, counted as one heel contact, to the next heel contact, for a single leg. The distance covered is the person's stride length. The stance phase begins when the foot hits the ground, and the swing phase begins when the foot leaves the ground (toe-off). In normal

adult-gait, 60% of the time is spent in stance phase and 40% in swing phase. Stance phase can be further split into double-support phase, (the first and last 10% of the stance phase, when both feet are in contact with the ground) and single support phase (when the opposing limb is swinging) [206]

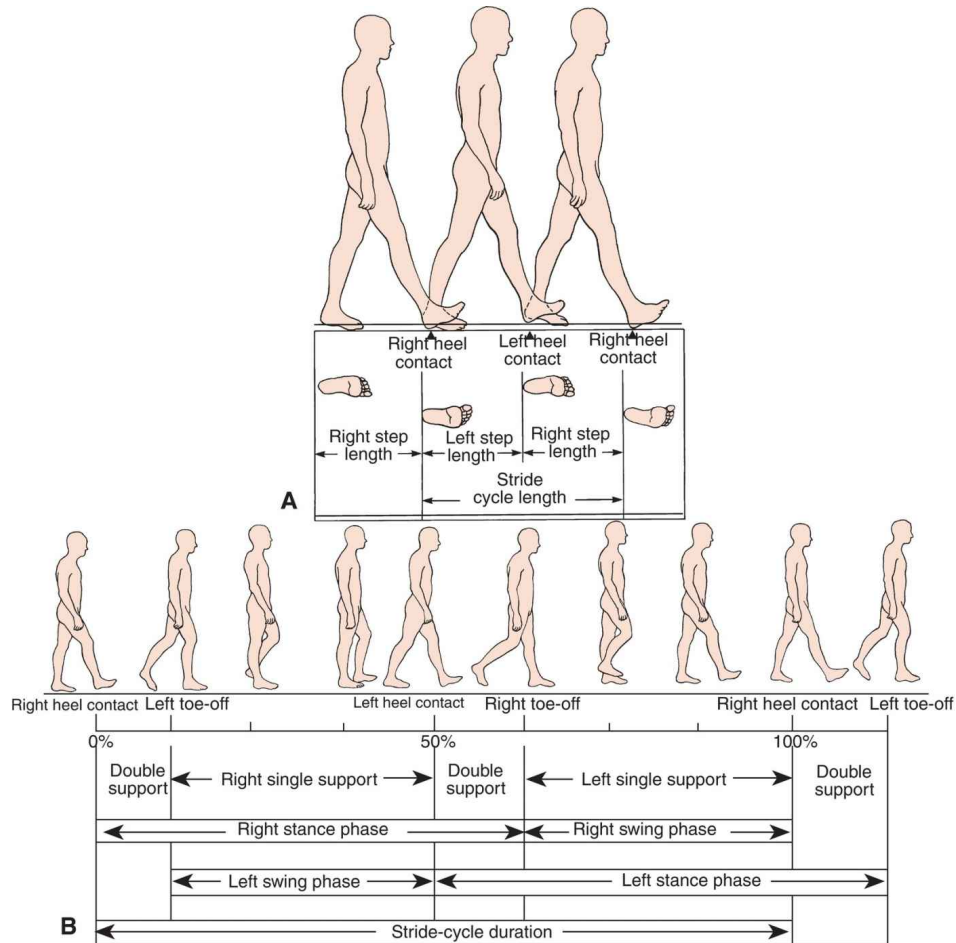


Figure 2.9: **Gait cycle:** A. Step length and stride length characteristics. B phases of the gait cycle (reproduced from [218])

Stance and swing phases can also be labelled as follows: Stance: 1) initial contact, 2) loading response, 3) mid stance, 4) terminal stance, 5) preswing. Swing: 1) initial swing, 2) mid swing, 3) terminal swing see Figure 2.10.

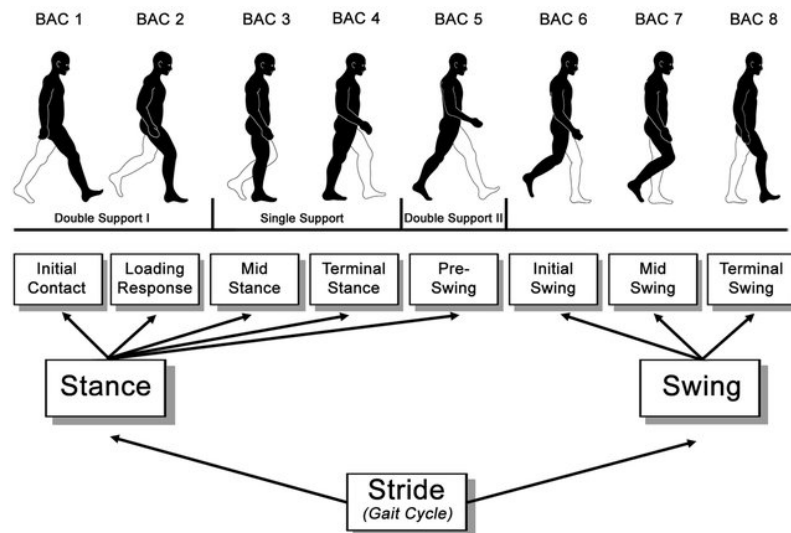


Figure 2.10: **Sub-phases of gait:** this figure show the sup-phases of gait, in relation to a single stride (reproduced from [231])

As touched on above, distance and temporal (spatio-temporal) metrics can be derived from the gait cycle. A selection of common metric is shown below. However, many more can be derived from the gait cycle and step cycle (Figures 2.9))

- **Velocity:** defined in its typical form found elsewhere, i.e. distance moved in a given time (m/s)
- **Cadence:** number of steps, taken in a given time (steps/min) (step frequency).
- **Step length:** the distance covered, between one foot strike to the alternate foot strike (m).
- **step width:** the distance between the mid line of the left and right heel (cm)
- **Stride length:** the distance covered, between one foot strike and the next, on the same foot (m).
- **Step time:** the time taken, between one foot strike to the alternate foot strike (s).
- **Stride time:** the time taken, between one foot strike and the next, on the same foot (s).
- **Stance time:** the time spent in stance phase (s)
- **Swing time:** the time spent in swing phase (s)
- **Double support time:** the time spent in double support (s)
- **Single support time:** the time spent in single support (s)

Kinematic measures can also be considered. Kinematics is the study of the geometry of motion. When applied to the human body, kinematics considers the movement of the body's joints throughout the gait cycle. Figure 2.11 shows how joint angles change over time during normal walking.

The use of spatio-temporal and kinematic metrics to assess abnormal gait, is discussed below.

Gait variability has, for a long time, been associated with increased falls-risk [7, 93, 30, 184]. Hausdorff et al. [93] suggested that a stride time variability

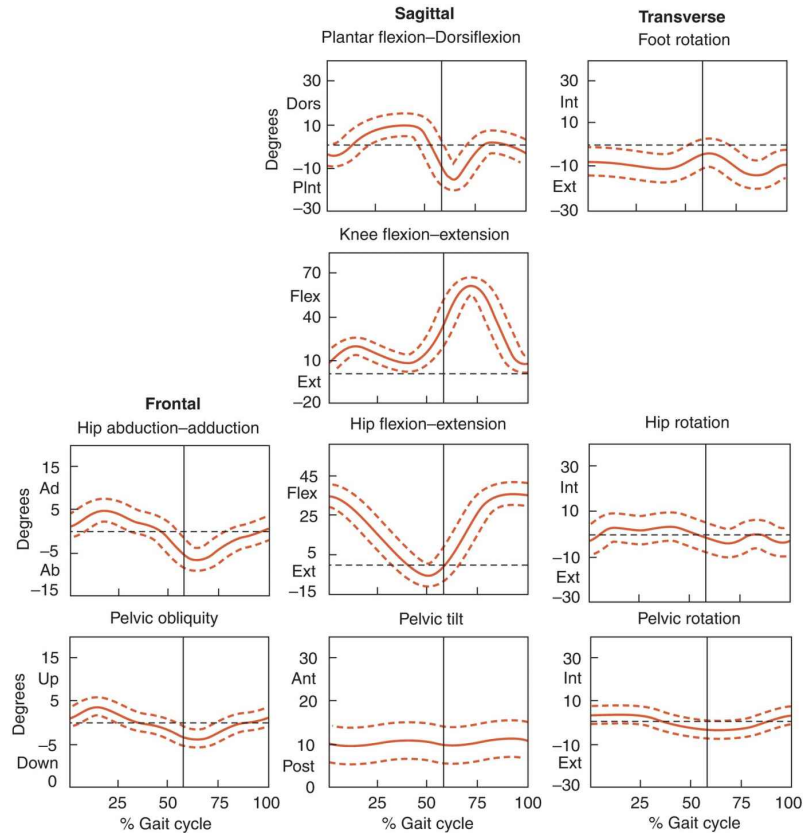


Figure 2.11: **Kinematics of gait:** this figure show the normal movement of the foot(ankle), knee, hip and pelvis throughout the gait cycle toe-off is marked with a solid vertical line (reproduced from [218])

of 106 ± 30 ms was indicative of future fallers, vs a stride time variability of 49 ± 4 ms for non-fallers. They went on to use logistic regression to predict fallers, in a cohort of 52 individuals. In their paper stride time and swing time were calculated from data collected using force-sensitive insoles, on a level, 6 minute walk, or as long as possible. Callisaya et al. [30] showed a similar result for step-time variability, in a much larger cohort ($n=411$). In addition, they found a relationship between falls risk and variability in the length of the Double Stance Phase (DSP). The data was collected from a 4.6 m computerised walkway. Follow-up questionnaires were posted out every two months, to record new falls. Interestingly, they noted that neither of these measures were associated with the risk of a single fall. This finding is in line with previous work [170, 138].

Gait metrics can also be derived from recordings made with the Kinect. Stone et al. [232] used Kinect V1 in a proof-of-concept, to demonstrate that gait velocity and stride-to-stride variation in velocity could be calculated in

the lab, using Kinect. A year later, he showed that Kinect could be used to continuously monitor gait in the home [233].

Dubois et al. [60], found good agreement between spatio-temporal metrics calculated from Kinect and a smart carpet (a device similar to the smart walkway, used in [30]). They used the background extraction method, described in [59], to estimate the CoM. The method utilises the raw depth data and uses the running average method [78] to identify the mobile pixels, which move relative to the static background. The CoM was calculated by averaging all the points belonging to the mobile object. The paper does not detail how well the calculated CoM relates to an anatomically correct CoM. However, it did allow them to create graphs of relative CoM displacement in the vertical and horizontal directions.

Using the vertical component of the estimated CoM, they were able to calculate the step length by measuring the distance between the maxima of the vertical com displacement. Measuring the time taken between steps also provided the step time. The speed was calculated as the time taken to travel across the cameras field-of-view, see Figure 2.12. The number of steps recorded was between 2-5 steps. This was due to the field-of-view of the Kinect camera, which is a major drawback to using a single Kinect camera for gait analysis.

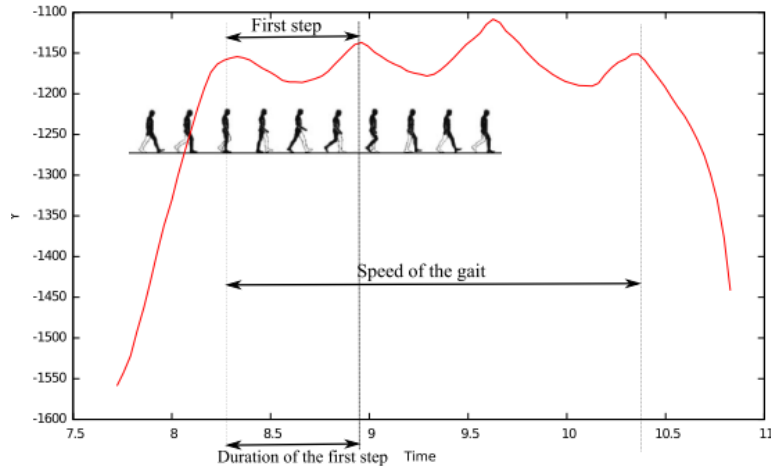


Figure 2.12: **Gait features, extracted from Kinect:** By tracking the vertical component of the CoM, estimated from the Kinect depth stream. step length, step time, and gait speed were calculated (reproduced from [60])

Dolatabadi et al. [55] wrote a case study detailing how they used features derived from Kinect to unobtrusively monitor recovery from hip replacement,

Table 2.2: **Results from [60]:** The results show % difference between gait metrics derived from the smart carpet and the Kinect, assuming the smart carpet to be the ground truth

	mean % error (SD)
Step Length	4.5 (3.8)
Step Time	6.6 (4.9)
Speed	3.69 (1.81)

in the home. Using the skeletal data from the Kinect (captured while walking towards the camera) they used the ankle joint to establish when the foot was in stance or in swing phase. From this data they calculated step length, stance time, stride length and cadence. Using this data, they were able to demonstrate a loss of function after surgery which returns and then exceeds the pre-surgery values within 9 weeks.

Now gaining popularity, for lab-based studies, a whole range of papers were published comparing kinematic, as well as spatio-temporal metrics, calculated from Kinect and marker-based systems (usually, though not exclusively VICON). e.g. [152, 64]

Mentiplay et al. [152] compared gait metrics, calculated from Kinect recordings to gait metrics captured by VICON and processed through 3DMA. Speed variability, step length, step time, step width, foot swing velocity metrics were compared. Along with, medial-lateral and vertical pelvis displacement, ankle flexion, knee flexion, knee adduction and hip flexion angles. The Kinect camera was placed in front of the participant (frontal-plane-view). The results are presented in Figure reffig:Mentiplay2015. They considered the relative agreement between devices and the inter-day reliability of each device. Both comfortable paced walking and fast-paced walking were considered. They, on the whole, found the spatio-temporal metrics had excellent relative agreement ($r > 0.75$) for both walking speeds. Except for fast-paced gait speed variability ($r > 0.73$) and mediolateral pelvis sway ($r > 0.45-0.46$), which should be considered modest agreement. They also found similar levels of inter-day reliability for the spatio-temporal metrics, calculated from both devices. When it came to the kinematic metrics, poor to week relative agreement was seen ($r < 0.50$).

Their discussion suggests some reason for the disagreement when in the Kinematic results. They point to the fact that it is difficult to compare systems that use different marker sets. They also note that the frontal position of

the Kinect is an optimal choice for collecting spatio-temporal data but may disadvantage the collection of kinematic data.

Figure 2.13: A comparison spatio-temporal and kinematic variables during the gait cycle, between the output of a Kinect camera and a 3DMA motion capture system (reproduced from [152]) Results are shown for conformable and fast paced walking. The validity column shows agreement between devices. The reliability columns show the reliability of each device, between days

Gait parameters	Day 1		Day 2		Validity		Kinect reliability		3DMA reliability			
	Kinect	3DMA	Kinect	3DMA	r	rc	ICC	SEM % ^a	ICC	SEM % ^a	ICC	SEM % ^a
Comfortable pace												
<i>Spatiotemporal variables</i>												
Gait velocity (m/s)	1.26±0.12	1.25±0.13	1.30±0.13	1.28±0.13	0.99	0.90	0.75 (0.53,0.88)	4.8	0.86	0.76 (0.53,0.88)	5.1	0.86
Gait velocity variability (m/s)	0.19±0.05	0.15±0.04	0.19±0.04	0.15±0.03	0.75	0.00	0.76 (0.55,0.88)	12.9	0.87	0.80 (0.61,0.91)	11.9	0.89
Ground contact time (s)	0.44±0.06	0.41±0.06	0.45±0.06	0.41±0.05	0.91	0.90	0.03 (-0.37,0.42)	13.4	0.06	0.21 (-0.21,0.56)	13.0	0.34
Step width (m)	0.13±0.03	0.19±0.03	0.13±0.02	0.20±0.03	0.94	0.00	0.71 (0.45,0.86)	12.4	0.83	0.79 (0.58,0.90)	7.2	0.88
Step time (s)	0.51±0.04	0.51±0.04	0.51±0.04	0.52±0.04	0.92	0.75	0.70 (0.45, 0.85)	4.3	0.83	0.71 (0.47,0.86)	4.2	0.83
Step length (m)	0.66±0.07	0.68±0.06	0.67±0.06	0.68±0.06	0.90	0.13	0.87 (0.75,0.94)	3.8	0.93	0.85 (0.71,0.93)	3.4	0.92
Pelvis ML range (cm)	4.39±1.05	3.62±1.05	4.64±1.15	3.58±1.04	0.45	0.00	0.55 (0.23,0.77)	16.8	0.72	0.63 (0.34,0.81)	15.2	0.77
Pelvis vertical range (cm)	4.53±0.96	3.86±0.96	4.67±0.79	3.94±0.81	0.87	0.00	0.76 (0.55,0.89)	9.8	0.87	0.84 (0.68,0.92)	10.0	0.91
Foot swing velocity (m/s)	3.84±0.35	4.33±0.40	3.94±0.40	4.40±0.38	0.79	0.11	0.72 (0.49,0.86)	4.8	0.84	0.66(0.39,0.83)	5.4	0.80
<i>Kinematic variables</i>												
Peak knee flexion-swing (deg)	30+3	67+5	31+3	66+5	-0.05	-0.02	0.85 (0.71,0.93)	3.9	0.92	0.79 (0.57,0.90)	3.4	0.88
Peak knee flexion-contact (deg)	26+4	16+4	26+3	18+5	-0.01	-0.01	0.72 (0.48,0.86)	8.1	0.84	0.58 (0.24,0.79)	16.2	0.73
Peak knee adduction-contact (deg)	4+3	3+5	4+3	2+4	-0.07	0.00	0.69 (0.42,0.84)	41.8	0.81	0.91 (0.81,0.96)	50.0	0.95
Total ankle flexion range (deg)	40+34	33+7	36+25	34+5	0.11	0.01	0.42 (0.02,0.71)	62.8	0.60	0.75 (0.51,0.88)	10.6	0.86
Hip flexion range (deg)	74+23	44+6	76+23	43+5	0.49	0.08	-0.10 (-0.57,0.42)	32.6	-0.23	0.55 (0.16,0.80)	9.1	0.71
Fast paced												
<i>Spatiotemporal variables</i>												
Gait velocity (m/s)	1.64±0.13	1.64±0.12	1.62±0.13	1.62±0.13	0.96	0.83	0.77 (0.54,0.89)	3.8	0.87	0.79 (0.89,0.90)	3.4	0.88
Gait velocity variability (m/s)	0.27±0.05	0.18±0.05	0.26±0.05	0.18±0.04	0.73	0.00	0.67 (0.38,0.84)	10.6	0.80	0.74 (0.50,0.87)	14.2	0.85
Ground contact time (s)	0.34±0.07	0.29±0.06	0.37±0.05	0.32±0.06	0.94	0.90	0.43 (0.04,0.71)	15.5	0.60	0.47 (0.07,0.74)	15.1	0.64
Step width (m)	0.13±0.02	0.20±0.03	0.13±0.03	0.20±0.03	0.92	0.00	0.74 (0.49,0.87)	7.8	0.85	0.78 (0.58,0.90)	7.0	0.88
Step time (s)	0.47±0.04	0.46±0.04	0.46±0.04	0.46±0.04	0.88	0.06	0.87 (0.74,0.94)	3.1	0.93	0.90 (0.80,0.96)	2.7	0.95
Step length (m)	0.80±0.08	0.80±0.07	0.78±0.07	0.78±0.07	0.95	0.88	0.94 (0.87,0.97)	2.4	0.97	0.85 (0.69,0.93)	3.4	0.92
Pelvis ML range (cm)	3.57±1.02	4.58±1.28	3.22±1.07	4.49±1.33	0.46	0.00	0.68 (0.41,0.84)	11.3	0.81	0.64 (0.35,0.82)	15.0	0.78
Pelvis vertical range (cm)	3.90±1.00	4.49±1.04	3.95±0.87	4.45±0.98	0.81	0.00	0.82 (0.64,0.91)	10.6	0.90	0.94 (0.88,0.97)	6.1	0.97
Foot swing velocity (m/s)	4.97±0.43	5.46±0.40	4.93±0.52	5.40±0.47	0.88	0.18	0.58 (0.26,0.79)	5.6	0.74	0.68 (0.40,0.84)	4.1	0.81
<i>Kinematic variables</i>												
Peak knee flexion-swing (deg)	33+4	69+5	33+3	67+5	-0.30	-0.09	0.75 (0.52,0.88)	6.1	0.86	0.63 (0.31,0.82)	4.4	0.77
Peak knee flexion-contact (deg)	28+4	20+4	29+6	18+5	-0.17	-0.19	0.56 (0.22,0.77)	9.5	0.72	0.57 (0.22,0.79)	13.1	0.73
Peak knee adduction-contact (deg)	5+4	3+5	5+3	2+4	0.23	0.01	0.38 (0.00,0.67)	63.0	0.55	0.88 (0.74,0.95)	57.7	0.94
Total ankle flexion range (deg)	41+28	32+5	44+33	32+6	-0.26	-0.02	0.44 (-0.04,0.75)	51.1	0.61	0.68 (0.38,0.85)	8.8	0.81
Hip flexion range (deg)	75+35	53+7	66+15	54+8	0.17	0.01	0.23 (-0.40,0.71)	40.9	0.38	0.34 (-0.05,0.64)	10.7	0.50

Eltoukhy et al., [64] compared recordings of healthy individuals walking on a treadmill at a comfortable pace, captured using Kinect V2 and the SMART-DX 7000 (BTS Italy) marker-based system. The Kinect camera was placed perpendicular to the subjects (sagittal-plane-view). This position favours the capturing of Kinematic data. This set up removed the issue of the small field-of-view of the Kinect camera but introduced the reliance on a large and expensive piece of equipment. They compared step length, step width, medio-lateral and vertical pelvic displacement, step time, stride time, and foot swing

velocity (spatio-temporal). Hip, knee, and ankle joint angles in the sagittal plane (kinematic). The results of this paper are shown in Figure 2.14.

Figure 2.14: A comparison kinematic and spatio-temporal variables during the walking gait cycle, between Kinect and SMART-DX 7000 (BTS Italy) motion capture system (reproduced from [64]) There is good agreement in Spatio-temporal measures between the two devices, along with Hip and knee ROM. However, ankle joints are less well tracked.

	Gait Speed	BTS System Mean \pm SD	Kinect System Mean \pm SD	p-value	Absolute Error	Relative Error	Agreement ICC (95%CI)	Consistency ICC (95%CI)	Correlation r (95%CI)	Concordance rc (95%CI)
Total Hip ROM (deg)	1.3 m/s	44.39 \pm 3.29	46.44 \pm 3.38	0.03*	2.67 \pm 1.65	-2.05 \pm 2.45	0.77 (0.05-0.95)	0.85 (0.38-0.96)	0.73 \dagger (0.17-1.25)	0.61 (0.13-0.86)
	1.6 m/s	47.42 \pm 4.06	49.69 \pm 3.71	0.03*	2.75 \pm 2.13	-2.27 \pm 2.69	0.80 (0.10-0.95)	0.86 (0.45-0.97)	0.77 \dagger (0.26-1.42)	0.64 (0.17-0.87)
Total Knee ROM (deg)	1.3 m/s	64.53 \pm 3.46	64.57 \pm 1.94	0.96	2.14 \pm 1.73	-0.04 \pm 2.84	0.68 (-0.45-0.92)	0.66 (-0.39-0.91)	0.57 (-0.17-2.21)	0.49 (-0.02-0.80)
	1.6 m/s	66.08 \pm 4.89	64.49 \pm 3.24	0.16	2.80 \pm 2.16	1.59 \pm 3.26	0.80 (0.26-0.95)	0.82 (0.27-0.96)	0.75 \dagger (0.32-1.95)	0.64 (0.20-0.87)
Total Ankle ROM (deg)	1.3 m/s	30.68 \pm 5.56	10.92 \pm 2.31	<0.001*	19.76 \pm 5.67	19.76 \pm 5.67	0.05 (-2.84-0.76)	0.01 (-0.06-0.20)	0.03 (-1.78-1.93)	0.01 (-0.03-0.03)
	1.6 m/s	31.22 \pm 5.33	10.58 \pm 2.44	<0.001*	20.63 \pm 6.32	20.63 \pm 6.32	-0.03 (-0.09-0.19)	-0.39 (-4.60-0.65)	-0.22 (-2.20-1.26)	-0.01 (-0.05-0.03)
Vertical Pelvis Motion (cm)	1.3 m/s	4.03 \pm 0.54	4.13 \pm 0.79	0.52	0.38 \pm 0.33	-0.11 \pm 0.51	0.84 (0.37-0.96)	0.83 (0.33-0.96)	0.77 \dagger (0.17-0.89)	0.71 (0.28-0.90)
	1.6 m/s	4.92 \pm 0.70	4.74 \pm 0.99	0.42	0.49 \pm 0.45	0.17 \pm 0.66	0.83 (0.35-0.96)	0.83 (0.30-0.96)	0.75 \dagger (0.15-0.92)	0.69 (0.24-0.90)
Mediolateral Pelvis Motion (cm)	1.3 m/s	4.38 \pm 0.53	4.01 \pm 0.79	0.02*	0.43 \pm 0.33	0.37 \pm 0.40	0.84 (0.14-0.96)	0.90 (0.60-0.98)	0.89 \dagger (0.34-0.85)	0.70 (0.35-0.88)
	1.6 m/s	4.66 \pm 0.80	4.53 \pm 0.95	0.45	0.44 \pm 0.28	0.13 \pm 0.52	0.91 (0.63-0.98)	0.90 (0.61-0.98)	0.83 \dagger (0.32-1.08)	0.52 (0.44-0.95)
Foot Swing Velocity (m s ⁻¹)	1.3 m/s	2.97 \pm 0.13	2.53 \pm 0.16	<0.001*	0.43 \pm 0.16	0.43 \pm 0.16	0.11 (-0.10-0.51)	0.51 (-0.98-0.88)	0.35 (-0.33-0.89)	0.05 (-0.06-0.17)
	1.6 m/s	3.23 \pm 0.12	2.71 \pm 0.17	<0.001*	0.52 \pm 0.14	0.52 \pm 0.14	0.14 (-0.06-0.55)	0.72 (-0.14-0.93)	0.60 \dagger (-0.40-0.86)	0.71 (-0.02-0.16)
Step Length (m)	1.3 m/s	0.87 \pm 0.11	0.77 \pm 0.08	<0.001*	0.10 \pm 0.05	0.10 \pm 0.05	0.76 (-0.17-0.95)	0.94 (0.76-0.99)	0.93 \dagger (0.84-1.65)	0.58 (0.31-0.76)
	1.6 m/s	0.90 \pm 0.11	0.80 \pm 0.07	<0.001*	0.09 \pm 0.06	0.09 \pm 0.06	0.67 (-0.26-0.93)	0.87 (0.48-0.97)	0.84 \dagger (0.62-1.96)	0.48 (0.13-0.72)
Step Width (m)	1.3 m/s	0.21 \pm 0.03	0.17 \pm 0.03	<0.001*	0.04 \pm 0.02	0.04 \pm 0.02	0.84 (0.35-0.96)	0.58 (-0.25-0.90)	0.73 \dagger (0.15-1.15)	0.38 (0.02-0.65)
	1.6 m/s	0.21 \pm 0.04	0.17 \pm 0.04	<0.001*	0.04 \pm 0.02	0.04 \pm 0.02	0.71 (-0.13-0.94)	0.95 (0.78-0.99)	0.91 \dagger (0.64-1.43)	0.52 (0.19-0.75)
Step Time (s)	1.3 m/s	0.54 \pm 0.02	0.56 \pm 0.03	<0.001*	0.02 \pm 0.01	-0.02 \pm 0.01	0.87 (-0.16-0.98)	0.96 (0.85-0.99)	0.96 \dagger (0.56-0.93)	0.75 (0.46-0.89)
	1.6 m/s	0.51 \pm 0.03	0.53 \pm 0.03	<0.001*	0.03 \pm 0.01	-0.03 \pm 0.01	0.82 (-0.13-0.97)	0.97 (0.88-0.99)	0.95 \dagger (0.76-1.34)	0.67 (0.35-0.85)
Stride Time (s)	1.3 m/s	1.05 \pm 0.04	1.05 \pm 0.05	0.88	0.01 \pm 0.01	0.00 \pm 0.01	0.98 (0.94-0.99)	0.98 (0.93-0.99)	0.97 \dagger (0.71-1.08)	0.97 (0.90-0.99)
	1.6 m/s	0.98 \pm 0.04	0.98 \pm 0.05	0.88	0.01 \pm 0.02	0.00 \pm 0.02	0.94 (0.74-0.98)	0.93 (0.72-0.98)	0.93 \dagger (0.43-0.85)	0.87 (0.68-0.95)

ROM = range of motion, deg = °, * significant between system difference ($p \leq 0.05$), \dagger indicates a significant correlation ($p \leq 0.05$).

The results of this paper showed acceptable agreement for Hip and Knee ROM. However, Kinect shows difficulty in tracking ankle joints, leaving kinematic analysis with Kinect somewhat limited. In addition, the agreement for the spatio-temporal metrics is adversely affected by the placement of the Kinect when compared to values obtained from [152].

Although Kinect might not be a suitable alternative to marker-based solutions for classic kinematic gait analysis, the spatio-temporal metrics could be enough to assess falls risk [7, 93, 30, 184]. However, the assessment of gait requires significantly more space to assess than other types of assessment, e.g. quiet standing and STS-5. In addition, the limited field-of-view [60] and depth-of-view [55] means only a hand-full of steps can be assessed. Moreover,

when the subject is at the extent of the Kinect's range, joint tracking is less accurate or may disappear altogether. It is for these reasons that the research detailed in this thesis did not use gait data in falls-risk analysis.

Rather than focusing on the innate differences between Kinect and other devices, a more constructive approach is to look at Kinect as a unique device that can provide a means of assessing movement quality in situations where other devices struggle. If one allies Kinect's abilities to machine learning, the product is a system that can provide new methods of assessing falls risk. The following section looks at the application of machine learning to gait.

The application of machine intelligence to gait assessment

The most fundamental implementation of machine intelligence is the application of a heuristic approach. Essentially, getting a machine to apply a set of pre-defined rules. Bigy et al. [17] applied heuristics to detect [Freeze of Gait \(FoG\)](#), a problematic symptom of Parkinson’s disease (in addition to falls and tremors). The rules-based approach is computationally undemanding, which makes this easily applied in real-time.

Moving away from rules-based solutions, Tupa et al. [273], used a shallow [Artificial Neural Network \(ANN\)](#) to identify individuals with Parkinson’s disease from gait characteristics. Using the same dataset, Prochazka et al. [191] achieved similar results by using a Bayesian Classifier.

Gabel et al. [70], extracted a feature set which expanded on gait analysis to include arm kinematics and additional body features, namely, COM, Direction of Progress and Acceleration. A state model was used to partition the gait cycle, and [Multiple Additive Regression Trees \(MART\)](#) was used to calculate the features. However, machine learning was not used to produce a predictive model for gait quality

2.10 Falls Detection

As discussed, falls are commonplace in elderly populations. The risks associated with someone who has fallen are compounded if that person is unable to get up from the floor [241]. Hence much research time has been spent on building falls detection systems.

The non-intrusive nature of Kinect, not having to wear a device, such as an accelerometer, makes it an appealing choice for this application. From the start, rules-based solutions were present, and soon machine models came in to use. Mastorakis et al. [146] used a two-stage process for falls detection, using Kinect depth images. In the first phase, the vertical-velocity between frames was used to detect a possible fall. However, the alarm was only raised if this event is followed by a period of inactivity. Stone et al. [234] refine this process by using an ensemble of binary decision trees to classify the period of inactivity, so guarding against false positives from events such as sitting down quickly. Although achieving high accuracy in the lab, this type of system

has not been extensively trialled in the home, a fundamental limitation being Kinect's range (0.4 - 3.5m).

To address this issue, Kalinga et al. [108] attached a Kinect camera to a service robot that is able to follow the person at risk, room to room. They also used the skeleton data in preference to the raw depth frames. This enabled them to develop the classification abilities of their system. Their system is able to identify three classes of post-fall events, prone, crawl and kneel. Fall detection systems also bring up an ethical problem. How do you validate your predictions on those most at risk? The usual solution is to use young, fit people to pretend to be old. However, this raises a problem of its own, how similar is the accidental fall of a frail person to the self-initiated fall of a young person?

On the other hand, it is difficult to justify asking vulnerable people to fall over in the lab in the hope of helping people just like them at some point in the future. Alternatively, you could install devices into a care home and wait for people to fall. Leaving a frail person on the floor to validate a crawl classifier seems unreasonably cruel. Necessarily, ethical issues like this have limited this area of research.

2.11 Rehabilitation

In rehabilitation, perhaps the most obvious use of Kinect is as a games controller. Exergames, are games designed to aid the repetition of exercise, which, while essential for recovery, can quickly become dull, and so compliance is notoriously low. This use of Kinect is sometimes referred to as the gamification of physiotherapy [37, 139, 176, 222, 236, 122]. As well as aiding compliance, it reduces the strain on physiotherapist staff, which frees them up to do more demanding work. All the studies reported improvements in both compliance and the patient's condition.

Away from gaming, Gonzalez-Ortega et al. [79] built a system that used a combination of Kinect and an RGB camera to automate the process of taking measurements needed to perform a cognitive test on patients with a wide range of brain damage issues.

Lin et al. [133] used a heuristic, template matching system to assess static Tai Chi poses. The patients pose was extracted from Kinect as a set of joints and Angles. The pose was then compared to and a template (a teacher with

the perfect pose), using 0-2 scoring system. If all joints and angles were perfect, the score would be 0, if both joints and angles exceed a threshold, the score was 2. The paper does not say what threshold they used. However, this approach reveals a fundamental truth that small changes in body position are a normal aspect of human pose.

Capecci et al. [32], worked with clinicians and used Kinect to record a set of exercises routinely used in the rehabilitation from back pain. From the recordings, they created a set of clinically relevant features based on both joint angles and joint distances. They validated the Kinect recording with a six-camera motion capture system and found good agreement between the two systems. This work was later developed into the KIMORE dataset [34].

2.12 Assessment of Balance and falls-risk

The assessment of falls-risk with Kinect has been considered using different movement types. Kargar et al. [111], used a combination of traditional gait metrics (step duration, turning duration, number of steps) and anatomical metrics (knee angle, leg angle and distance between elbows) as features to train an SVM which was able to identify those at high risk of falls. Gianaria et al. [77], found a correlation between scores on a frailty index and several gait metrics. They also found a correlation between falls-risk and variability in the torso angle while walking.

Others have chosen to automate pre-existing tests or gain new insights from commonly used clinical tests. Garcia et al. [73] demonstrated the potential use of Kinect in place of an instrumented mat for the Choice Stepping Reaction Time (CSRT). They demonstrated a similarity of results between the two devices. However, this work used healthy volunteers and was not validated with potential fallers.

Ejupi et al. [61] used Kinect to record the 5x sit-to-stand of 79 participants. In the non-instrumented assessment of falls-risk, the Sit-to-stand test gives a good indication of lower body muscle function, i.e. sarcopenia, a key element in the cycle of frailty (see Figure 1.1). As such, it has been shown that slow chair rise is associated with falls-risk [256]. Ejupi et al. found the mean velocity of the sit-to-stand transitions discriminated well between fallers and non-fallers.

Another common, non-instrumented test is TUG. TUG combines Sit-to-stand with gait. Various studies have automated both of these tests. [91]

Considered the TUG test. They segmented the sit-to-stand portions of the TUG test of young and older participants using an SVM. They then extracted three features, shoulder path curvature, trunk angle movement duration, as well as the traditional TUG duration. Using these features, they were able to show differences between the young and old populations but did not consider the population of fallers.

In this thesis, the use of STS-5 and postural sway metrics (derived from Kinect data rather than force plates), are used in the assessment of falls-risk. These tests were selected because they can be carried out using less space than gait-related tests.

2.13 Working with Skeletal Data

When considering the application of skeletal data for balance assessment, CoM is an attractive way to represent upright balance. CoM provides everything you would wish for in a representation. It is compact and explainable. i.e. it elegantly reduces the high dimensional data into a low dimensional representation that is easy to understand and interpret.

In any consideration of representation, there is a tension between hand-crafted features, automatically extracted features and explainability. This can be thought of as a scale where, on the extreme right is automatically extracted features, which can work well but are difficult to explain (the black box of deep learning) and on the other linear regression of two easily understood metrics, e.g. weight and [Body Mass Index \(BMI\)](#), which can be represented by a straight line.

Added to this conundrum is the curse of dimensionality. How much data is required to explain the difference you are looking for? As discussed in [Section 2.2](#). The jointed structure of the human skeleton means that it has inherent redundancy. This means the same movement can be achieved in different ways. So how does one identify the significant dis-coordinations, which are the physical signs of frailty?

Raptis et al. [\[197\]](#) noted that the joints of the torso have very strong correlations. By applying [Principal Component Analysis \(PCA\)](#), as a linear form of dimensionality reduction, they were able to reduce the seven joints of the torso to a 3-dimensional vector, which they called the torso basis. Using the torso basis as an origin point, they created a hierarchy of joints, related

by their spherical coordinates. Joints directly connected to the torso, e.g. elbow and knee, were called first-level joints and second level joints were those joints attached to the first level joints, e.g. ankle and wrist. Head, hands and feet were ignored. This generated 8×2 joint angles. This feature set is invariant to the orientation of the camera and the individual, as it uses local angles between joints as descriptors of movements, independent of the global frame of reference. Miranda[156] refined this feature set to include the torso inclination. This feature set achieved high recognition accuracy for a set of well defined and large gestural movements.

In their work, related to the machine-evaluation of a dancer’s performance, Alexiadis et al. [3] temporally align the movements of amateur dancers with ground truth provided by professionals. Inspired by this work, Su et al. [235] developed a system which uses Dynamic [Dynamic Time Warping \(DTW\)](#), a method previously used in relation to handwriting and audio recognition, to compare the movements of patients in their everyday life to a standard set of movements. The aligned sequences were then classified (bad, good, excellent), using an [Adaptive Neuro-Fuzzy Inference System \(ANFIS\)](#) which uses a combination of ANN and fuzzy logic.

A drawback with DTW is that it does not perform well for periodic movements, like waving. To address this issue, Wang et al. [253] proposed the scaling of skeletons to a common standard, e.g. the mean distance between the neck and spine-base joint of all the skeletons in the dataset. This allows for the pair-wise distance between joints to be used as a robust and discriminating feature. Following scaling, all the skeletons in a particular sequence were aligned to the spine mid joint, as you would for any approach that uses local descriptors. Vox et al. [249], suggest that there is an issue with this type of normalisation. It tends to reduce the variance in movement for joints, close to the origin joint. They found that moving the origin to the right-ankle joint improved action recognition when using relative angles as features.

In spite of its criticism, DTW is still used to great effect. Anton et al. [5] applied a template approach to exercise recognition, using three different shoulder rehabilitation exercises, utilising DTW in the process. They scored the quality of the movement by measuring the distance from the template to the recognised movement, using dynamic time warping to align the movement to the template.

In a similar way, Gholami et al. [76] used DTW in the creation of a distance measure to quantify the degree of dissimilarity between the gait cycle of Multiple Sclerosis Patients and healthy patients of a similar age. *A distance approach is useful because it allows for scaling between ideal and severely impaired. Also, distance metrics provide a useful scale to monitor progress following during a course of rehabilitation*

2.14 Automatic Feature Extraction and Representational Models

So far, the use of handcrafted features has been discussed, which, in themselves, can act as dimensional reduction. Along with the explicit use of PCA to reduce the dimension of features with high covariance, i.e. the torso joints. The following section will discuss representational models as 1) a way of modelling the inherent variance in skeleton features 2) the automatic extraction of features from skeleton data.

2.14.1 Automatic Feature Selection

[Convolutional Neural Networks \(CNN\)](#)s have become the de facto means of automatically extracting features, for 2D images, inspired by the brain's visual cortex and pioneered by Yann LeCun [121]. In 2012 an implementation of this technique won the ImageNet competition [116] and sparked the revolution in deep visual computing.

Du et al. [56], used a CNN to extract salient features from stacked vectors of skeleton joint positions that represent a whole movement. To allow the CNN to extract features, the matrix was converted to an image of a set size, thus enabling movements of different lengths to be accommodated. *This type of feature extraction creates features that naturally capture local dependencies which are scale-invariant.*

1D convolutional networks are also possible. The essentials of convolving a filter, learned by backpropagation, is the same as for 2D CNNs. However, the signal and filter have only one dimension. 1D convolutions have found uses in all kinds of signal processing, and it is by recasting human movement as a multi-channel times series problem that allows for the use of 1D CNNs in this context. Chi et al. [39] used data from an array of body-worn accelerometers,

placed on key positions, to train a 1D CNN to classify a series of static and dynamic movements.

2.14.2 Representational Models

As discussed above, a templating approach can be useful in creating distance metrics, which can be used to indicate the severity of a particular condition or to monitor recovery. The downside of the templates, discussed so far is that they have a low tolerance for spatio-temporal variation within movements. Unfortunately, this is a key characteristic of human movement.

To address this issue, one can build models which learn their own internal representation of the essence of the variation. Once trained, these models can be used, in inference instead of the input data, so making the over-all system more robust.

Houmanfar et al. [101] demonstrated the use of a [Hidden Markov Model \(HMM\)](#) model to calculate a distance score between healthy individuals and those who had undergone hip or knee surgery. The model was, not only able to quantify the current status, but it was able to track improvements during rehabilitation.

Capecci et al. [33] proposed a [Hidden Semi-Markov Model \(HSMM\)](#) to score the performance of patients during rehabilitation.

In the same year that Du et al. published [56], they also published [57] the paper suggested that splitting the skeleton into five parts (Torso, left and right arms, left and right legs). In their paper, they used a hierarchical [Recursive Neural Network \(RNN\)](#) to model movements at different scales, so combining local and global features into a cohesive map of human movements.

In the sections above, a distinction has been drawn between feature extraction and representation. However, in reality, CNNs build compact representations of inputs, separated by distance or time, depending on how the network and its input are configured. For instance, Zhu et al. [272] proposed an automated method for “data mining” joint co-occurrence, using LSTM Li et al. [132] proposed an alternative system of discovering co-occurrence using CNNs. In this network, the x,y,z positions of the skeleton joints were treated as separate channels, as one might, the three channels of an RGB image. The CNN was able to automatically learn the co-occurrence, between joints.

CNNs and LSTMs, can also work well together, each with a distinctive role. Reyes et al. [198] used a combination of 1D convolutions and [Long Short Term Memory \(LSTM\)](#) to build a model that can differentiate between Parkinson’s Patients and healthy individuals.

2.14.3 Autoencoders

The models, discussed above are trained by supervised methods. However, there is a class of models that are trained in an unsupervised fashion, Autoencoders [26]. They learn a more compact representation of the input by, first encoding the input to a latent vector and then decoding it back to the original input. Although no separate labels are used, hence unsupervised, the network still needs an error signal to train properly. The label used for this type of training is the original input, and it is through the process of backpropagation that the essential features are discovered. Autoencoders can provide a non-linear version of PCA. The compact features (latent vectors) can be used to train separate discriminative models. Alternatively, autoencoders can be considered a model in their own right and can be used directly in inference. This type of model is often used for anomaly detection. Autoencoders, can be constructed from any normal ANN structure, [Multilayer Perceptron \(MLP\)](#), CNN, RNN or a combination.

Vakanski et al. [1], used an LSTM autoencoder to reduce the dimensionality of skeleton data. They then used a mixture density network to produce a log-likelihood score, which they appropriated as a movement quality score.

Jun et al. [107] compared the performance of features extracted from two autoencoders, based on RNN structures (LSTM / [Gated Recurrent Unit \(GRU\)](#)) to raw skeleton data. All three representations were passed to an existing discriminating model. Both sets of features, extracted using the autoencoder, performed better than the raw data. The LSTM autoencoder achieved the best performance.

Butepage et al. [29] proposed an autoencoder that was extensively trained on generic mocap data. They suggested that this model could then be fine-tuned (in the transfer learning sense), to achieve good generalisation with small quantities of specific data.

2.15 Clinical Datasets

As discussed in section 2.8, HAR is leading the way when it comes to new techniques for exploring Kinect data. Jegham et al. [104] provides a good overview of the state-of-the-art, and Firman’s review [66] provides a good idea of the types of dataset available.

While HAR datasets are plentiful, datasets containing recognised Clinical assessments are scarce. To address this gap, the KINECAL dataset was created, detailed in chapter 6. It is hoped that research carried out using the dataset will lead to a range of objective assessments, for balance and movement impairment, which can be carried out away from the lab.

2.16 Machine Learning

In this section, a background to machine learning is presented. Both generic concepts and details of specific techniques are discussed. The application of many of the techniques in this section have already been covered. This section provides a background to accompany what has come before.

2.16.1 Types of Machine Learning

Supervised learning

The task of supervised learning is to estimate a function $f(x)$, which can map an input to an output. During training, this function is learned by comparing pairs of inputs, typically an array or matrix of values, to a label, typically a single value. Once trained, the model can then infer labels from unseen inputs. The labels can be continuous, in the case of regression or discrete, in the case of classification.

The model learns by minimising the distance between the estimates and the labels. The distance provides an error signal and guides the model to find the optimum solution for the training set. The general assumption is that the training set is a good sub-sample of the general population. If the model fits the training data and a wide range of unseen data, it can be said that the model generalises well. Often a regularisation term is added to the optimiser to help the model to generalise better to unseen data.

Unsupervised Learning

Unsupervised learning asks the question “can underlying relationships be discovered through examining the data alone, without the direction of labels.” It essentially is trying to find the probability distribution of $p(x)$. A Classic example of unsupervised learning is clustering. Common techniques include K-Means clustering and Expectation-Maximisation (EM). The fundamental assumption of clustering is that data is not evenly spread across data space. Instead, it clusters into high data-density areas, which contain innately similar things (things belonging to the same class). In between, there are areas of low data density, which is where the decision boundaries lie. Furthermore, the transition from high to low-density regions should be smooth. Training a model on a single class (the normal case) produces a model which can be used in anomaly detection. Any sample that does not fit into the distribution of the normal case can be thought of as being anomalous. This is useful when the event that is to be detected is rare. Moreover, distance metrics can be constructed that quantify how far away from the normal case the detected event lies. This approach is common in bank fraud detection, as new methods of fraud constantly appear.

Principal Component Analysis (PCA) can also be thought of as a form of clustering and so unsupervised learning. The assumption here is that high dimensional data can be projected onto a low-dimensional manifold, thereby capturing the essence of the high-dimensional data while removing redundant elements. PCA achieves this by first calculating the co-variance matrix between all of the high dimensional features, then calculating the eigenvectors (principal components) and associated eigenvalues (magnitude of the eigenvectors) for each dimension. The dimensionality reduction is achieved by keeping only those principal components that explain the majority of the variance between the features. i.e. those with the largest eigenvalues. Graphing the relationship between principal components reveals the clusters.

2.16.2 Machine Learning Algorithms

Bayes' theorem

Broadly speaking, Machine Learning is the ability of a system to make predictions. Modern implementations of machine learning rely on powerful computers, but its origin starts back in the 18th-century when Thomas Bayes

discovered the theory that bears his name, first described in Philosophical Transactions of the Royal Society of London [10]. Bayes' theorem extends basic probability to allow you to change your belief that something will happen based on past events, described as follows:-

- $P(A)$ is the probability of event A occurring
- $P(B)$ is the probability of event B occurring
- $P(A | B)$ is the probability of A occurring given B occurred
- $P(B | A)$ is the probability of B occurring given A occurred
- $P(A,B)$ is the probability of A and B occurring simultaneously (joint probability of A and B)

The joint probability of A and B happening together is

$$P(A, B) = P(A|B) * P(B) = P(B|A) * P(A) \quad (2.1)$$

Which simplifies to

$$P(B | A) = \frac{P(A | B) P(B)}{P(A)} \quad (2.2)$$

This is the classic form of Bayes' Theorem. The power of Bayes' theorem is that you can use iteration to refine your estimates, collecting new data as you go. The posterior probability of one iteration becomes the prior probability for the next round. As you proceed, your estimate gets better. Eventually, your estimate will converge to a stable state. An iterative approach is the basis of most machine learning algorithms

Regression

In 1805 Adrien-Marie Legendre published the least square method for finding the best-fit line through a graph, that defines a linear relationship [123]. This was the first form of regression analysis. Linear regression is still used today but has now been joined by a range of other forms of regression which can take into account a wide variety of non-linearities. Polynomial Regression: Joseph Diaz Gergonne, 1815 [230], Logistic regression: David Cox, 1958 [46], Ridge regression: Hoerl and Kennard, 1970 [98]

Markov Chains

In 1913 Andrey Markov developed the idea of a Markov chain [145]. A Markov chain allows you to make future predictions based on the present state and the likelihood of transitioning to a different state. All of the transitional probabilities are clearly stated.

Hidden Markov Models

In the mid 1960's Baum, Leonard developed the idea of hidden Markov models [9]. In hidden Markov models, the probability of the transition from one state to the next is not known and is not observable directly. However, you can observe the emissions from the system. Hidden Markov Models have been used to model sequence problems like speech recognition and human action recognition. The hidden layers work in a similar way to the hidden layers of a multi layer perceptron, discussed later, and are able to model complex systems.

Perceptrons

Developed by Frank Rosenblatt in 1957 [205]. The perceptron represented a radical departure in inference. Inspired by the networks of organic neurons, in the brains of animals, Rosenblatt constructed ANN using valves. Like modern ANNs, Rosenblatt's ANNs were able to learn mappings from input to outputs, using gradient descent to optimise a set of weights between neurons. He demonstrated how perceptrons could be used as a linear classifier or a linear predictor.

The expectation for this new type of machine learning was high, but research stalled as the perceptron proved difficult to train, especially for more complex problems. In 1969 the idea of building artificial neural networks was all but killed, due to a wilful misinterpretation of Minsky and Papert's book *Perceptrons* [155]. The suggestion was that this type of network could only model linear relationships. Although this is true for single layer perceptrons, the issue goes away when you construct networks of perceptrons with more than one layer, i.e. MLP, a fact recognised by Minsky and Papert at the time. However, the damage was done, and it would be nearly 20 years until the subject was revisited. This is commonly known as the dark ages of neural networks.

2.16.3 Statistical Machine Learning Models

During the years when neural nets were out of favour, statistical forms of machine learning were developing rapidly, K - Nearest Neighbour - 1967 [143], Decision Trees - 1975 [195] , K-mean Clustering - 1982 [136], Bayesian Networks - 1985 [182] , SVM - 1993 [45], Random Forests - 1995 [240]. These methods form the backbone of statistics-based machine learning.

Nearest Neighbour

The Nearest Neighbour algorithm, classifies data based on similarity to a previously classified set of points i.e. clustering. The simple [Nearest Neighbour Search \(NNS\)](#) [115] algorithm was quickly superseded by the [K-Nearest Neighbours \(K-NN\)](#) approach [67]. The K refers to the number of neighbours taken into consideration, so a K of one is just the NNS algorithm, a K of 5 would consider the 5 nearest neighbours. A new data point is classified based on the majority rule. The K value is usually arrived at either by trial and error or by using the elbow method [237].

K-mean Clustering

To some extent, K-mean clustering can be seen as an extension of the K-NN approach. The term was first coined by Mac Queen in 1967 [143]. K-mean clustering tries to assign new data to an existing partition based on the mean value or centroid of the existing partitions (to start with, these mean values are randomly generated). However, each assignment is then followed by an update step in which the centroids are updated, in light of the new data. K-mean came to prominence in the 1980s after Stewart Lloyd published the accepted method for determining k-means clustering in 1982 [136]. Although, a similar method was published by Forgy in 1965 [69].

Decision Trees

Decision trees were first described by Ross Quinlan in 1975, in the book *Machine Learning*, vol. 1, no. 1. [195] The first formal publishing of the ID3 method of constructing Decision Trees was published in 1986 [194]. This method was then superseded by the C4.5 method [196]. The method essentially recursively applies 2 rules. Given a set of X cases 1) if all cases in X are labelled with the same class, the leaf node is labelled with that class. 2) If there

is more than one class, choose an attribute of the data which has 2 or more variations, i.e. gender (male, female). Partition X into the subsets X_1 and X_2 . now recursively apply rule 2) to each subset. Decision trees are powerful, simple and quick to calculate. However, they can suffer from overfitting.

Random Forests

Random Forests were first described by Tin Kam Hoin 1995 [240] in relation to handwriting recognition. Random Forests are constructed of a large number of decision trees. However, by deliberately restricting the number of features, each tree represents the overfitting issues associated with decision trees do not arise. The features which are included are chosen randomly. Each tree then represents a subspace of the overall space. By using the assembly of all of the trees, you get a model that is quick to calculate and reduces the likelihood of over-fitting.

Support Vector Machines

In 1993 Vladimir Vapnik demonstrated that his [Support Vector Machine \(SVM\)](#) [45] could out-perform the neural networks that his colleagues, at Bell Labs, were using for hand writing recognition. He came up with the ideas of SVMs, 30 years earlier while working on his PhD at the Institute of Control Sciences in Moscow. The technique defines a hyperplane that can separate the two classes, using the maximum margin to define the line of best fit, as defined by equation 2.3.

$$f(x) = w^T + b \quad (2.3)$$

where b is the bias and w is weight vector, that is normal to the line. To separate two classes with labels -1 and 1 solve the equation so that for class 1, $w^T + b = 1$ and for class 2, $w^T + b = -1$. Therefore the line with the biggest margin between the two classes is described by $w^T + b = 0$. The total margin is computed by maximising $\left\| \frac{2}{w} \right\|$

Initially, SVMs were used as linear classifiers but, soon the use of kernel tricks were employed, which projected the data to be separated, into higher dimensional space [25]. This allows for more complex hyperplanes to be described. Although, generally thought of as a binary classifier, multi-class classification systems can be constructed by building several one vs all classifiers,

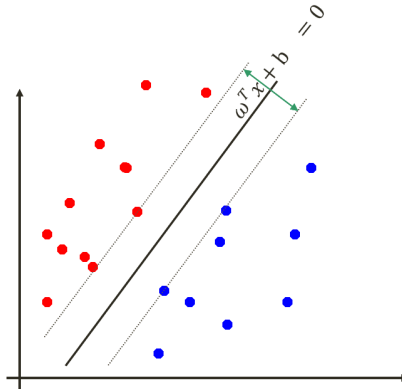


Figure 2.15: Linear separation by SVM

i.e. class 1 vs all other classes, class 2 vs all other classes etc. In the classification step, all the classifiers are run, and the one that produces the greatest margin between classes is declared the appropriate class for that particular sample [228]. Until the recent rise of deep learning, SVMs were seen as the first best candidate for binary classification problems.

Gaussian Naive Bayes GNB

Gaussian Naive Bayes (GNB) [257] use Bayes theorem to separate samples using the maximum likelihood that a sample is drawn from a particular distribution. The 'naive' in the name refers to the assumption the model makes that each parameter, used in the estimation, is independent, even and maybe especially if they are not.

2.16.4 Neural Networks - reborn

During the dark ages, some kept the faith. Chief amongst the proponents of Neural Networks was Geoff Hinton. However, the lack of an elegant method of error correction meant neural nets were still not seen as a robust method of machine learning. This issue was addressed in 1986 when Rumelhart, Hinton and Williams applied back propagation to the problem [207]. In the same year, Rina Dechter coined the phrase Deep Learning [51]. Hinton went on to published a set of landmark papers on various applications of multi layer architectures and popularised the phrase deep learning, as applied to artificial neural networks. His efforts were helped by the huge increase in computing power over the same period. But it was not until Krizhevsky, Sutskever,

and Hinton published their seminal paper "ImageNet Classification with Deep Convolutional Neural Networks" in 2012 [116], that Deep Learning rose to its current popularity. Key to the success of their approach was the use of Graphics Processing Units or GPUs, until then the preserve of gamers.

Multi Layer Perceptrons (MLP)

With the difficulties of training, ANNs addressed the promise of Rosenblatt's work became a practical reality. MLPs are the classic universal approximator, i.e. they are able to approximate most functions [100, 127]. A three-layer MLP is regarded as the simplest practical configuration, consisting of an input layer, an output layer and a hidden layer sandwiched in between. While to some extent, the input layer is directed by the input signal and the output layer is directed by the label, the hidden layer is free to set its weights to best approximate $f(x)$. These layers can be stacked much deeper and, as will be discussed shortly, can contain other types of neurons besides perceptrons. These highly layered or deep networks is where deep learning derives its name.

Modern MLPs use a variety of activation functions, including sigmoid, tanh and ReLU, the latter being the most common in MLPs. These activation functions introduce non-linearity between layers and so allow MLPs to estimate non-linear functions, while allowing the network to smoothly adjust its weights and biases. Like earlier ANNs modern MLPs use gradient descent during learning. However, modern networks use the process of back propagation, outlined by Yann Lecun in his 1986 paper [120] to transmit a set of corrections back through the network. These corrections are guided by an error signal, calculated as a loss between the output and a known label. As with activation functions, the modern computer scientist has a large array of loss functions to choose from, mse, mae, binary cross-entropy, to name but a few. Through repeated rounds of training and error correction, the $f(x; \theta)$ required to transform x to y is learned, where θ represents the learned parameters.

Deep Networks

In the case of just one hidden layer, one can think of the function being $f(x; \theta)$, as stated above. For networks with more layers, each layer can be thought of as contributing a function in a chain, which can be represented as $f(x_1(f(x_2f(x_3))); \theta)$ where $_{[1:3]}$ represent layers. Essentially the more layers a

network has, the wider range of functions it is able to estimate, and so the better the network is able to generalise [13, 80]. Weighed against this factor must be the need for more data when training deeper networks and the spectre of over-training.

Regression via Neural Networks

In regression, the purpose of the network is to estimate a continuous variable, for example, estimate the asking price of a house, based on an input vector of features, such as footprint, number of floors, number of bedrooms, etc. In this case, a good option for the output layer would be a single neuron with a sigmoid activation function.

Classification via Neural Networks

For a classification task, you would change the single output neuron used for regression. For n number of neurons were $n =$ the number of classes needed to be modelled. By applying a softmax activation function, the network converts the probability of an input lying in a particular class to a hard category.

2.16.5 Recurrent Neural Networks (RNN)

The networks discussed so far are regarded as feed-forward networks as training takes place in the forward direction and error correction in the backwards direction. If you take a feed-forward network and loop it back on itself, you get a Recurrent Neural Network. This looping makes RNNs ideally suited to learning repeating patterns in time series data. At every step in the time series, the network sees new information X_t plus the output of the previous step h_t . Figure 2.16 shows this loop for a single neuron in a similar way to HMM. This architecture gives two distinct advantages over feed forward networks. 1) they can handle inputs of arbitrary lengths 2) they share weights across several time steps. The shared weights act as a memory of what came before. If one extends the universal approximation idea, an RNN, with enough hidden units, it should be able to approximate any sequence-to-sequence mapping [88]. However, the problem of uncontrolled feedback rears up. Hence, the gradients used in back propagation either explode or vanish all together [106, 12, 96].

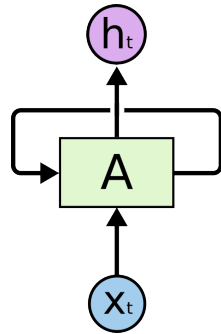


Figure 2.16: **RNN**: conceptually an RNN is just a feed forward network which at each time step can take in new information and a memory of the past outputs, X_t is the input plus h_t , the output of the previous step. Reproduced from [173]

Long Short Term Memory(LSTM)

To address the issue of exploding and vanishing gradients Hochreiter and Schmidhuber [97] introduced LSTM cells. Replacing simple neurons with LSTM cells, addresses the gradient problem by, allowing one LSTM cell to control the flow of data from the previous LSTM one. Figure 2.17 shows the parts of an LSTM cell in detail. In addition to the output of the previous cell (h_{t-1}) Each LSTM cell has a cell state (C_t), that carries information from one cell to the next. 3 gates, Forget, Input, and Output, (each consisting of a sigmoid activation and a pointwise multiplication), add or remove information from the cell state signal based on the input of h_{t-1} and x_t . Information flows through the cell in the following manor. 1) the forget gate calculates f_t by looking at h_{t-1} and x_t and outputs a number from 0-1 for each number in the cell state (1 meaning remove this and 0 meaning keep this and all shades inbetween, this also applies to the other two gates). 2) i) a tanh activation is used to create the vector \tilde{C}_t , by scaling h_{t-1} and x_t between -1 and 1 ii) the input gate uses a sigmoid activation to decide what should be input (i_t), iii) a candidate vector ($i_t * \tilde{C}_t$) is generated by the pointwise multiplication of the two vectors. 3) in this step C_t is created, by multiplying f_t and adding $i_t * \tilde{C}_t$. 4) finally the output of the cell (h_t) is calculated i) first a tanh is used to scale the cell state value between -1 and 1 ii) then this output is multiplied by the output, of the output gate, which is passed out as h_t .

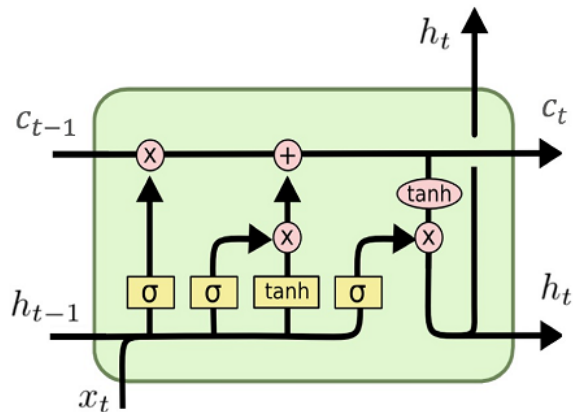


Figure 2.17: **LSTM cell:** The structure of an LSTM cell, is a MLP in its own right. Multiple layers of LSTM cells can learn complex time-series relationships, without the issues of exploding or vanishing gradients. Recreated from commons.wikimedia.org.

Gated Recurrent Units (GRU)

GRU units are a related, but computationally simpler than the LSTM cells [40]. In a GRU unit, the cell state and the hidden states are merged, as are the forget gate and input gate, shown in 2.18. Both kinds are popular, but LSTM has become the default architecture for RNN applications.

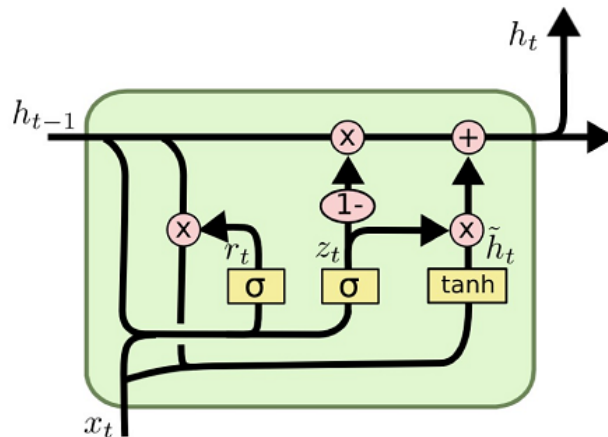


Figure 2.18: **GRU:** Similar to an LSTM unit but the the cell state and the hidden states are merged, as are the forget gate and input gate. Recreated from commons.wikimedia.org.

2.16.6 Autoencoders

Autoencoders are a class of unsupervised neural network which learn a more compact representation of the input by, encoding and then decoding the input. This output is then compared to the input and by back propagation the essential features are discovered. The encoder takes an input of x and produces a lower dimensional version (z). This process can be generalised to the equation $z = q(x)$. The decoder then reconstructs the original input, generalised as: $x' = p(z)$. The structure of a typical autoencoder is shown in Fig 2.19.

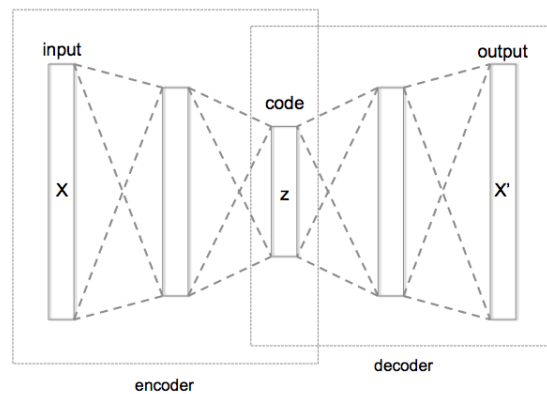


Figure 2.19: **Autoencoder:** The layers of an autoencoder are arranged to allow for the encoding and decoding of an input. The original input is used as an error signal in training. Recreated from commons.wikimedia.org

Autoencoders can use any type of neuron or even gated units (LSTM or GRU). By applying the same naming convention used with MLPs, any autoencoder with more than three layers is called a deep autoencoder. Autoencoders are often used as a form of dimension reduction. In this mode, you can think of them as a non-linear version of PCA [95]. The latent representation is then used as the input to any of the models discussed so far.

However, in truth, they are models in their own right [8]. by learning, in an unsupervised way, to reconstruct inputs from the latent layer they must have learned a model of the data [207]. If the autoencoder is trained on “normal cases” for instance, healthy adult participants carrying out a test for movement impairment, the autoencoder will build a model of a healthy movement and will be able to reconstruct that movement with a high degree of faithfulness. If the trained network tries to reconstruct the recording of someone with impairment,

the Autoencoder will make errors in the reconstruction because it has never seen this type of input before. The reconstruction error can be quantified using any number of metrics (MSE, euclidean distance, cosine distance, etc) and can serve as a measure of distance from normal.

2.17 Conclusion

The assessment of falls-risk is still principally assessed by clinical tests carried out by trained staff. As well as the inherent variation in such measures, the number of people available to undertake such assessments makes preemptive screening for falls-risk impractical. This means that anyone referred for help at a falls clinic will have already suffered a potentially life-changing fall.

In research, force plates have become the most widely used tool for balance assessment. In spite of inherent issues, force plates can still provide powerful insights. However, their use has never become widely incorporated into clinical practice. The cost and setup requirements still remain a barrier. Some commercial devices have been developed, but they are more general in nature and try to identify deficits in the systems of balance rather than looking at metrics that can be more directly associated with falls-risk.

An alternative to the use of force plates can be found in motion capture. Motion capture can track each joint, individually, and so provides a more complete picture of balance. However, they are expensive, and their setup-time can be longer than the time needed to carry out a clinical assessment. Marker-less motion capture, such as Kinect, provides a practical alternative method of capturing human movement. When used in conjunction with machine models, this area of research could provide an alternative approach to the assessment of physical impairment.

Much effort has been put into the field of HAR, leaving the clinical use of Kinect a much smaller field of research. This is perhaps surprising as an ageing worldwide population need cost-effective solutions to identify those at risk of falls.

Appropriate publicly available data is an issue which the KINECAL dataset goes some way to address. Recent research into internal data representations of complex data shows promise in disentangling overlapping classes. Furthermore, the application of appropriate distance functions can provide an objec-

tive method of quantifying impairment. In addition, this approach provides a method of monitoring long term changes.

Chapter 3

Techniques and Methods

3.1 Introduction

In this chapter, the techniques and methods, either used directly in this thesis or discussed in related work, is discussed. The intention is to provide a technical background. The equations detailed here are referred to throughout the subsequent chapters.

3.2 Joints and Skeletons

Whether collected by marker-based or markerless systems, joint positions can be described as points in 3D space. For the Kinect, the world view is right-handed, the origin is the centre of the camera, as shown in Figure 3.1

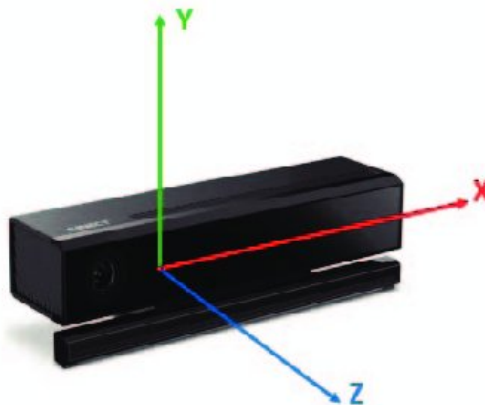


Figure 3.1: **Kinect coordinate system:** Z axis projects from the depth camera, with x and y orthogonal to it his image is recreated from [here](#).

3.2.1 The Human Body

Mapping the x,y,z axis of the connect onto the recognised anatomical directions maps x to **ML**, y to **Superior-inferior (SI)** and z to **AP**. The three-axis of the Kinect can be mapped to the recognised anatomical planes of the human body. These are the sagittal, frontal(also called coronal) and transverse planes, as shown in Figure 3.2. The sagittal plane maps to the ZY plane of the Kinect. Similarly, the frontal plane maps to the XY plane, and the transverse plane maps to the XZ plane.

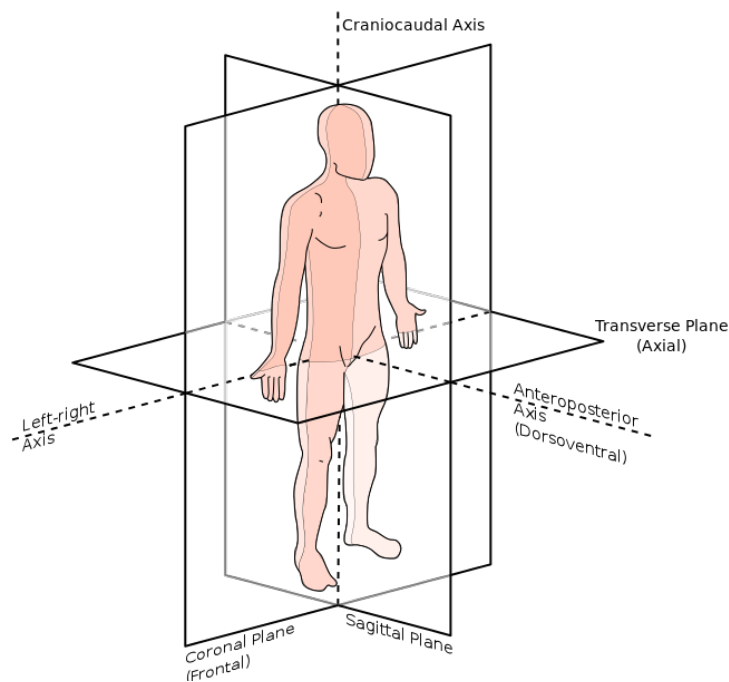


Figure 3.2: **Body planes:** The planes of the body, are Sagittal, which bisects the body left to right; Coronal (Also know as Frontal), which bisects the body, front to back and Transverse, which bisects the body head to tail. This image is adapted from [an open-sourced figure](#).

3.3 Working with Kinect skeletons

3.3.1 Filtering

As with any system that digitises real-world data, Kinect’s signal is bound up with noise. To address this issue, the recordings were filtered using a Butterworth fourth-order zero-lag filter. The low-pass cut-off frequency was

established as described by Winter [263]. The frequency used to filter the data used in this thesis was 8 Hz.

3.3.2 Pose Normalisation

The skeleton output of the Kinect gives the distance from the camera to the subject, in metres. This data was converted from the camera coordinate system to a person-coordinate system, with the spinebase joint at the origin. This was achieved by subtracting the spinebase coordinates of the first frame from the joint coordinates of all subsequent frames, using equation 3.1.

$$p_{n,i}(x, y, z)^* = P_{n,i}(x, y, z) - P_{0,SPINE_BASE}(x, y, z) \quad (3.1)$$

where $p_{n,i}(x, y, z)^*$ represents the normalised position of the x, y, z axis of joint i in frame n . $P_{0,SPINE_BASE}(x, y, z)$ represents the position of the *SPINE_BASE* joint in first frame of the recording, and $P_{n,i}(x, y, z)$ represents the positions of joint i in frame n .

3.3.3 General Method for Calculating CoM

The centre of mass of any regular object can be calculated simply by the plumb bob method [259]. The centre of mass of an irregular object is somewhat more tricky. The Total Body Centre of Mass (TBCM), of a human body, can be calculated by segmenting the body as described by Dempster [263]. The CoM is calculated for each segment, TBCM is then calculated as a weighted average of the CoM of all segments, using equation 3.2.

$$\begin{aligned} {}^xTBCM &= \frac{\sum m_i x_i}{M} \\ {}^yTBCM &= \frac{\sum m_i y_i}{M} \end{aligned} \quad (3.2)$$

where ${}^xTBCM, {}^yTBCM$ are coordinates of *TBCM*; x_i, y_i are coordinates of the i -th segment; m_i is mass of the i -th segment; and M is the total mass of all of the segment.

3.3.4 Centre of Mass from Force Plate Data

Several methods of deriving CoM from CoP when using force plates have been suggested. The Balance master [204] used for comparison in chapter 5 estimates a vertical projection of the Centre of Mass (CoM) from CoP data using the method described by Morasso et al. [158]. This method assumes that the body is rigid, and the CoP is mid-way between the two feet with a single pivot at the ankle. The position of the CoM is assumed to be the vertical projection of the CoP by 0.5527 of the person's height and inclined by -2.3° (estimated to be the average anterior lean when standing). See section 5.2.4

3.3.5 Centre of Mass from Kinect Data

To provide a method of calculating CoM, which does not require the weight of an individual to be known, a method is used that estimates the position of CoM directly from the skeletal structure of a human body. First described in [124], it calculates CoM to be the 3D Euclidean mean of 3 joints of the Kinect skeleton, Hip left, Hip right, Spine mid. as described in equation 3.3.

$$\begin{aligned} CoM_x &= \frac{J1_x + J2_x + J3_x}{3} \\ CoM_y &= \frac{J1_y + J2_y + J3_y}{3} \\ CoM_z &= \frac{J1_z + J2_z + J3_z}{3} \end{aligned} \quad (3.3)$$

where $J1 = HIP_LEFT$, $J2 = HIP_RIGHT$, and $J3 = SPINE_MID$. The x, y, z components were calculated individually and then concatenated to form a CoM triplet. i.e. $[CoM_x, CoM_y, CoM_z]$. This essentially defined a 26th joint in the skeleton graph.

3.4 Conclusion

This chapter provides a background to the common techniques used throughout this thesis. However, it should be considered a background chapter as salient details are provided in the methods sections of the experimental chapters.

Chapter 4

Preliminary Research

4.1 Introduction

As discussed in Chapters 1-3, Kinect is a portable and inexpensive device that allows for the automatic tracking of anyone placed in front of it. The area of HAR has seen many datasets created to help in that field. Sadly the same is not true when it comes to the clinical use of Kinect. When this preliminary research was undertaken, the largest dataset of clinically relevant movements was the K3Da dataset [125]. It consists of, 26 young and middle-aged people (18-48 years, 17 male and 9 female) and 28 older age people (61-81 years, 14 male and 14 female) carrying out the SPPB [85], plus the unilateral stance [24]. In this study, not all of the movements available in the K3Da dataset were considered. The movements used and the reason for their inclusion are detailed in table 4.1

The K3Da dataset contains details of age, height and weight but does not contain information about falls history. Therefore this work asks the question, can one tell the difference between young and older base solely on their movement?

This research was presented at the [IEEE Systems Man and Cybernetics conference in Banff in 2017](#).

Table 4.1: Movements used in this work, along with the rationale for inclusion

Movement Name	Description	Reason for inclusion
STS-5	Starting from a seated position, rise up with legs fully extended, then sit down again, arms are held across the chest. Repeat five times, as quickly as possible.	This measure is indicative of leg muscle power, associated with falls and physical impairment [239].
Quiet standing, eyes open	Standing feet close together, eyes open and arms extended parallel to the floor. Test is terminated after 10 seconds.	This is used to provide an indication of postural sway in a quiet stance, two feet on the floor.
Quiet standing, eyes closed	Standing feet close together, eyes closed and arms extended parallel to the floor. Test is terminated after 10 seconds.	Removing the visual cues make the participant rely on vestibular and somatosensory feedback. Both these systems are affected by age [61].
ULS, eyes open	Standing on one leg, 6 inches off the ground, arms extended horizontally, eyes open. Test terminated after 10 seconds or when the second leg touches the ground.	Balancing on one leg provides a small base of support, inducing postural sway.
ULS, eyes closed	Standing on one leg, 6 inches off the ground, arms extended horizontally, eyes closed. Test terminated after 10 seconds or when the second leg touches the ground.	During this exercise, the individual must use the vestibular and somatosensory systems to maintain balance.

4.2 A Method to Distinguishing Young from Older, in the KD3a Dataset

For this preliminary investigation, a pipeline was constructed, which takes an exemplar approach to identify key poses which, when put together in time-order, can represent a whole movement. This chapter demonstrates that these exemplar motions can be used to separate young from old, using a range of machine models. The machine models were SVM, random forest (the most popular statistical approaches for binary classification) and a MLP. This was done to see if a neural network could out-perform the statistical approaches.

Using the methods outlined in Figure. 4.1, the process of feature encoding and then the classification of an individual’s age-class, based upon their motion alone, was automated. The data processing steps were carried out using

Matlab. Matlab was also used for classification by statistical machine learning. Theano was used for classification by neural network. The following section covers each step in detail.

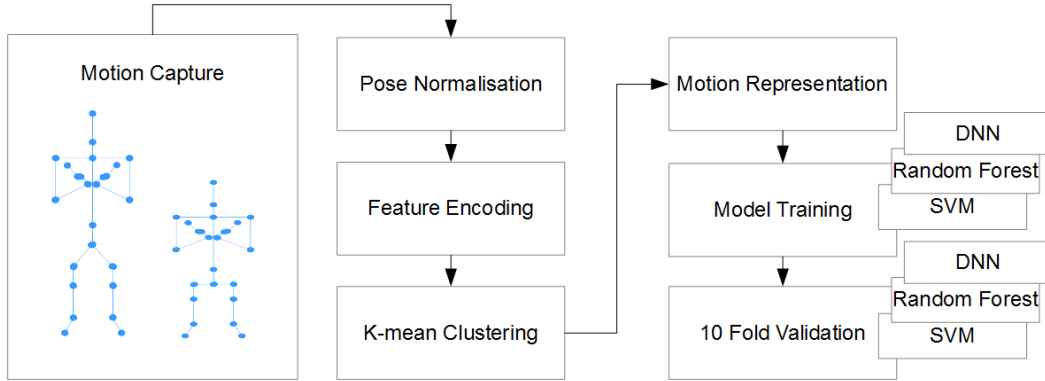


Figure 4.1: **Data processing pipeline:** this pipeline was used to extract features from the K3Da dataset.

4.2.1 Pose Normalisation

From the skeleton data, a series of matrices were constructed, one for each frame of the movement (30 fps). The skeletons were normalised by aligning all frames to the *SPINE_BASE* joint of the first frame, using equation 4.1. This moves the coordinate system from being camera centred to being skeleton centred, and all measurements become relative to the start of the recording.

$$p_{n,i}(x, y, z)^* = P_{n,i}(x, y, z) - P_{0,SPINE_BASE}(x, y, z) \quad (4.1)$$

where $p_{n,i}(x, y, z)^*$ represents the normalised position of the x, y, z axis of joint i in frame n . $P_{0,SPINE_BASE}(x, y, z)$ represents the position of the *SPINE_BASE* joint in first frame of the recording, and $P_{n,i}(x, y, z)$ represents the positions of joint i in frame n .

4.2.2 Feature Encoding

In this study, the torso features detailed in [124], and described here, in Table 4.2 where used. Details of how each feature was calculated is shown below. In addition to the CoM position, this feature set includes the torso’s inclination, the body’s inclination, the torso joint positions and the x,y coordinates of skeleton joints in the torso.

Table 4.2: The features used in this study

Feature	Description	Vector length
CoM	Mean position between Spine mid, Hip left and Hip right	3
Body Lean Angle	Angle between Spine Mid and the ground plain	1
Torso Angle	Angle between Spine base and Neck	1
Spine Distance	Euclidean distance between Spine base and Head	1
Torso positions (ML plane)	XY position of the torso joints	10

Body Lean Angle was calculated as the angle between the 3D coordinates of the the *SPINE_MID* joint and the *GROUND PLAIN*, using equation 4.2. The *GROUND PLAIN*, was calculated as the euclidean average of the *FOOT_RIGHT* and *FOOT_LEFT* joints. Figure 4.2 shows the relative position of each joint.

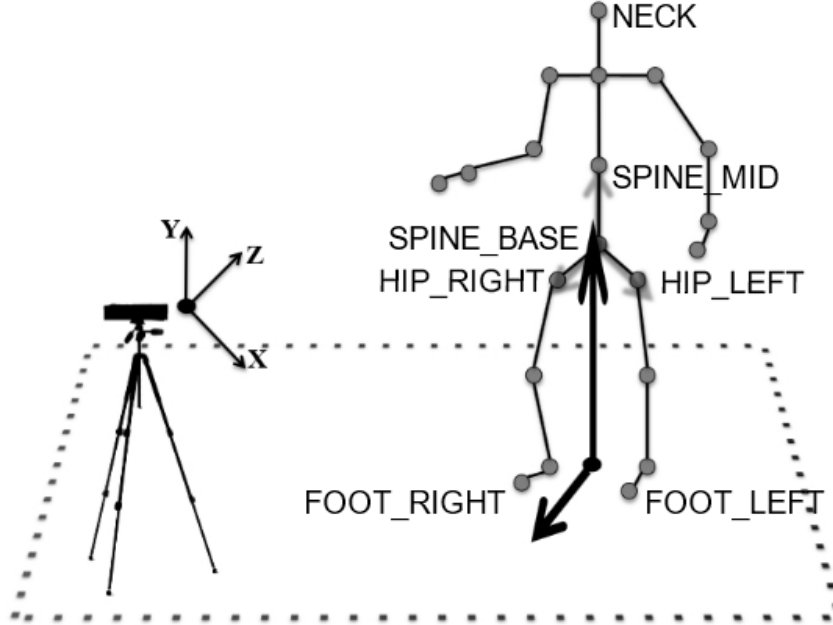


Figure 4.2: A diagram of the relationship between, an individual, being recorded and the Microsoft Kinect camera. The salient joints are shown. The *BodyLeanAngle*, is the angle between *SPINE_MID* and *NECK* joints. The *TorsoAngle*, is the angle between *SPINE_BASE* and *NECK* joints. The **CoM** is calculated as the euclidean average of the *HIP_LEFT*, *HIP_RIGHT* and *SPINE_MID* joints (modified, from [124])

$$Body\ Lean\ Angle = \arccos\left(\frac{S_{mid} \cdot G_p}{\|S_{mid}\| \|G_p\|}\right) \quad (4.2)$$

where S_{mid} is the *SPINE_MID* (x,y,z) vector and G_p is the *GROUND_PLAIN* (x, y, z) vector.

Torso Angle was calculated, in a similar fashion as **Body Lean Angle**, using equation 4.3.

$$Torso\ Angle = \arccos\left(\frac{S_{base} \cdot N_k}{\|S_{base}\| \|N_k\|}\right) \quad (4.3)$$

where S_{base} is the *SPINE_BASE* vector (x,y,z) and N_k is the *NECK* vector (x, y, z)

Centre of Mass (CoM) of any body, is the mean point that the mass of that body acts. For a human body standing erect, the centre of mass is located around the navel. CoM was calculated using equation 4.4. The x, y, z components were calculated individually and then concatenated to form a CoM triplet.

$$\begin{aligned} CoM_x &= \frac{HIP_LEFT_x + HIP_RIGHT_x + SPINE_MID_x}{3} \\ CoM_y &= \frac{HIP_LEFT_y + HIP_RIGHT_y + SPINE_MID_y}{3} \\ CoM_z &= \frac{HIP_LEFT_z + HIP_RIGHT_z + SPINE_MID_z}{3} \end{aligned} \quad (4.4)$$

$$CoM = [CoM_x, CoM_y, CoM_z]$$

where *HIP_LEFT*, *HIP_RIGHT*, *SPINE_MID* are the joints, indicated on Figure 4.2

Spine Euclidean Distance was calculated between the 3D coordinate of the spine base and head joints, using equation 4.5.

$$distance = \sqrt{(S_B_x - H_x)^2 + (S_B_y - H_y)^2 + (S_B_z - H_z)^2} \quad (4.5)$$

where subscript x, y, z represent the x, y, z axis of the *SPINE_BASE* (S.B) and *HEAD* (H) joints.

Torso positions in ML plane represents the x,y positions of the torso joints, calculated using equation 4.6

$$ML_TORSO_POS = [S_B_x, S_M_x, S_S_x, N_x, H_x, S_B_y, S_M_y, S_S_y, N_y, H_y] \quad (4.6)$$

4.2.3 K-mean Clustering

K-mean clustering (covered in section 2.16.3) was used to convert a time-series of differing lengths (depending on individual recordings), into a set of representative poses of a known length. The k was determined empirically for each type of motion, 5 for chair rise and 2 for all other movements.

4.2.4 Motion Representation

The data frames nearest to each centroid were concatenated together, in time-order to produce a 1D vector that provides an example of the whole motion. A label was then added, 1 for young and 0 for older.

Simply choosing the centroid would not provide enough examples to train the models. So more examples were collected using the following method:-

1. Each member of a cluster were ranked using Euclidean distance from the centroid.
2. The closest 50% were selected. To ensure that each vector represents the whole motion, only n number of motions were produced from each time-series. Where n is the number of members in the smallest cluster.

This method produced a family of feature-sets that are representative of a person's motions. By providing a family of similar examples, the number of examples retrieved from a time-series was increased, many times, without the need to resort to synthesising data. This approach makes the models more robust as they are trained on a diverse but representative feature-set.

4.2.5 Model Training

Three classification methods were compared, SVM, Random Forests and Deep Neural Networks. The SVM and Random Forrest were trained using Mat Lab, and the Neural network was trained using Keras, with a Theano back end. The neural network used was an MLP with two hidden layers and a 0.5% dropout layer. The final class determination was made via two neuron softmax layer.

10-fold cross-validation was used to assess the effectiveness of each approach. This allows the results to be averaged over ten combinations of the dataset.

4.3 Results

The results, summarised in Table 4.3, demonstrates the proposed method is able to generate example motions that can be used to separate young from older people, using a range of well know machine models.

The method identified mean exemplars of a motion and then collected many similar examples of that motion from the time-series. In this way, enough examples were generated to allow both statistical and deep learning methods to discriminate between young and older people, with a high degree of certainty, STS-5 marginally producing the best overall classification.

Table 4.3: **A comparison of the different machine models:** All three machine models were able to separated the extracted features

	Model	Acc	Prec	Recall	F1score	MCC
ULS, eyes open	SVM	0.999	1.000	0.998	0.999	0.998
	Random Forest	0.998	0.998	0.998	0.998	0.998
	Deep Learning	0.977	0.977	0.979	0.978	0.976
ULS, eyes closed	SVM	0.998	1.000	0.996	0.998	0.995
	Random Forest	0.999	0.998	1.000	0.999	0.999
	Deep Learning	0.985	0.983	0.993	0.988	0.986
Quiet Standing, eyes open	SVM	0.999	1.000	0.998	0.999	0.997
	Random Forest	0.999	1.000	0.998	0.999	0.997
	Deep Learning	0.991	0.994	0.994	0.994	0.985
Quiet Standing, eyes closed	SVM	0.995	0.994	0.994	0.996	0.992
	Random Forest	0.999	0.998	1.000	0.999	1.000
	Deep Learning	0.998	0.998	0.998	0.998	0.988
STS-5	SVM	1.000	1.000	1.000	1.000	1.000
	Random Forest	1.000	1.000	1.000	1.000	1.000
	Deep Learning	1.000	1.000	1.000	1.000	1.000

4.4 Discussion

There is a pressing need to develop a portable system that can help in the assessment of falls risk. This need was recognised by Leightly et al. [125], when they compiled the K3Da dataset. Currently, the most common way physical impairment is assessed is through assessment against a clinical scale. This can lead to inconsistency from assessor to assessor, and location to location [221]. K3Da is a dataset of movements used in clinical tests, captured, objectively by Kinect V2.

This chapter details the first steps in developing a tool that could be used by clinicians in detecting the changes in motion that advance with age. Its utility was demonstrated by separating a random sample of young and older individuals from K3Da.

As discussed in section 1.1 and chapter 7, while falls risk increases with age, age cannot be the cause of different levels of falls risk between individuals of similar ages. Unfortunately, K3Da lacks the labels, such as falls history, essential for research into assessing falls-risk.

Working within the limitations of K3Da, a method was developed which created feature vectors able to separate young from older, based solely on their

movements. Looking at the result section, all of the models produced similar results, no form of classification was better than another. The research, detailed in this chapter, developed a method of feature extraction, not a method of binary classification. The method provides feature vectors that clearly show differences between ages. However, no effort was put into explaining how the encoding achieved this. Ultimately, this avenue of research was put to one side, in favour of methods that could separate individuals of similar ages based on falls risk. Although, future work could revisit this question.

That said, these results were encouraging and demonstrated that data derived from Kinect could identify differences between groups of people based solely on their movements. More importantly, this research was seminal in shaping the question which this theses addresses, i.e. “can methods be developed which can identify those at risk of falls from a population of > 65 years of age.” As distinct from “can methods be developed which can identify older people based on their movements.” It also posed the question “what would a dataset look like, that is well suited to answering the first question.”

4.5 Conclusion

In this work, an exemplar-based method was developed that can identify age-related changes captured using a Kinect camera, looking at the age profile of the KD3a dataset, shown in Fig 4.3. It is clear that this dataset is very polarised. This makes it ideal for studying gross age differences, but it is difficult to answer the fundamental question posed by this Thesis, can machine models be created that can identify physical impairments and relating to increased falls-risk?

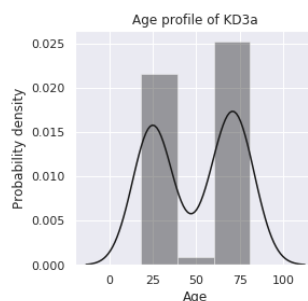


Figure 4.3: **The age profile of KD3a:** The graph shows the polarised nature of the kD3a dataset, while this is perfect of looking at age related changes, it makes identify those at risk of falls difficult

The proposed method, detailed here, works well for a simple binary split on age. Chapters 6 and 8 look at methods that focus on identifying physical changes, which relate to mobility issues, and falls-risk in preference to age.

To enable this research, the KINECAL dataset was established, detailed in chapter 6

Chapter 5

A New Process to Measure Postural Sway, Using a Kinect Depth Camera

5.1 Introduction

Clinical tests for balance and physical impairment suffer from variation between assessors [221]. Conversely, posturography provides an objective measurement of a person's postural sway [92], based on the movement of the body's Centre of Mass (CoM), as calculated from quantitative ground reaction forces as measured using a force plate. The work of Nashner et al. [167], Hasselkus and Shambes [92] lead to the development of the SOT, which is implemented in the SMART Balance Master (BM). SOTs involves static and reactive balance assessments that place emphasis on visual (eyes open/closed), vestibular, or proprioceptive afferents that govern postural control.

The Balance Master's SOT was selected because it is regarded as a valid tool to investigate different aspects of balance [134, 157, 21] including falls-risk amongst older adults [250, 162, 27], proprioceptive decline [47], the effects of age and gender on postural control [87], and the effectiveness of balance-based exergaming [215]. However, high costs and low availability of the specialist equipment needed for posturography and SOT means they are not practical for wide-scale screening [150].

The Kinect depth camera offers the potential to accurately and reliably assess many aspects of human movement. However, their use as a posturographic

device is underexplored. They are affordable, portable and can potentially be used in a wide range of home or clinical settings. Previous studies [41, 71, 163] have considered the use of Kinect as a way to replace marker-based systems (e.g. Vicon, Qualisys). The near-universal conclusion of these studies is that Kinect can be considered equivalent to the marker-based systems. However, the use of depth cameras to assess postural sway as an indicator of postural control is rarely considered. Our proposed approach addresses this gap. It seeks to measure postural control by tracking CoM in an equivalent fashion to the way it is measured by the most widely used means of assessing standing postural control, i.e. force plates. Force plates are used in the assessment and diagnosis of many conditions, including falls-risk [248, 165], and it is with force plates that the Balance Master measures sway.

Yeung et al. [269] did consider Kinect’s use in posturography. The authors outline an approach that uses Kinect to calculate the **Total Body Centre of Mass (TBCM)** by segmenting the body, as described by Dempster [263]. In the current study, a much simpler method of calculating CoM is demonstrated, first used by Leightley et al. [124]. Leightley’s method takes the euclidean mean of 3, well-tracked joints (*HIP_LEFT*, *HIP_RIGHT*, *SPINE_MID*) to be a good estimate of the CoM position. Previous studies [269, 255] have demonstrated that the accuracy of Kinect’s joint tracking is related to the angle between the Kinect and the joint. This means that ankle and foot joints are tracked poorly. Joints that have a less steep angle to the Kinect (e.g. the hip joints) are tracked with high accuracy. Poor tracking of joints can cause issues when estimating the TBCM, an issue that Leightley’s method avoids. The human skeleton can be considered as a chain of connected joints meaning the positions of knee, ankle, and foot joints affect the CoM position without the need to consider them directly. Thus for an upright stance, the lengthy calculation of TBCM is not required for our application.

5.2 Methods

5.2.1 Participants

This study was approved by the Manchester Metropolitan University Research Ethics Committee. All participants provided written informed consent. Fifteen injury-free individuals (mean \pm SD age: 42.3 \pm 20.4 yrs; height: 172 \pm

11cm; weight: $75.1 \pm 14.2\text{kg}$; BMI: $25.3 \pm 3.3 \text{ kg/m}^2$; male = 11) took part in 346 trials during the completion of the six components of the SOT used by the SMART Balance Master (NeuroCom International, USA), to assess postural sway during static and dynamic challenges. A wide age-range was selected to ensure a wide range of postural sway was recorded. Postural sway is known to increase with age, as part of the normal ageing process. [2]. The age profile of the participants was 6 young (20-30 years), 5 middle age (31-59 years) and 4 older (>60 years). More details are shown in table 5.1

For this study, no individuals with a history of falls were included. Also, several participants took part in more than one set of trials. This is a valid choice, as this is a study of agreement between two methods, not an investigation to identify those with balance impairment. Note: this population is not included in the KINECAL dataset, detailed in chapter 6, and the data collected here is not used elsewhere.

Table 5.1: **Table of participants:** The table provides a breakdown of Age, Sex, Weight, BMI and Age Class: Young (20-30 years), Middle Age (31-59 years) and Older (>60 years)

ID	Age	Hight	Weight (kg)	BMI (kg/m2)	Gender	Age Class
304	20	1.60	55	21.5	Male	Young
303	23	1.79	90	28.1	Male	Young
6020	24	1.81	82	25.0	Male	Young
7020	24	1.8	75	23.1	Male	Young
8020	25	1.73	81	27.1	Female	Young
4000	24	1.81	66	20.1	Male	Young
401	32	1.81	76	23.2	Male	Middle age
5020	36	1.77	105	33.5	Male	Middle age
3021	40	1.70	80	27.7	Male	Middle age
9020	48	1.70	73	25.3	Male	Middle age
10020	59	1.71	70	23.9	Male	Middle age
3020	62	1.52	56	24.2	Female	Older
4020	68	1.88	93	26.3	Male	Older
501	74	1.56	67	27.5	Female	Older
601	76	1.6	57	22.3	Female	Older

5.2.2 Procedure

The participants were simultaneously recorded using the EquiTest software that comes bundled with the SMART Balance Master and the Skel recorder. Skel recorder is custom software, detailed in section 5.2.4. It processes the output of the Kinect depth camera into a 2D CoM path. Participants performed

the six components of the SOT while standing on the force plates incorporated into the Balance Master. The Balance Master was controlled, and data recorded using the EquiTest software. The Kinect was controlled using the Skel recorder. Participants wore a safety harness throughout all assessments to prevent falls. All six components of the SOT (outlined below) were carried out in accordance with the Balance Master operator instructions. The instructions require participants to stand on two legs approximately shoulder-width apart with heels aligned to markers on the force plates [204].

The six components of the SOT are as follows: (a) eyes open, platform fixed; (b) eyes closed to remove visual input; (c) eyes open with moving surround, to create sensory conflict between visual input (simulating a moving room) and vestibular inputs (a stable room); (d) eyes open and the platform support rotating freely to disrupt somatosensory and proprioceptive feedback from the feet and ankles; (e) eyes closed and the platform support rotating freely; and (f) eyes open with moving surround and the platform support rotating freely.

Two consistent trials for each condition were included in this study. Inconsistent trials and fails were excluded from further analysis. All assessments were conducted in the sequence of (a) to (f), as recommended by the operator instructions. This increases difficulty progressively. Each trial (an instance of an individual carrying out one aspect of the SOT) was repeated twice, except if the second trial was inconsistent with the first or was marked as a fail, in which case the participant was allowed a third attempt. A trial was marked as a fail if a participant touched the upright supports on the Balance Master frame or relied on the safety harness to maintain an upright posture for any reason.

5.2.3 Experimental Setup

Participants stood upright on the force plates of the Balance Master, facing towards the large surround approximately 1m away. The surround is used to create visual-vestibular conflict, but obscured the front view of the participant (Fig. 1). Therefore, the Kinect was positioned to capture the rear-view of the participant 2.5 m from the participant at a height of 1.2 m from the floor. The distance was selected after pilot trials to confirm that people of all heights

could be captured equally well while their feet were placed correctly, along the foot markers on the force plates (Fig. 5.1).

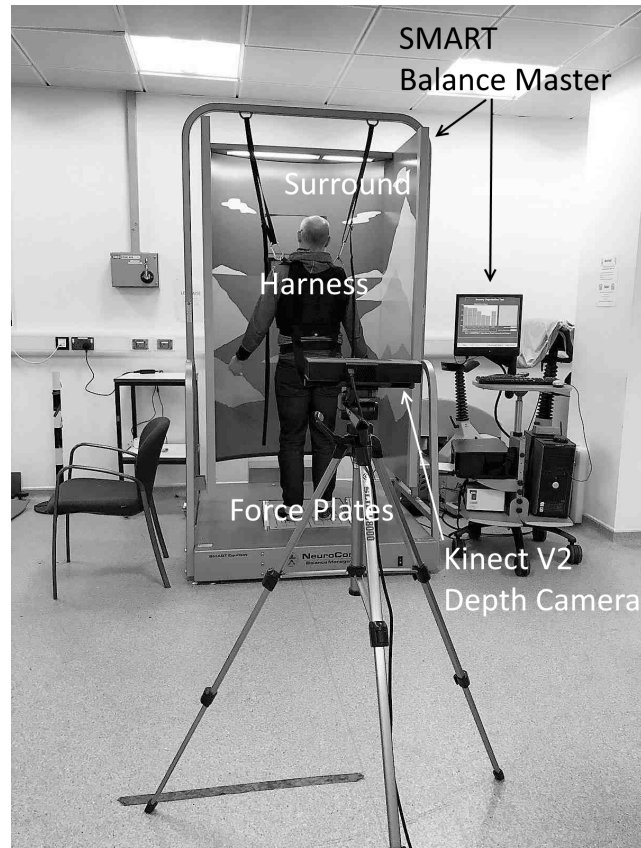


Figure 5.1: Setup of Balance Master and Kinect V2, Depth Camera.

5.2.4 Recording of CoM path

Recording of CoM, using SMART Balance Master

The Balance Master [204] estimates a vertical projection of the Centre of Mass (CoM) from Centre of Pressure (CoP) data using the method described by Morasso et al. [158]. This method assumes that the body is rigid and the CoP is mid-way between the two feet with a single pivot at the ankle (Fig. 5.2). The vertical projection of the CoM is estimated to be 0.5527 of the person's height (represented by length c in Fig. 5.2). The value for a is obtained by taking the CoP value from the force plates and inclining it by -2.3° , estimated to be the average anterior lean when standing. The force plates have a sampling rate of 100 Hz.

The CoM path was recorded using the EquiTest software, bundled with the SMART Balance Master. The CoM path is plotted in two dimensions, mediolateral and anterior-posterior.

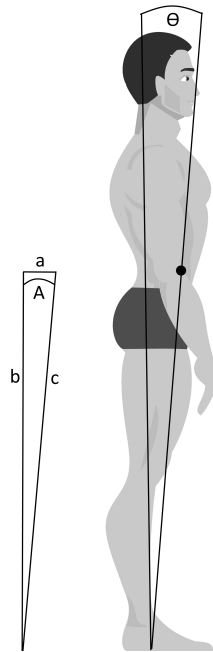


Figure 5.2: **Diagram of sway angle calculation used by the Balance Master [204].**

Recording of CoM path, using Skel recorder

Kinect measures the distance from the participant to the camera in three dimensions, using the time-of-flight of an infrared beam, at a rate of 30 Hz. From this information, Kinect fits a human skeleton to a 25-joint model [216], which has good agreement with skeletons generated from marker-based systems [269].

The Skel recorder is custom software, written in C# using Visual Studio and the Kinect SDK 2.0. It takes a series of skeleton frames and derives a CoM path. The pipeline of the Skel recorder is shown in Fig. 5.3. The steps of the pipeline are as follows: 1) The ML-axis of the skeletons are reversed, to take into account the rear position of the Kinect camera; 2) Each skeleton frame, is aligned to the first frame of the recording, making all subsequent movements relative to this initial position [246]; 3) The position of CoM is estimated, as described, in the section “Frame-wise calculation of CoM”; and 4) The ML and AP elements of the CoM path are saved to disk.

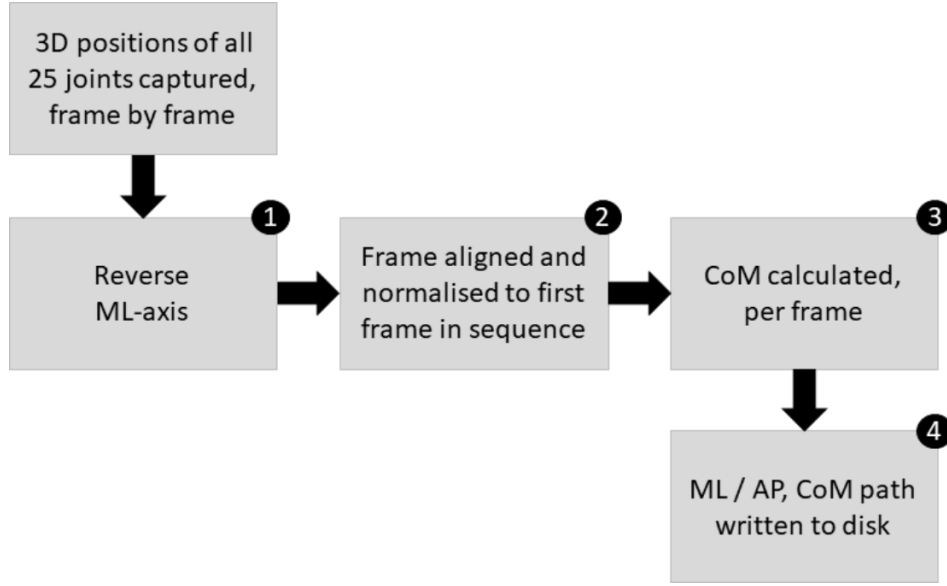


Figure 5.3: **The pipeline of the Skel recorder.**

Frame-wise calculation of CoM The position of the CoM was calculated, frame-by-frame by taking the euclidean average of the left-hip, right-hip and mid-spine joints, as defined by equation 5.1, first used by Leightley et al. [124]. This method estimates the position of CoM in three dimensions without needing to rely on the assumptions made by the Balance Master.

$$\begin{aligned}
 CoM_{ML} &= \frac{HIP_LEFT_{ML} + HIP_RIGHT_{ML} + SPINE_MID_{ML}}{3} \\
 CoM_{SI} &= \frac{HIP_LEFT_{SI} + HIP_RIGHT_{SI} + SPINE_MID_{SI}}{3} \\
 CoM_{AP} &= \frac{HIP_LEFT_{AP} + HIP_RIGHT_{AP} + SPINE_MID_{AP}}{3}
 \end{aligned} \tag{5.1}$$

$$CoM = [CoM_{ML}, CoM_{SI}, CoM_{AP}]$$

where HIP_LEFT , HIP_RIGHT , $SPINE_MID$ are joints, defined by Kinect. The ML , SI , AP components were calculated individually and then concatenated to form a CoM triplet.

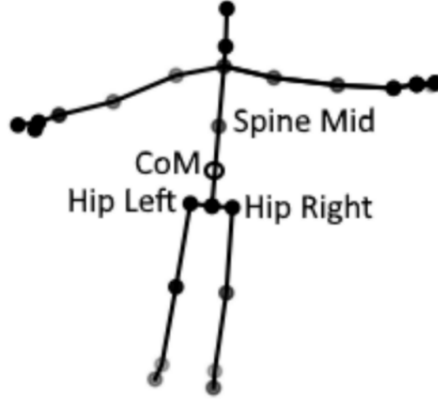


Figure 5.4: Kinect V2 Skeleton, the joints used to estimate CoM and the CoM position, are labelled.

5.2.5 Creation of CoM Time Series

As noted by Prieto et al. [189], when calculating sway, precise foot placement is hard to achieve. This makes meaningful comparison between individuals difficult. The same can be said for the comparison between methods. A more robust approach is to centre the time series on the mean position of each recording. In this study, this is achieved using equation 5.3. The mean position for the raw ML and AP time series (ML_{raw} and AP_{raw}), was calculated using equation 5.2. In both equations, n is the number of time steps, and i represents the frame index.

$$ML_{raw}^- = \frac{1}{n} \sum_{i=1}^n ML_{raw}_i \quad (5.2)$$

$$AP_{raw}^- = \frac{1}{n} \sum_{i=1}^n AP_{raw}_i$$

$$ML_i = ML_{raw}_i - ML_{raw}^- \quad (5.3)$$

$$AP_i = AP_{raw}_i - AP_{raw}^-$$

The straight-line-distance, in two dimensions, between the current CoM position, and the Mean CoM value, at each time step, was calculated, using

equation 5.4, this is also known as the resultant distance.

$$RD_i = \sqrt{(ML_i)^2 + (AP_i)^2} \quad (5.4)$$

Concatenating the calculated values, for each time step (i) produces the final resultant distance time series (RD), one for each method. These time series were used in subsequent analysis of the two methods.

5.2.6 Calculation of Sway

RMS of sway ($Sway_RMS$) was calculated, for each method using equation 5.5, where RD is the time series calculated in equation 5.4 and n is the number of time points in the time series [189, 110]. MATLAB 2019a was used to implement equations 5.2, 5.3, 5.4 and 5.5

$$Sway_RMS = \sqrt{\frac{\sum_{i=1}^n RD^2}{n}} \quad (5.5)$$

5.2.7 Data Exclusions

A total of 56 recordings were removed for various reasons, as detailed in Table 5.2. The remaining 288 records were used in the analysis.

Table 5.2: Table of Exclusions

Reason for exclusion	Description	#
Extra recordings	For each trial, if a participant did not complete two consistent trials, they were offered a third trial. Only the two most representative trials were used.	29
The participant fell	The participant fell while attempting a trial.	3
Recordings out-of-sync	The start of the Kinect recording was not coincident with the start of the balance master recordings.	14
Over-recording of a previous trial	One trial was recorded over another trial.	6
Malformed skeletons	Kinect was not able to track all the joints consistently during the recording.	5
The harness caused confusion	Kinect mistook the harness for a limb.	1
Total		58

5.2.8 A priori Sample Size Calculation

A priori sample size estimation was carried out to ensure there was enough power to detect differences between the two methods, using recordings made

while experimenting with the best position for the Kinect camera. Utilising the mean and standard deviation of this data, the sample size required for each trial was calculated, using G*Power. The results are shown in Table 5.3, along with the actual sample size used for analysis. In each case the sample size used exceed the number calculated from G*Power.

Table 5.3: **A priori power calculations** G*Power was used to calculate the sample size required for 95% power. The data came from an initial study, used to ensure the placement of the Kinect camera was correct.

	Sample size @0.95 power	Actual Sample Size
a) Quiet standing eyes open	12	44
b) Quiet standing eyes closed	11	48
c) Surround moving eyes open	29	50
d) Support moving eyes open	45	50
e) Support moving eyes closed	5	48
f) Support & surround moving eyes open	11	48

5.2.9 Statistical Tools

The main analysis used in this study was the Bland-Altman test for agreement between methods [19]. In addition, several supporting analysis were carried out. below are details of the tools used for each analysis

- Descriptive statistics and t-tests were carried out using SPSS (v. 21. IBM, US). Significance was accepted at $p < 0.05$.
- Normality was assessed using the D'Agostino-Pearson [50] method, implemented in the scipy python library [210].
- Bland-Altman plots were created (Fig. 5.6), using all available data for each method, without averaging over repeated measures. Repeatability and Bland-Altman tests were carried out using the Analyse-it plugin for excel (v. 5.40.2).

5.3 Results

This section explains the test that were used to compare the two methods of assessing, upright postural sway.

5.3.1 Repeatability

Repeatability, also known as Precision, was calculated for each method, expressed as standard deviation (SD) and Repeatability Coefficient (CR), providing the 90% CI of standard deviation, so removing outliers [130]. Both the proposed pipeline and the Balance Master, show increasing variability with increasing balance challenge. With eyes open conditions showing the best agreement (Table. 5.4).

Table 5.4: **Repeatability of each method, Balance Master (BM) and the Proposed Pipeline (PP)**, has measured by the Standard Deviation (SD) and Repeatability Coefficient (CR).

	Method	SD (mm)	95% CR
a) Quiet standing eyes open	PP	0.85	2.35
	BM	0.88	2.45
b) Quiet standing eyes closed	PP	0.84	2.33
	BM	0.72	2.00
c) Surround moving eyes open	PP	1.19	3.31
	BM	1.14	3.16
d) Support moving eyes open	PP	1.50	4.17
	BM	1.49	4.15
e) Support moving eyes closed	PP	3.40	9.41
	BM	2.86	7.93
f) Support & surround moving eyes open	PP	7.37	20.43
	BM	7.94	22.00

5.3.2 Agreement of Postural Sway Measurement

As presented in many papers, initially, the two methods were compared using a Pearson correlation coefficient. The values generated from each method show a high correlation to each other. See Table 5.5 for details.

Table 5.5: **Pearson correlation coefficient between the two methods:** The Pearson correlation coefficient demonstrates a high correlation between the two methods

	Parson's r
(a) Quiet standing - eyes open	0.951
(b) Quiet standing - eyes closed	0.928
(c) Surround moving - eyes open	0.947
(d) Support moving - eyes open	0.929
(e) Support moving - eyes closed	0.930
(f) Support & surround moving - eyes open	0.977

However, correlation does not necessarily mean agreement. To explore further the relationship between the values generated by both methods, a set of plots was created which graph the two sets of values, one against the other. A line of equality was also plotted (solid black). If the two sets were in perfect agreement, values for each would lineup along this line. These plots are shown in Figure: 5.5. The dotted line is a trend line that shows the direction of the agreement. Bias between the two methods can be thought of as the space between the line of equality and the trend line. Broadly, the bias increases as the difficulty increase, but is there a way to quantify the bias? This is a question which Bland and Altman address in their 1986 paper [19]. The paper suggests a plot of the difference between the methods against their mean may be a better choice, as it is difficult to know the true value, so the mean of the two is the best estimate possible. This plot is known as the Bland-Altman plot.

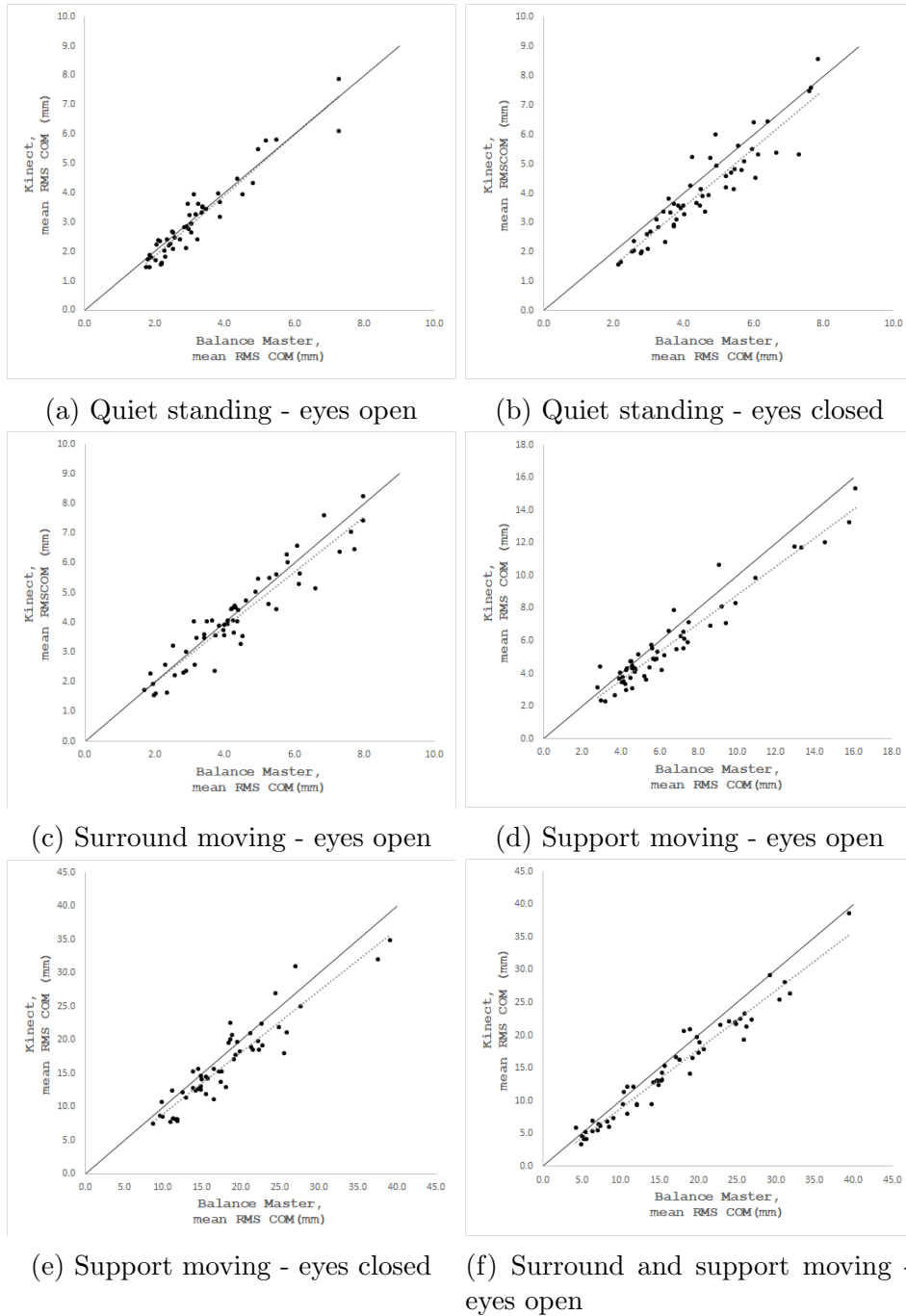


Figure 5.5: Correlation of postural sway derived from the SMART Balance Master and Kinect depth camera. The line of equality is shown (continuous line) as well as the linear regression (dotted line).

For a Bland-Altman plot to work well, the data should be normally distributed. More particularly, the difference between values for each method should be normally distributed. Table 5.7, shows that difference values were

normally distributed. However, Table 5.6 shows that the range of values produced by each method was not normal, in 3 out of the 6 cases. Bland and Altman noted that this is often the case when dealing with biological data. [19]

Table 5.6: **The normality of the difference between the two methods** given by D’Agostio-Pearson tests for normality.

	Balanced Master $\alpha = 0.05$	p	Proposed Pipeline $\alpha = 0.05$	p
a) Quiet standing eyes open	No	0.00	No	0.00
b) Quiet standing eyes closed	Yes	0.25	Yes	0.08
c) Surround moving eyes open	Yes	0.24	Yes	0.31
d) Support moving eyes open	No	0.00	No	0.00
e) Support moving eyes closed	No	0.00	No	0.01
f) Support surround moving eyes open	Yes	0.22	Yes	0.11

Table 5.7: **The normality of the difference between the two methods** given by D’Agostio-Pearson tests for normality.

	The difference between the two methods $\alpha = 0.05$	p
a) Quiet standing eyes open	Yes	0.83
b) Quiet standing eyes closed	Yes	0.16
c) Surround moving eyes open	Yes	0.28
d) Support moving eyes open	Yes	0.10
e) Support moving eyes closed	Yes	0.17
f) Support surround moving eyes open	Yes	0.41

Figure. 5.6) shows the output of the two methods plotted on a Bland-Altman plot. The bias can be quantified as the difference between 0 (the perfect agreement) and the mean difference between methods. This provides a measure of disagreement. The bias is plotted on the figure as a bold horizontal line. The Bland and Altman paper, suggest that ultimately the acceptable level of disagreement is up to interpretation and use case. The bias seen in this comparison is between 0.12mm (0.38) for quiet standing eyes open and 1.69 (1.63) for the most dynamic movement ((f) support and surround moving) even young, healthy people fall over when attempting it.

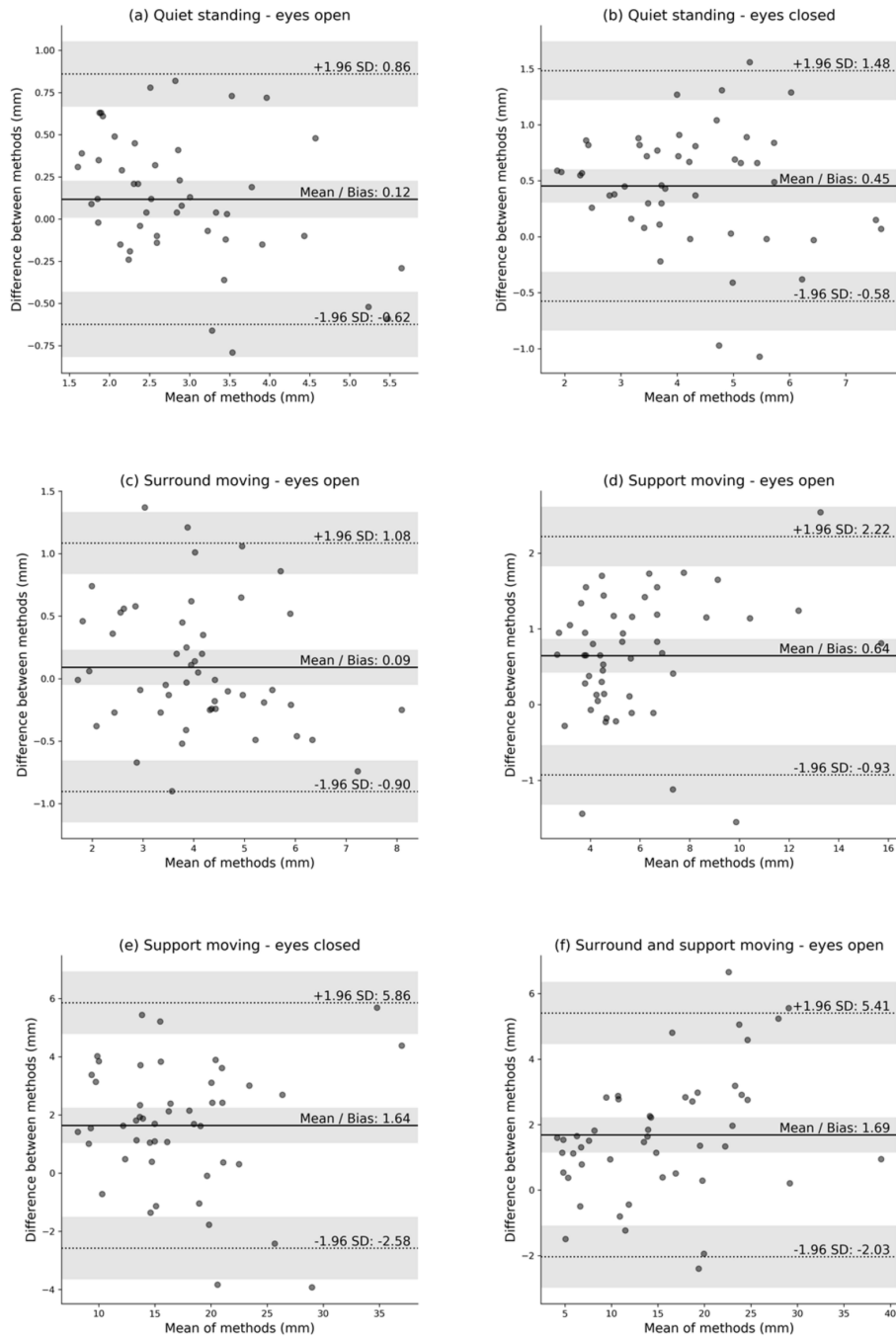


Figure 5.6: **Bland-Altman plot of the SMART Balance Master vs the Proposed Pipeline’s estimates of postural sway.** Bold horizontal line indicates the mean, dashed horizontal lines indicate two standard deviations from the mean. The shaded areas represent associated confidence intervals. The figures marked a-f represent the six conditions of the SOT test.

The most severe interpretation of the Bland-Altman plot is to carry out a one-sample t-test on the difference between all of the values for each condition, using a hypothesised difference of 0. When this test is carried out, only the eyes open conditions (a) and (c) show no significant difference. All of the results are summarised in table 5.8.

Table 5.8: **A summary of the agreement of postural sway derived from the two methods: Balance Master (BM) and the Proposed Pipeline (PP).** The mean, standard deviation (in brackets) - within each method, mean standard deviation (in brackets) - between the methods (bias), the 95% Confidence Interval (CI) and Limits of Agreement (LOA) and the significance of the t-test are shown. Eyes open conditions show no significant difference between methods, shaded in grey

	BM mean sway (mm)	PP mean sway (mm)	Mean difference BM-PP (bias) (mm)	95% CI for Bias	LOA	t-test (p)
a) Quiet standing eyes open	2.96 (0.94)	2.84 (1.10)	0.12 (0.38)	0.01 to 0.23	-0.62 to 0.86	0.16
b) Quiet standing eyes closed	4.45 (1.36)	3.99 (1.45)	0.45 (0.53)	0.30 to 0.61	-0.58 to 1.48	3.39E-07
c) Surround moving eyes open	4.10 (1.35)	3.99 (1.46)	0.09 (0.50)	-0.06 to 0.24	-0.90 to 1.08	0.21
d) Support moving eyes open	6.12 (2.84)	5.53 (2.68)	0.64 (0.82)	0.41 to 0.88	-0.93 to 2.22	9.10E-07
e) Support moving eyes closed	17.93 (6.29)	16.29 (6.37)	1.64 (2.18)	1.0 to 2.27	-2.58 to 5.85	3.99E-06
f) Support surround moving eyes open	16.12 (8.51)	14.43 (7.79)	1.69 (1.63)	1.13 to 2.24	-2.03 to 5.41	1.93E-07

5.3.3 Implications of the Increased Disagreement

The eyes open condition show the most similarity in repeatability. Looking at the bias between the two samples, conditions where the participant is standing on a firm surface, with eyes open, agree the best. However, as the balance challenge increases, either by removing vision or by perturbing balance by standing on a pivoting platform, the two results increasingly disagree.

The differences seen in these results may be explained by the fundamentally different approaches each method takes to estimate the CoM position and are discussed in the following section.

5.4 Discussion

In this study, a pipeline is proposed that is able to assess upright human postural sway. It makes use of an inexpensive and portable depth camera (Kinect V2), in combination with custom software that calculates CoM directly from skeleton joints. A pilot study was carried out, that compares the postural sway calculated from the proposed pipeline and a Balance Master, obtained during a Sensory Organisation Test (SOT).

The repeatability of each method was assessed (Table. 5.4), i.e. the agreement between repeated measures. The comparison was based on the (SD) and reliability coefficients (CR), for each method. Both methods show an increase in variability with task difficulty. The SOT test uses this variability to identify balance defects. In the SOT, the ratio of sway measured in quiet standing eyes closed (b) vs quiet standing eyes open (a) is used as a measure of the reliance on the somatosensory system to balance. This is also known as the Romberg Ratio. The reliance on the visual system is given by the ratio of support moving, eyes open (d) vs quiet standing eyes open (a) (the measures with the greatest similarity in the repeatability test) and the reliance on the vestibular system is given by support moving eyes closed (e) vs quiet standing eyes open (a). In all these assessments, quiet standing eyes open (a) is used as a baseline measure[204]. This matches the intuition that in a given population, the ability to balance with eyes open is essential and so well-practised. However, the ability to balance well, when challenged in unfamiliar ways produces a wider range of scores, seen as increasing variance, for the most challenging tasks.

The agreement between the two methods was examined, using Bland-Altman plots (Fig. 5.6), and one-sample t-tests, with an hypothesised, mean difference of zero. The plots show the mean difference between measures (bias) is smallest for the most every-day tasks (eyes open with the least challenge), but bias increases with increasing task difficulty. The t-test suggests that the two methods only agree well for eyes open conditions with a firm surface. To understand how these disagreements may occur, it is worthwhile considering two elements. 1) the way the human body reacts to quiet standing vs its reaction to perturbation. Winter, in his paper on human balance [265] noted that the human body pivots about the ankle (the ankle strategy) in quiet stance and about both hip and ankle in reaction to a perturbation (the hip strategy), such as standing on a pivoting platform. The Balance Master uses a pivoting

platform to induce perturbation in the tests which generated the biggest disagreement between methods (*d* to *f*). The induced perturbation, causing an increase in postural sway amplitude. Black et al. [18] noted that quite standing with eyes closed also increases postural sway amplitude, and so a switch to a hip strategy, for some people. In condition (b) quiet standing with eyes closed, an increase in bias was seen, compared to condition (a), although the increase is less than for conditions d-f, where the pivoting platform induces a greater postural sway. These observations lead to the second point. 2) The way the two methods estimate CoM is quite different. The Balance Master uses the most common method of estimating CoM, when using force plates, the inverted pendulum model, which ignores the hip and knee joints. In order to estimate the position of the CoM, using this method, an average value for the static incline of the body and an average offset from the position of the CoP, proportional to a person’s height, is used to relate the CoP to the CoM [204]. The proposed pipeline calculates CoM from the Kinect data, as described in equation 5.1; its estimate of CoM relates directly to the skeletal structure. Although it uses the values of only 3 joints (left hip, right hip and spine mid), these joints do not exist in isolation. Their movements are influenced directly by the movements of other anatomical structures such as the ankle, knee and hip joints, as well as the spine, arms and head. Previous reports questioned the assumptions used routinely to estimate CoM from CoP data. For example, Cretual et al. [48] suggested the single pendulum model should be used with caution to estimate CoM during more challenging conditions. Lafond et al. [118] also found error in this method of calculating CoM for more difficult poses, and Yeung et al. [269] demonstrated that Kinect performed better when recording more challenging balance tasks compared with force plates. Benda et al. [11] demonstrated that the accuracy of CoM estimated from CoP reduces with increased dynamics. As discussed in [19] it is difficult to get at the ground truth with any form of measurement. Using the theory of large numbers, the intuition is that a mean value of an event, measured by two methods, should come closer to that ground truth. However, this assumption can come in stuck when, as in the current case, the two methods of assessing a quantity are based on differing assumptions. So which assumption is closer to the ground truth?

Cretual et al. [48] point out the fact Winters original work [265] concerning the bodies control of CoM, discusses CoP as a way of understanding CoM,

based on the available technology at the time i.e. force plates. In the intervening time, CoP displacement and CoM are sometimes conflated, often because CoP is easy to measure directly using force plates. Even when CoM is used, too often, the single pendulum model is seen as a gold standard, when in fact it has many limitations. After examining many methods of estimating CoM, the paper's recommendation is the use of marker-based motion capture. The paper then goes on to say how this is not feasible for widespread clinical use because of cost and set up time.

Yeung et al. [269] carried out a three-way comparison between VICON (a well established marker-based motion capture system), Kinect V2 and a force plate (AMTI OR6 series, Advanced Mechanical Technology Inc. USA) to capture Total Body Centre of Mass (TBCM), under 4 conditions (1) Quite standing, on a firm support - eyes open, (2) Quite standing, on a firm support - eyes closed, (3) Quite standing, on a foam pad - eyes open, (4) Quite standing, on a foam pad - eyes closed. Based on the findings of [48]. There is strong evidence for saying that the VICON system gets closer to the ground truth concerning CoM. Yeung's paper found acceptable agreement between all three devices when measuring quite standing on a firm surface, but Kinect outperformed the force plate for Quite standing on a foam pad - eyes closed. The paper concludes that "Overall, Kinect is a cost-effective alternative to a motion capture and force plate system for clinical assessment of TBCM sway".

From the literature, there is evidence to say that the disagreement between methods is due to the limitations of the way the Balance Master measures CoM. Moreover, the values for CoM measured by the proposed method may be closer to the real CoM value. Certainly, it suggests values for CoM, provided by the proposed method, can be used in objective and useful measures of postural sway. Cost-effectively in locations away from the lab. Ultimately this is the aim of the work presented in this thesis.

However, future work is warranted to empirically demonstrate the reasons for the differences, seen here. This future work should provide a three-way cross-validation between CoM, measured using the proposed pipeline, a high quality marker-based system and a high quality force plate. Separately, future work should examine the potential of the proposed pipeline in the identification of individuals with balance impairments.

For now, one can say that the proposed pipeline shows no significant difference to the Balance master when measuring sway for quiet standing, eyes

open and quiet standing with a moving surround, eyes open.

This study was designed as a proof of concept and shows that assessment of postural control by depth camera is worth pursuing. Especially for applications where devices, such as the Balance Master, are too expensive or too cumbersome to be practical.

5.4.1 Limitations, Considerations and Future Work

(1) Our assessments were completed in laboratory conditions. In more informal settings, there is the potential for Kinect to confuse non-human elements, such as table and chair legs for human limbs. (2) The current study only includes healthy individuals. Future work should extend these initial findings, to a larger group, including individuals who suffer from recurrent falls. (3) In this study, the Balance Master was used to automate the SOT. The Balance Master uses pivoting force plates and a pivoting surround to produce challenging balance conditions. In order to further the cause of machine-based balance assessments in informal settings, future work will need to utilise more portable means of challenging balance. These include compliant foam pads and visual conflict domes. For instance, the Clinical Test of Sensory Integration and Balance (CTSIB) [217] uses these items to replicate the SOT test, without the need for costly equipment. (4) Balance Master's force plates are not as accurate as more modern designs. Future work should incorporate the newer plates, ideally as part of a three-way validation with a marker-based system.

5.5 Conclusion

In this study, a novel pipeline to assess upright postural sway is proposed. The pilot study compared the results of the proposed pipeline to results from a Balance Master, obtained from simultaneously testing 15, healthy individuals (age: 42.3 ± 20.4 yrs, height: 172 ± 11 cm, weight: 75.1 ± 14.2 kg, male = 11). Our initial findings suggest that the methods agree well for static assessments of balance, with eyes open, but the agreement reduces under more challenging conditions. That said, the pipeline warrants further investigation, with a larger cohort, including people for whom falling is an ongoing issue.

In chapter 6, the creation of a large dataset of clinical movements is detailed, captured using the pipeline discussed here. The dataset was recorded in the lab, community centres and private homes. It contains the recordings of healthy adults, healthy older and older fallers. Each participant was asked to carry out a range of movements regularly used in clinical assessment. It also contains rich medical, demographic and socioeconomic data

Chapter 6

KINECAL: A Dataset of Clinically Significant Movements

6.1 Introduction

There is a dichotomy at the heart of falls risk assessment. Lab-based research tends to use expensive equipment (force plates and marker-based motion capture) to quantify balance impairment. Even here, the costs mean that force plate data tends to dominate. As discussed in section 1.2.1, in clinical practice, observational tests are the dominant form of assessment. This means there is difficulty in translating state of the art research into clinical practice. In addition, clinical tests which have shown great utility in falls risk assessment, such as the [STS-5](#) and 3m walk, are difficult to instrument, using a force plate. These tests could be instrumented using marker-based motion capture, but even if one ignores the cost of such systems, the space required and set up time makes this option impractical for everyday assessment. Markerless motion capture could provide a practical solution to bridge the gap between research and practice. As demonstrated in this thesis, markerless solutions can provide joint angles, akin to those derived from marker-based solutions, and sway metrics, akin to those derived from force plates. As discussed in section 2.5.3, these systems are not without issues, but they can provide insight, difficult to achieve any other way, away from the lab. However, research into their use as an objective method of assessing balance, frailty and falls risk is under

researched. As is often the case, there is a chicken and egg situation when it comes to appropriate data on which to base the development of useful methods of assessment using these devices. The proposed dataset, named *KINECAL* addresses this need.

Kinect, and more generally [Red Green Blue + Depth \(RGB+D\)](#) data, is used extensively in HAR research [104]. This area of research has made huge strides in recent years, driven mainly by the availability of a diverse range of publicly available datasets [66, 211, 135]. On the face of it, it would seem this type of dataset would be useful in the clinical study of human movement. However, the focus is quite different. The purpose of HAR, is to identify a small set of human movements (actions) from a nearly infinite set of possibilities. The clinical use of motion capture seeks to quantify the quality of a prescribed set of movements. In addition, anonymised clinically-important, metadata such as age, height, weight, and meaningful labels of impairment are rarely included in HAR datasets.

Firman [66] in his review of RGB+D datasets, detailed 45 datasets, 44 of which were recorded using Kinect. Of these datasets, only one, the K3Da dataset [125] had movements that are useful in the assessment of balance disorders. This dataset was used in the work detailed in chapter 4. It has some metadata, but it is limited to age, height and weight.

Since the publication of the Firman paper [66], a few datasets have been created to address these issues. The Multimodal Dataset [15] contains clinically relevant movements (Timed get-up-and-go (TUG), a single 30 second chair stand, a 45 second unilateral stance, and 2-minute step test). However, the dataset comprises just 21 subjects, evenly split between young, and old and none of the participants had known movement impairment at the time of testing. The KIMORE Dataset [34], has 78 subjects, 44 healthy mean age 36.7 ± 16.8 years and 32 suffering from motor dysfunction mean age 60.44 ± 14.2 years. The dataset includes clinical scoring of the movements. However, the movements do not relate directly to falls likelihood. Table 6.1 provides a comparison between other datasets, containing clinical movements and *KINECAL*.

Table 6.1: **A comparison of datasets:** Comparing KINECAL to previous datasets that contain clinically significant movements, the advantages of KINECAL can clearly be seen.

	Multimodal Dataset [15]	K3Da [125]	KIMORE [34]	KINECAL
Number of participants	21	54	78	90
Depth		✓	✓	✓
Skeletons	✓	✓	✓	✓
Clinical evaluation			✓	✓
Falls related labels				✓
Postural Sway Metrics				✓
Rich metadata				✓
Recordings in informal settings				✓

6.2 Clinically Significant Movements

For KINECAL, 90 participants were recorded performing eleven movements commonly used in the clinical assessment of balance impairment, frailty and falls-risk. Details of how each movement was carried out are shown in Table 6.2. This list of movements was chosen because they are widely used singularly or in combination to assess falls-risk. [23, 256, 141] used the STS-5 to assess falls-risk. [75, 144, 129] found unilateral stance could distinguish between faller and non-fallers. 3m walk is used in many assessments of gait and falls risk 2.9, and [153] found an association between slow walking and falls risk. [187, 219] suggest the use of TUG as in falls risk assessment.

Together Quiet standing, eyes open (EO) and eyes closed (EC), Semi-tandem stance, Tandem stance, 3m walk and 5x sit to stand (STS-5) constitute the SPPB [83]. Another test that combines, Quiet standing on a firm surface and quiet standing on a foam surface, EO/EC is the mCTSIB [43]. Using KINECAL, Many more combinations can be synthesised from existing literature or invented anew.

The data from the recordings are made available as depth videos and joint positions (skeleton data). The RGB videos are not part of this dataset due to privacy concerns.

Upright stances are the most commonly used stance when assessing balance

using force plates. From the output of a force plate, a range of sway metrics can be derived. The KINECAL dataset also includes the most commonly used sway metrics, calculated for each recording. These are discussed later in section 6.6.

Table 6.2: A description of each movement in the dataset, and how they were explained to the participants.

	Description
5 times sit to stand (STS-5)	From a seated position, with your arms crossed over your chest, rise extending your legs fully, then sit down again. Repeat five times, as quickly as possible.
Quiet standing, Eyes open, Firm surface	Stand feet close together, eyes open and arms by your side. The test is terminated after 20 seconds, or if lost balance.
Quiet standing, Eyes closed, Firm surface	Stand feet close together, eyes closed and arms by your side. The test is terminated after 20 seconds, or if lost balance.
Quiet standing, Eyes open, Foam	Same instructions as for standing on a firm surface.
Quiet standing, Eyes closed, Foam	Same instructions as for standing on a firm surface.
Semi-tandem Stance	Stand with the toe of the back foot against the side of the heel of the front foot. Either foot can be forward, whichever is most comfortable. The test is terminated after 20 seconds.
Tandem Stance	Stand with the toe of the back foot against the back of the heel of the front foot. Either foot can be forward, whichever is most comfortable The test is terminated after 20 seconds.
Unilateral stance, Eyes open	Stand on one leg, whichever is most comfortable, with the other leg flexed 6 inches off the ground, hands by your side, eyes open. The test is terminated after 20 seconds or when the lifted leg touches the ground.
Unilateral stance, Eyes closed	Stand on one leg, whichever is most comfortable, with the other leg, flexed 6 inches off the ground, hands by your side, eyes closed. The test is terminated after 20 seconds or when the lifted leg touches the ground.
TUG	From a seated position, stand, and walk to a marker 3m away and return to the seat
3m walk	From a standing position, walk to a marker 3m away, and return to the seat

In designing KINECAL, previous studies relating to ageing and falls-risk were examined. Some studies have compared extreme populations, e.g. young (<35 years old) vs older (≥ 65 years old) populations [189, 114, 63]. This polarisation is useful if the question is, “how does postural sway change with age”. However, using this type of data alone can be problematic when applied to falls-risk, making it difficult to differentiate between factors relating to age and factors relating to falls-risk. Other studies [58, 151, 192] exclusively compared older populations of fallers and non-fallers. However, this approach can make it just as difficult to separate the two types of changes. The KINECAL dataset contains recordings from a range of ages, grouped to help aid the separation of falls-risk from age effects. As with the majority of studies, the proposed dataset uses self-reporting history of falls as a key label [160, 174, 199, 4]. Inspired by studies, such as [177, 200, 244]. The dataset has also been labelled using several well-known clinical tests. Falling into the impaired range ≥ 2 these test labelled an individual as being **Clinically-Impaired** (discussed in section 6.4.3). As well as labels of impairment, The dataset incorporates rich metadata, derived from a questionnaire which the over 65’s were asked to fill in, details of which are provided in section 6.7

6.3 Participants

90 participants were recorded for the KINECAL dataset, carrying out a range of well recognised clinical tests. The recordings were made using a Kinect V2 and custom software, written using Visual Studio 2015 and the Kinect SDK 2.0. Ethical approval was obtained from the University Research Ethics Committee (ethics approval ref: 020517-ESS-CC(1), and ref: SE161757). All participants provided written informed consent. Participants were excluded if they had any of the following:

- Treatment for cancer in the previous 2 years
- Joint replacement in the previous year
- Broken a leg, or hip bone or had a joint replaced, e.g. hip or knee, in the previous 2 years
- Any lower limb amputation

- Suffering from neuromuscular conditions (e.g. multiple sclerosis)
- Have been diagnosed with Alzheimer’s or Dementia
- Cannot read and communicate in English, either verbal or written.

6.4 Dataset Labelling

6.4.1 Self-reported Labels

All participants were asked the following question. “**Have you had any fall including a slip or trip in which you lost your balance and landed on the floor or ground or lower level in the past 12 months?**”. This is the standard question used when collecting falls history [258]. Possible answers were [**None, One, Two, Three, Four or more**].

Based on the answer they gave and their age, participants were split into the following groups:

- **Healthy-Adult**, members of this group, were all < 65 years old and gave the answer **None**
- **Non-Faller**, members of this group, were all ≥ 65 years old and gave the answer **None**
- **Self-reported-Faller**, members of this group, were all ≥ 65 years old and gave the answer **One, Two, Three, Four or more**

Table 6.3 details the numbers in each group, along with their age range and the gender split.

Table 6.3: **Grouping of Self-reported Labels:** This table shows the split between the different groups, in terms of mean age, total numbers and gender split. A description of each group is also included.

	Description	Age (\pm 95% CI)	Total Number	Male	Female
Healthy-Adult	< 65 years, no history of falls in the last 12 months	mean age 46.2 (\pm 22.7)	33	22	11
Non-Faller	\geq 65 years, no history of falls in the last 12 months	mean age 73.3 (\pm 11.7)	33	16	17
Self-Reported-Faller	\geq 65 years, reported \geq 1 falls in the last 12 months	mean age 72.6 (\pm 13.6)	24	15	9

6.4.2 Single and Multiple Fallers

Someone who answered **one** to the falls history question might simply be the victim of bad luck and not someone with a high likelihood of future falls. Someone who declared they have fallen multiple times is more likely to suffer future falls and could be thought of as a “true faller”. The **Self-reported-Faller** group can be further split, using this distinction into:

- **Self-reported-Faller_s**, members of this group, were all \geq 65 years old and gave the answer **One**
- **Self-reported-Faller_m** members of this group, were all \geq 65 years old and gave the answer **Two, Three, Four or more**

Table 6.4 details the numbers in each group, along with their age range and the gender split.

*Note: the **Self-reported-Faller_s** and **Self-reported-Faller_m** groups are made up of members of the **Self-Reported-Faller** group. Participants are multipally labelled, which provides flexibility in use. However, it is up to the individual researcher to decide how to best use these labels*

Table 6.4: **Grouped Sub-labelling of Self-reported-Fallers** : This table shows the split between the different single (_s) and multiple fallers (_m), in terms of mean age, total numbers and gender split. A description of each group is also included.

	Description	Age (\pm 95% CI)	Total Number	Male	Female
Self-reported-Faller_s	\geq 65 years, reported 1 fall, in the last 12 months	mean age 72.3 (\pm 15)	15	7	8
Self-reported-Faller_m	\geq 65 years, reported >1 fall, in last 12 months	mean age 73.1 (\pm 11.7)	9	2	7

6.4.3 Clinical labelling

As discussed in section 6.2 KINECAL consists of recordings of 11 movements, commonly used in clinical tests. The recordings provided an alternative means of labelling participants. Moreover, one which relates to clinical tests of physical impairment, hence clinical labelling.

The clinical labelling was a two-stage process. 1) The recordings, for each participant were played back and marked against accepted thresholds for physical impairment and falls risk, for each of the following tests: SPPB [85]; Slow 3m walk [153]; TUG [187, 219] and slow time to complete STS-5 [256]. 2). Any individual categorised as impaired for a least two of these tests was labelled **Clinically-Impaired** in the dataset. Using this method, six people were identified as belonging to the **Clinically-Impaired** group. Details of this group are shown in Table 6.5. The thresholds of impairment for each test are discussed below.

*Note: the **Clinically-Impaired** group is made up of members of the **Non-Faller** group (2) and **Self-Reported-Faller** group (4). Participants are multiply labelled, which provides flexibility in use. However, it is up to the individual researcher to decide how to best use these labels*

Table 6.5: **Details of the Clinically-Impaired group:** Details of, mean age, total numbers and gender split. A description of this group is also included.

	Description	Age (\pm 95% CI)	Total Number	Male	Female
Clinically-Impaired	\geq 65 years identified as impaired by \geq 2 clinical tests	mean age 80.3 (\pm 11.8)	6	1	5

6.4.3.1 Thresholds of Clinical-Impairment

This section details the thresholds applied to each clinical test.

SPPB

The SPPB test was carried out and scored using the protocol in Appendix A.1. Based on the SPPB score, the participant was classified using the scheme from [83] and detailed in Table 6.6. Those who were classified as having **Moderate Limitations** or **Severe Limitations** were marked as impaired, for this test.

Table 6.6: SPPB classification

Score	Classification
0-3	Severe Limitations
4-6	Moderate Limitations
7-9	Mild Limitations
10-12	Normal

3m walk

Quach et al. [193] used a 3m walk, alone to assess falls risk in an 18 month long, longitudinal study of 764 community-dwelling older people, mean age: 78 ± 5 years. They concluded that a walking speed of < 0.6 m/s was associated with an increased risk of falling inside. For a 3 m walk, this is equivalent to a time of > 5 seconds to complete. Applying this threshold to the 3m walks in KINECAL, anyone who took >5 seconds to complete the 3m walk, was marked as impaired, for this test.

STS-5

Another longitudinal study was undertaken by Ward et al. Over 4 years they studied 755 community-dwelling older people, mean age: 78.1 ± 5.4 years. The study looked at SPPB as a predictor of injurious falls. The conclusion was that the STS-5 alone was, enough to assess falls-risk. They suggested that a time to complete ≥ 16.7 second may be sufficient to identify those at risk of future falls. Applying this threshold to KINECAL, anyone who took >16.7 seconds to complete the STS-5 test was marked as impaired, for this test.

TUG

Shumway-Cook et al. [219] found TUG to be a powerful test for fallers. They used a population of 30 people, split evenly between two groups **Non-Fallers**, (no historic falls in last 6 months) mean age: 78 ± 6 years, **fallers** (≥ 2 falls in the last 6 months) by history mean age: 86.2 ± 6 years. They suggested that those who take > 14 seconds to complete the TUG are at **elevated risk of falls**. The Mc Kinly Laboratory [149] provides a reference for normative scores for TUG, synthesised from the Shumway-Cook paper and 3 more [187, 142, 119]. This reference extends the recommendations of Shumway-Cook et al. [219], as presented in Table 6.7. In spite of the other work, the value presented in [219] remains the current recommendation to identify those at **elevated risk of falls**. Applying this threshold to KINECAL, anyone who took >14 seconds to complete the STS-5 test was marked as impaired, for this test.

Table 6.7: **TUG classification**

Time	Classification
30 seconds	Problems, cannot go outside alone, requires gait aid
20 seconds	Good mobility, can go out alone, mobile without gait aid
14 seconds	Elevated risk of falls
10 seconds	Normal

6.5 Methods

This section details the methods used to compile the KINECAL dataset.

6.5.1 Experimental Setup

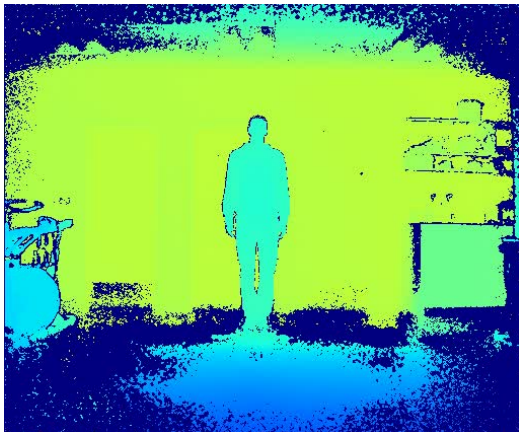
The Kinect camera was mounted on a tripod, at a height of 1.14m from the ground plane. Participants were asked to stand 3m from the camera for static stances, and 4m for TUG and 3m walk (the additional meter was needed to capture the entire 3m walking section).

6.5.2 Data recording

The participants were recorded using custom software i.e. Skel recorder, Skel recorder was initially written for the study detailed in chapter 5. Skel recorder was written using Visual Studio 2015 and the Kinect SDK 2.0. The software captures RGB, Depth and Skeleton data and stores it to disk. In chapter 5 the x axis was reversed, in recording this dataset the x axis was not reversed, as the participants were facing the Kinect. Figure 6.1 shows the view from the Kinect. This image was taken in laboratory conditions but other recording in KINECAL were made in more informal settings, such as church halls.



(a) RGB



(b) Depth



(c) Skeleton

Figure 6.1: **Kinect point-of-view** This figure is of a young participant in quiet stance. (a) is an RGB image, (b) is a depth image, (c) is the 25 joint skeleton, created by Kinect. *Permission was obtained from the person in the frame for their image to be used.*

6.5.3 Signal Processing

Filtering

Filtering was achieved using a Butterworth fourth-order zero-lag filter. The low-pass cut-off frequency was established as described by Winter [263]. The frequency used to filter the data, used in this thesis, was 8 Hz.

Pose Normalisation

Pose Normalisation, alters the coordinates system, from a camera-centred system to a person-centred system. To achieve this, each skeleton frame was aligned to the first frame of the recording, making the *SPINE_BASE* joint of the first frame of each recording $[0_x, 0_y, 0_z]$, using equation 6.1. All subsequent movements were related to this initial position.

$$p_{n,i}(x, y, z)^* = P_{n,i}(x, y, z) - P_{0,SPINE_BASE}(x, y, z) \quad (6.1)$$

where $p_{n,i}(x, y, z)^*$ represents the normalised position of the x, y, z axis of joint i in frame n . $P_{0,SPINE_BASE}(x, y, z)$ represents the position of the *SPINE_BASE* joint in the first frame of the recording, and $P_{n,i}(x, y, z)$ represents the positions of joint i in frame n .

6.5.4 Estimation of CoM

The position of the CoM was calculated as the 3D Euclidean mean of 3 joints of the Kinect skeleton: *HIP_LEFT*, *HIP_RIGHT*, *SPINE_MID*, shown in Figure 6.2, using equation 6.2. The x, y, z components were calculated individually and then concatenated to form a CoM triplet. Stacking these CoM triplets, over time, creates the **3D CoM time series**.

$$\begin{aligned} CoM_x &= \frac{HIP_LEFT_x + HIP_RIGHT_x + SPINE_MID_x}{3} \\ CoM_y &= \frac{HIP_LEFT_y + HIP_RIGHT_y + SPINE_MID_y}{3} \\ CoM_z &= \frac{HIP_LEFT_z + HIP_RIGHT_z + SPINE_MID_z}{3} \end{aligned} \quad (6.2)$$

$$CoM = [CoM_x, CoM_y, CoM_z]$$

where *HIP_LEFT*, *HIP_RIGHT*, *SPINE_MID* are Kinect joints, indicated on Figure 6.2. The Figure also shows the resultant position of the CoM for a single frame.

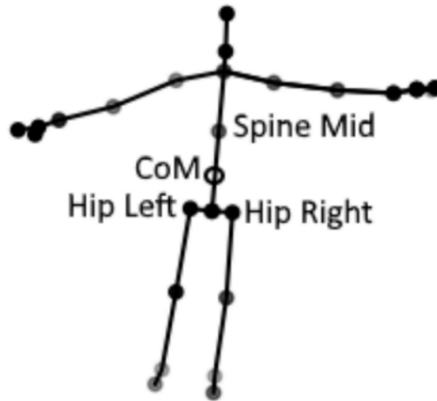


Figure 6.2: Kinect V2 Skeleton, the joints used to estimate CoM and the CoM position, are labelled.

6.6 Generation of sway metrics

The **3D CoM time series** is a useful asset for researchers, as is the full depth and skeleton data. However, to make the dataset more instantly useful to those more used to using force plates, a set of common force plate metrics has been included. In doing this the dataset simulates lab-based metrics, so in one dataset you have clinical and lab-based tests for, each participant.

Generally, when working with sway metrics derived from force plates, the CoM position is expressed in only two dimensions, i.e. the anatomical directions **AP** and **ML**. To provide equivalence between the two systems, the z-axis of Kinect was mapped to movement in the AP direction of the person being recorded. Similarly, the x-axis was mapped to movement in the ML direction. For this application, the y axis was ignored.

6.6.1 Sway Metric - Time Series

As discussed in section 5.2.5 it is good practice to centre the time series. Centring was achieved by subtracting the mean CoM position, for an entire recording, from the CoM value at each time step. This was done separately for movement in the AP and ML directions using equations 6.4. The mean position was calculated using equations 6.3.

The output of equations 6.4 were concatenated to produce the *AP* and *ML* time series. A third time series was calculated, which takes into account movements in the AP and ML directions in a single value. Known as the

resultant distance time series (RD), it was calculated as the vector distance from the mean CoM position to a pair of points in the AP and ML time series, at each time step. Values for each time step were generated using equation 6.5 and then concatenated to produce RD. Each of the calculated sway metrics was calculated using all three-time series.

$$ML_{raw}^- = \frac{1}{n} \sum_{i=1}^n ML_{raw}_i \quad (6.3)$$

$$AP_{raw}^- = \frac{1}{n} \sum_{i=1}^n AP_{raw}_i$$

$$AP_i = AP_{raw}_i - AP_{raw}^- \quad (6.4)$$

$$ML_i = ML_{raw}_i - ML_{raw}^-$$

$$RD_i = \sqrt{(ML_i)^2 + (AP_i)^2} \quad (6.5)$$

If the AP is graphed, against ML , the CoM path, for each recording is revealed. Figure 6.3 compares the CoM paths of members of the **Healthy-Adult** and **Clinically-Impaired** groups Standing Quietly with eyes open (blue line). The 95% confidence ellipse is also shown (red ellipse) (the calculation of the 95% confidence ellipse is detailed in section 6.6.2).

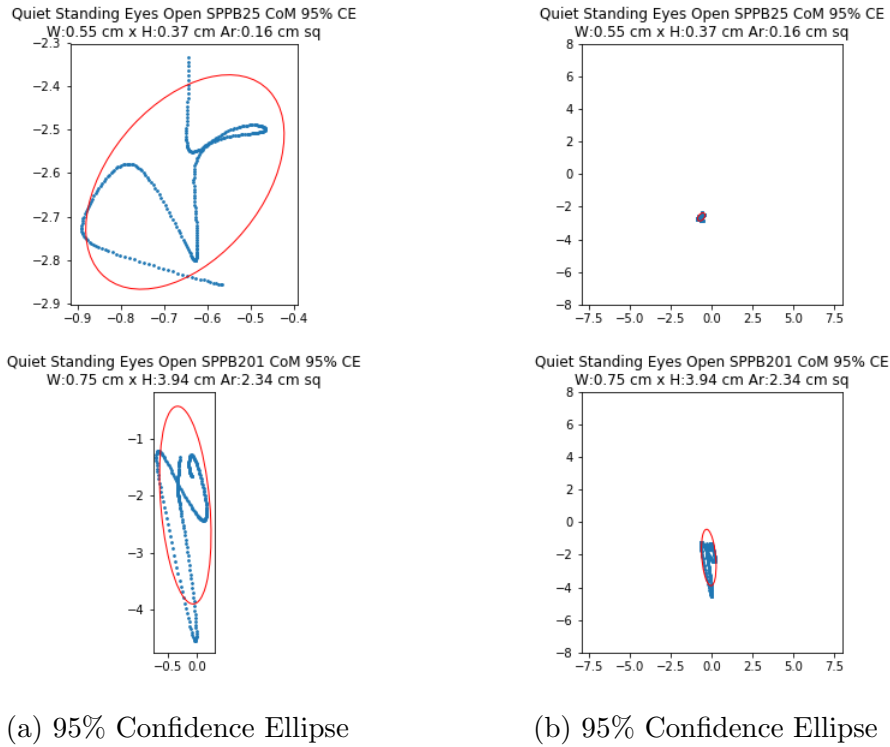


Figure 6.3: **95% Confidence Ellipse and CoM path:** This figure compares CoM paths and associated 95% Confidence Ellipses of a person labelled **Healthy-Adult** (SPPB25) to someone labelled **Clinically-Impaired** (SPPB201), Standing Quietly. Column (a) shows a tight view. Column (b) shows the 95% Confidence Ellipses plotted on the same scale.

6.6.2 Calculation of Sway Metrics

The following section gives details of the equations used to calculate the sway metrics. In these equations, $_AP$ relates to the AP time series (AP). For the most part, these equations were also used to calculate the metrics in the ML and RD directions. The exceptions being MFREQ and the 95% confidence ellipse.

Mean Distance of CoM

The most straightforward metric to understand, and to calculate, is the mean distance of the CoM. This is simply the mean, absolute distance moved, from the mean position of the CoM over the time of each trial. Equation 6.6 was used to calculate [Mean distance of the AP time series \(MDIST_AP\)](#)

$$MDIST_{AP} = \frac{1}{n} \sum |AP_i| \quad (6.6)$$

where AP is the AP time series, i is a single time step and n is the total number of times steps, in the time series. ML was used in place of AP , to calculate the [Mean distance of the ML time series \(MDIST_ML\)](#). RD was used in place of AP , to calculate the [Mean distance of the RD time series \(MDIST\)](#).

RMS Distance

The root mean squared process removes the sign and gives more prominence to values further away from the mean CoM position. Equation 6.7 was used to calculate [RMS distance of the AP time series \(RDIST_AP\)](#).

$$RDIST_{AP} = \sqrt{\frac{1}{n} \sum AP_i^2} \quad (6.7)$$

where AP is the AP time series, i is a single time step and n is the total number of times steps, in the time series. ML was used in place of AP , to calculate the [RMS distance of the ML time series \(RDIST_ML\)](#). RD was used in place of, AP to calculate the [RMS distance of the RD time series \(RDIST\)](#).

Total excursion (CoM Path Length)

Total excursion, is calculated by summing the distance between successive time steps. This is also known as the CoM path length. Equation 6.8 was used to calculate [Total excursions of the AP time series \(TOTEX_AP\)](#).

$$TOTEX_{AP} = \sum |AP_{i+1} - AP_i| \quad (6.8)$$

where AP is the AP time series and i is a single time step. ML was used in place of AP to calculate the [Total excursions of the ML time series \(TOTEX_ML\)](#). RD was used, in place of AP , to calculate the [Total excursions of the RD time series \(TOTEX\)](#).

Mean Velocity

Mean velocity is the total excursion divided by the time of the sample in seconds. Equation 6.9 was used to calculate the the [Mean velocity of the AP time series \(MVELO_AP\)](#).

$$MVELO_AP = TOTEX_AP/t \quad (6.9)$$

where *AP* is the AP time series and *t* is the time for the trial in seconds. *ML* was used in place of AP to calculate the [Mean velocity of the ML time series \(TOTEX_ML\)](#). *RD* was used, in place of, *AP* to calculate the [Mean velocity of the RD time series \(MVELO\)](#).

Mean angular frequency AP and ML

[Mean frequency of the AP time series \(MFREQ_AP\)](#) is the frequency, in Hz, of a sinusoidal oscillation with an average value of the mean *MDIST_AP* and a total path length of *TOTEX_AP*. This was calculated using equation equation 6.10.

$$MFREQ_AP = \frac{MVELO_AP}{4\sqrt{2}MDIST_AP} \quad (6.10)$$

where *MVELO_AP* is defined by equation 6.9 and *MDIST_AP* is defined by the equation 6.6. *MVELO_ML* was used in place of *MVELO_AP* and *MDIST_ML* was used in place of *MDIST_AP* to calculate the [Mean frequency of the ML time series \(MFREQ_ML\)](#)

Mean Angular Frequency

[Mean frequency of the RD time series \(MFREQ\)](#) is the mean angular frequency is the rotational frequency in Hz. This is the number of revolutions per second of the CoM, if it had travelled the total excursion around a circle with a radius of the mean distance. It is calculated using values derived from *RD*, given by Equation 6.11

$$MFREQ = \frac{MVELO}{2\pi MDIST} \quad (6.11)$$

where *MVELO* is defined by equation 6.9 and *MDIST* is defined by equation 6.6

95% confidence elliptical area

The **95% Confidence Area (AREA-CE)** is given by the set of equations below (6.12). The elliptical area is an estimate of the area described by the maximum and minimum AP and ML values of the time series. To reduce the effect of rapid changes in direction, this value is scaled to 1.96 standard deviations of the mean values.

$$p = \frac{COV_{AP,ML}}{\sigma_{AP}\sigma_{ML}}$$

$$AP_r = \sqrt{1 - p}\sigma_{AP}1.96 \tag{6.12}$$

$$ML_r = \sqrt{1 + p}\sigma_{ML}1.96$$

$$area = \pi AP_r ML_r$$

where p is the Pearson correlation coefficient, ML_r is the ML elliptical radius scaled to the 95% Confidence Interval (CI), and AP_r is the AP elliptical radius scaled to the 95% CI.

Table 6.8, shows the file format of the metric file, for Quiet standing, eyes open. *Note, due to size the page width of the is document, not all of the calculated metrics are shown.*

Table 6.8: Truncated Table of Sway Metrics: This table provides a truncated view of the sway metric data, comparing just two participants over a selection of metrics, for quiet standing, eyes open. *Note: **Group HA:** Healthy-Adult, **FHm:** Self-reported-Multiple-Faller, **Sex 0:** Male, **1:** Female, **Self-Rep:** Self-Reported-Faller, **Clin-imp:** Clinically-Impaired.*

PART_ID	GROUP	AGE	SEX	Self-Rep	Clin-imp	MDIST_ML	MDIST_AP	MDIST	TOTEX_ML	TOTEX_AP	TOTEX	AREA_CE
SPPB25	HA	25	0	0	0	0.089714	0.110692	0.15911	0.937892	1.088324	1.648861	0.16
SPPB201	FHm	81	1	1	1	0.189479	0.662605	0.724661	2.268462	9.155649	9.627409	2.34

6.7 Questionnaire

In addition to the falls history question, all participants ≥ 65 years were asked to complete a wide-ranging questionnaire. The question covered the following topics: Demographics; Health status (current disease, current medication); Smoking; Alcohol; Grip strength - anecdotal; Mood; Menopause; Current and historical physical activity; Bone fractures; Joint Pain; Joint Replacements; Falls history; Confidence in every-day-tasks and details of any walking aids. The full details of this questionnaire can be found in Appendix [B.1](#)

6.8 Open Source Code

It is our intention that on the release of the KINECAL dataset, the code used to record the data and calculate the sway metrics will also be released. This is done to allow for the expansion of the dataset by other researchers.

Skel-Recorder

Skel-Recorder was used to capture Kinect data and save it to disc.

Skel-Metrics Python Library

The skel-metrics Python library allows Kinect skeletons to be converted in to the range of metrics described in section [6.6](#). In addition, it also contains methods to filter and normalise the skeletons.

Summary of the contributions of the KINECAL dataset

The hope that the dataset will provide a useful resource for fellow researchers and will lead to solutions for objective balance assessments, which can be carried out away from the lab.

Here is a list of contributions, made by the KINECAL dataset

- Dataset of 90 participants
- The recordings were made in the lab and in more informal conditions, such as private homes and a community centre.

- Labels: self-reporting falls history and clinically assessment.
- Rich metadata, including socio-economic and medical data
- Raw skeletal and depth recordings (RGB images are excluded to protect the privacy of participants)
- Common sway metrics for each participant

6.9 Conclusion

The assessment of physical impairment is an increasingly important field. With an ageing worldwide population, the early identification of those at risk of injurious falls is of particular import. Currently, the majority of balance assessments are carried out by trained professionals, using clinical test, which take a substantial amount of time to complete. This puts additional strain on already stretched health services. The adoption of automated methods of balance assessment could help to ease that burden. One approach to automation is to use devices that can achieve markerless motion capture, such as the Kinect camera, which are portable, easy to set up and can be used outside of the lab. However, in order to progress such research, there is a need for datasets that researchers can use to avoid the time-consuming process of collecting their own data. The KINECAL dataset addresses this need.

Chapter 7

An Investigation of Sway Metrics Associated With Falls

7.1 Introduction

In this chapter the sway metrics, included in the KINECAL dataset are investigated. In KINECAL, sway metrics have been calculated for each of the upright stances (quiet standing on a firm surface [EO/EC](#), quiet standing on foam [EO/EC](#), semi-tandem stance [EO](#), tandem-stance [EO](#), [ULS EO/EC](#)). These are the most commonly used stances to assess balance, in a lab situation, using force plates.

While a range of stances and metrics are included, in KINECAL, not everyone could complete all of the upright stances. These included people labelling themselves as Non-Fallers who could not complete the single leg stand or the tandem stance. One very impaired individual could not complete the quiet standing with eyes closed for 10 seconds. When using a scoring paradigm such as the SPPB score, counting a fail as 0, has a purpose, but when considering sway metrics, it is difficult to extract meaning from a failed trial. The ultimate goal is to develop an objective machine model to help in the diagnosis of falls-risk and frailty. Therefore, this study opted to examine the one upright stance that was completed universally and so has the most data, i.e. quiet standing [EO](#). Even quiet standing on foam [EO](#) requires the orchestration of the whole musculoskeletal system as discussed in section [1.1](#), and so provides insights into the physical indications of impairment and falls-risk

Age and frailty are associated, as signs of frailty tend only to become an

issue over the age of 65. However, increasing age does not necessarily mean increasing frailty. This chapter considers if a distinction can be made between sway metrics related to normal ageing vs those related to falls-risk. In addition, using a series of machine models, the KINECAL Clinical labelling schema is validated, and the use of a machine model, which could be used to identify those with a high falls-risk, is explored.

7.2 Sway Metrics Identification

7.2.1 Sway Metrics

All of the upright stance of the KINECAL dataset have common, precalculated sway metrics for each trial, (although, many more types of metric can be created from the raw data). In this investigation, quiet standing EO was used.

Table 7.1 shows the abbreviations used for each metric, alongside a description of each metric. The abbreviations follow the form laid out in Prieto et al. [189]

Table 7.1: **Table of sway metrics:** This table details the sway metrics from the KINECAL dataset. RD refers to the Resultant Distance, AP Anterior-posterior and ML Medio-lateral directions, details of how these metrics were calculated can be found in section 6.6

	Description
MDIST	Mean distance of the RD time series
RDIST	RMS distance of the RD time series
MVELO	Mean velocity of the RD time series
TOTEX	Total excursions of the RD time series
MFREQ	Mean frequency of the RD time series
MDIST_AP	Mean distance of the AP time series
RDIST_AP	RMS distance of the AP time series
MVELO_AP	Mean velocity of the AP time series
TOTEX_AP	Total excursions of the AP time series
MFREQ_AP	Mean frequency of the AP time series
MDIST_ML	Mean distance of the ML time series
RDIST_ML	RMS distance of the ML time series
MVELO_ML	Mean velocity of the ML time series
TOTEX_ML	Total excursions of the ML time series
MFREQ_ML	Mean frequency of the ML time series
AREA_CE	95% Confidence Area

7.2.2 Participant groups

Participants of the KINECAL dataset are grouped age-wise, i.e. below and above 65 years. Those ≥ 65 years are further split by falls-risk, i.e. Non-Fallers, by history, Fallers by history and those at risk of falls by clinical test. Table 7.2 details the the criteria for inclusion into these groups.

Table 7.2: **Participant groups used in this investigation:** The groups shown here are the standard groups of participants from the KINECAL dataset, along with a description of the criteria for inclusion.

	Description
Healthy-Adult	< 65 years, no history of falls in the last 12 months
Non-Faller	≥ 65 years, no history of falls in the last 12 months
Self-reported-Faller	≥ 65 years, reported ≥ 1 fall in the last 12 months
Clinically-Impaired	≥ 65 years identified as impaired by ≥ 2 clinical tests

7.2.3 Outlier Detection

In this investigation, the **Healthy-Adult** and **Non-faller** groups were used as a baseline in this analysis. To ensure the sample was representative, those whose sway lay outside the normal range, for these groups, were excluded. The chosen method of outlier detection was Median Absolute Deviation (MAD), with a threshold level of 3.5. MAD was used in preference to 1.96 SD from the Mean value because the Median is less affected by sample size [131].

7.2.4 Assessment of Significant Difference, Between Participant Groups

To identify sway metrics that could be useful in identifying fallers, a set of pairwise comparisons was made. This was done in two parts. 1) the first comparison identified metrics that are significantly different with age. This was achieved by comparing groups of healthy individuals of different ages

(**Healthy-Adult** and **Non-Faller** groups). 2) the second comparison identified metrics which show significant difference between groups of fallers (**Self-reported-Fallers, Clinically-Impaired**) and non-fallers (**Healthy-Adult , Non-Fallers**). By carrying out the investigation in this fashion, metrics that are associated with both age and falls-risk could be discounted, for inclusion in the machine model detailed in section 7.3. This is only achievable because of the structure of the KINECAL dataset.

To assess the difference between groups, a two-step process was used, on a per metric basis. 1) The normality of the distribution of the metric in the two groups being considered, was assessed using the D'Agostino-Pearson method, implemented in the scipy python library (`scipy.stats.normaltest`). 2) Based on the result of step 1), if the distributions were normal, a t-test was used. Otherwise a Mann Whitney U test was performed. Both of these tests were carried out using the appropriate method from the `scipy.stats` python library.

Significance was accepted at a level of $p < 0.05$. However, candidate metrics, those deemed useful for the assessment of falls-risk by a machine model, were only accepted at the $p < 0.01$ level, although some metrics showed a significant difference at the $p < 0.001$ level.

7.2.5 Age-related Sway Metrics

7.2.5.1 Grouping of Participants

For this comparison, a new group **Healthy-Young**, was created. This group was made up of members of the **Healthy-Adult** group who were < 35 years old. The **Healthy-Young** group is not a permanent feature of the dataset but was created to relate the results shown here to the literature.

These two groups were then compared to the **Non-Faller** group. The makeup of these groups is shown in Table 7.3, after outliers have been removed. In this investigation, members of the **Healthy-Young** group also belong to the **Healthy-Adult** group. However, no members of the **Non-Faller** group belong to either of the other two groups.

Table 7.3: **Participant groups used:** The groups described here were used in the identification of metrics useful in falls-risk assessment. The numbers shown here were after outliers had been removed. Each participant belonged to only one group.

	Description	Age (\pm 95% CI)	Total Number	Male	Female
Healthy-Young	< 35 years, no history of falls in the last 12 months	mean age 28.2 (\pm 8.4)	6	4	2
Healthy-Adult	< 65 years, no history of falls in the last 12 months	mean age 46.0 (\pm 22.7)	30	20	10
Non-Faller	\geq 65 years, no history of falls in the last 12 months	mean age 72.6 (\pm 10.1)	29	15	14

7.2.5.2 Results

Healthy-Young vs Non-Fallers

The results, detailed in this section, are summarised in Table 7.4. The first step was to compare young vs older, in a similar way to other studies [189, 87], that consider age-related changes of healthy individuals.

To achieve this, the **Healthy-Young** group, was compared to the **Healthy-Adult** group. Column 1 of Table 7.4, shows the results for this polarised case. MFREQ_AP, TOTEX, MEVLO, TOTEX_AP and MEVLO_AP were found to be significantly different, between these groups. These findings are in line with those found in the literature [189, 87].

Healthy-Adult vs Non-Fallers

The group in the KINECAL dataset, regarded as being a healthy norm, is the **Healthy-Adult** group (non-fallers < 65). This group has a mean age of 46 (± 22.7 years), the oldest member being 64 years old.

When comparing the **Healthy-Adult** group to the **Non-Faller** group (who have a mean age of 72.6 ± 10.1 years), the significant difference in TOTEX_AP and MEVLO_AP was lost, and the significance level of MFREQ_AP was reduced. However, MFREQ_AP, TOTEX, MEVLO remain significantly different between the healthy populations, either side of 65 years of age.

Table 7.4: **Results of analysis of the difference in sway metrics, between different groupings:**. The shading of the background signifies the degree of significance (light grey = $p < 0.05$, dark grey = $p < 0.001$).

	Healthy-Young * vs Non-fallers ‡	Healthy-Adult † vs Non-fallers ‡
MFREQ_AP	0.00085	0.01085
TOTEX	0.02058	0.02408
MVELO	0.02058	0.02408
MVELO_AP	0.02091	>0.05
TOTEX_AP	0.02091	>0.05
MFREQ_ML	>0.05	>0.05
MVELO_ML	>0.05	>0.05
TOTEX_ML	>0.05	>0.05
AREA_CE	>0.05	>0.05
RDIST_AP	>0.05	>0.05
RDIST	>0.05	>0.05
MDIST	>0.05	>0.05
MDIST_AP	>0.05	>0.05
MDIST_ML	>0.05	>0.05
RDIST_ML	>0.05	>0.05
MFREQ	>0.05	>0.05

footnote:

* **Healthy-Young** < 35 years old, no history of falls in the last 12 months

† **Healthy-Adult** < 65 years old, no history of falls in the last 12 months

‡ **Non-Fallers** \geq 65 years old, no history of falls

7.2.6 Falls-Risk related Sway Metrics

This section considers if there are sway metrics that align better with impairment and falls-risk rather than age. To achieve this, two healthy groups (**Healthy-Adult** and **Non-Fallers**) were independently compared to the two impaired groups (**Self-reported-Fallers** and **Clinically-Impaired**). The results detailed in this section are summarised in TABLE 7.6. For the sake of brevity, the metrics identified above as most likely to increase with age (MFREQ_AP, TOTEX, MEVLO, TOTEX_AP and MEVLO_AP) shall, from now on, be referred to as *age-biased metrics*

7.2.6.1 Grouping of Participants

For this investigation the participant groups **Healthy-Adult**, **Non-Faller**, **Self-reported-Faller** and **Clinically-Impaired** were used. Table 7.5 shows the makeup of each group, after outliers have been removed. In this investigation, group membership was exclusive, and no participant appears in more than one group.

Table 7.5: **Participant groups used:** The groups described here were used in the identification of metrics useful in falls-risk assessment. The numbers shown here were after outliers had been removed. Each participant belonged to only one group. In this investigation, group membership was exclusive, and one participant does not appear in more than one group.

	Description	Age (\pm 95% CI)	Total Number	Male	Female
Healthy-Adult	< 65 years, no history of falls in the last 12 months	mean age 46.0 (\pm 22.7)	30	20	10
Non-Faller	\geq 65 years, no history of falls in the last 12 months	mean age 72.6 (\pm 10.1)	29	15	14
Self-reported-Faller	\geq 65 years, reported \geq 1 fall in the last 12 months	mean age 71.6 (\pm 13.8)	20	9	11
Clinically-Impaired	\geq 65 years identified as impaired by \geq 2 clinical tests	mean age 80.3 (\pm 11.8)	6	1	5

Table 7.6: **Results of analysis of the difference in sway metrics between levels of impairment:** The shading of the background signifies the degree of significance (light to dark grey $p < 0.05$, $p < 0.01$, $p < 0.001$). The final column gives a grouping for the metrics.

	Healthy-Adult † vs Clinically Impaired ◊	Healthy-Adult † vs Self-reported-Fallers *	Non-fallers ‡ vs Clinically Impaired ◊	Non-fallers ‡ vs Self-reported-Faller *	
MFREQ_AP	0.00748	0.00038	> 0.05	0.04787	Differences related to age and impairment
TOTEX	0.00067	0.00725	0.02359	0.02223	
MVELO	0.00067	0.00725	0.02359	0.02223	
MVELO_AP	0.00067	0.00605	0.01246	0.01393	
TOTEX_AP	0.00067	0.00605	0.01246	0.01393	
MFREQ_ML	0.00404	> 0.05	> 0.05	> 0.05	No difference between \geq 65 year old groups
MVELO_ML	0.00878	0.04726	> 0.05	> 0.05	
TOTEX_ML	0.00878	0.04726	> 0.05	> 0.05	
AREA_CE	0.00278	0.00345	0.00842	0.00822	Target
RDIST_AP	0.00430	0.03910	0.00165	0.01986	
RDIST	0.00509	0.04650	0.00636	> 0.05	
MDIST	0.00602	0.00724	0.00878	0.00800	Target
MDIST_AP	0.00790	> 0.05	0.00112	0.01638	
MDIST_ML	> 0.05	> 0.05	> 0.05	> 0.05	
RDIST_ML	> 0.05	> 0.05	> 0.05	> 0.05	
MFREQ	> 0.05	> 0.05	> 0.05	> 0.05	

footnote:

† **Healthy-Adult** < 65 years old, no history of falls in the last 12 months

‡ **Non-Fallers** \geq 65 years old, no history of falls in the last 12 months

* **Self-reported-Fallers** \geq 65 years old, reported \geq 1 falls in last 12 months

◊ **Clinically-Impaired** \geq 65 years old, identified as being impaired by \geq 2 clinical tests

Healthy Groups vs High Falls-risk Groups

Looking across all of the comparisons in 7.6, differences in the *age-biased metrics*, seen in the first set of comparisons, can be seen to be not entirely related to age alone. Differences related to impairment and falls-risk can also be seen. However, the smallest difference in significance, is seen when comparing

groups, whose ages are closest together. I.e. either of the groups containing individuals, with high falls-risk. The age difference between **Clinically-Impaired**) vs **None-Faller** is 7.7 years (column 3). for **Self-reported-Fallers** and **None-Faller** it is -1 year (column 4) Now consider, the age difference between **Clinically-Impaired** and **Healthy-Adult**, 34.3 years (column 1), and between **Self-reported-Fallers** and **Healthy-Adults**, 25.6 years (column 2).

Hence, changes in these metrics seem to be affected by both age and impairment. However, there is a bias towards age. As discussed in 1.1, age-related changes, ultimately lead to frailty. However, some people are better at adapting to those changes. Future work may examine this in a cross-discipline fashion to understand the processes which underpin this, but this is beyond the current line of enquiry.

Piirtola et al. [185] points to an increase in ML sway being related to impairment, and looking at column 1 and 2, it would seem that MFREQ_ML, MVELO_ML and TOTEX_ML could be good candidates for metrics relating to impairment. However, column 3 and 4 show no significant difference in these metrics, between **Non-Fallers** and either of the groups showing high falls-risk (**Self-reported-Fallers** or **Clinically-Impaired**).

The only metrics that showed significant difference at the $p < 0.01$ level, when comparing Healthy individuals of any age to **Self-reported-Fallers** or **Clinically-Impaired** were AREA_CE and MDIST.

In summary, MFREQ_AP, TOTEX, MEVLO, TOTEX_AP and MEVLO_AP showed significant difference associated with age and falls-risk. AREA_CE and MDIST showed the highest significant difference associated with falls-risk. From now on, AREA_CE and MDIST will be referred to as *falls-risk-biased metrics*. In the next section, the identified sway metrics are used to assess the effectiveness of the labelling scheme, by training machine models to identify those who would be classified as having a high falls risk, based on self-reporting and clinical-labelling 6.4.3.

7.3 Machine Learning Methods

7.3.1 Sliding Window

When posturographic metrics are used for human interpretation, the values are averaged over the entire length of the trial, such that each provides a single, easy to understand value, per person, per metric. Machine learning models require many more examples in training. To generate a range of similar, but not identical values for each trial, a sliding window method was used to generate 10 values, per metric, for each participant. The size of the window was 300 frames (out of a total of 600 frames for each recording), with an overlap of 10 frames.

7.3.2 Monte Carlo Cross-Validation and Rebalancing

While the KINECAL dataset is the largest of its type, it is still small compared to the total population of fallers. A semi-synthetic bootstrap approach was used to model values one might expect to see in a larger population.

That is to say, bootstrapping [53] was used, to produce a family of samples which, using the law of large numbers, will tend towards the values you might expect in a larger sample. This method is also known as Monte Carlo Cross-Validation (MCCV) [213]. This technique was used in combination with SMOTE-ENN. In common with many medical datasets, KINECAL is unbalanced, i.e. there are many more examples of unimpaired, when compared to impaired. Unfortunately, Most machine models, used for classification, do not train well with unbalanced data. In order to rebalance the training data, SMOTE-ENN was used. SMOTE-ENN combines the SMOTE algorithm [38] with Wilson’s Edited Nearest Neighbour (ENN) [262], to remove outliers from the synthetic data, effectively increasing the boundary between classes. *Note, SMOTE-ENN was used to aid training alone, the test subset was unprocessed and so reflects the distribution of the KINECAL dataset.* The overall method is outlined in Figure 7.1, the caption provides step-by-step details of the process.

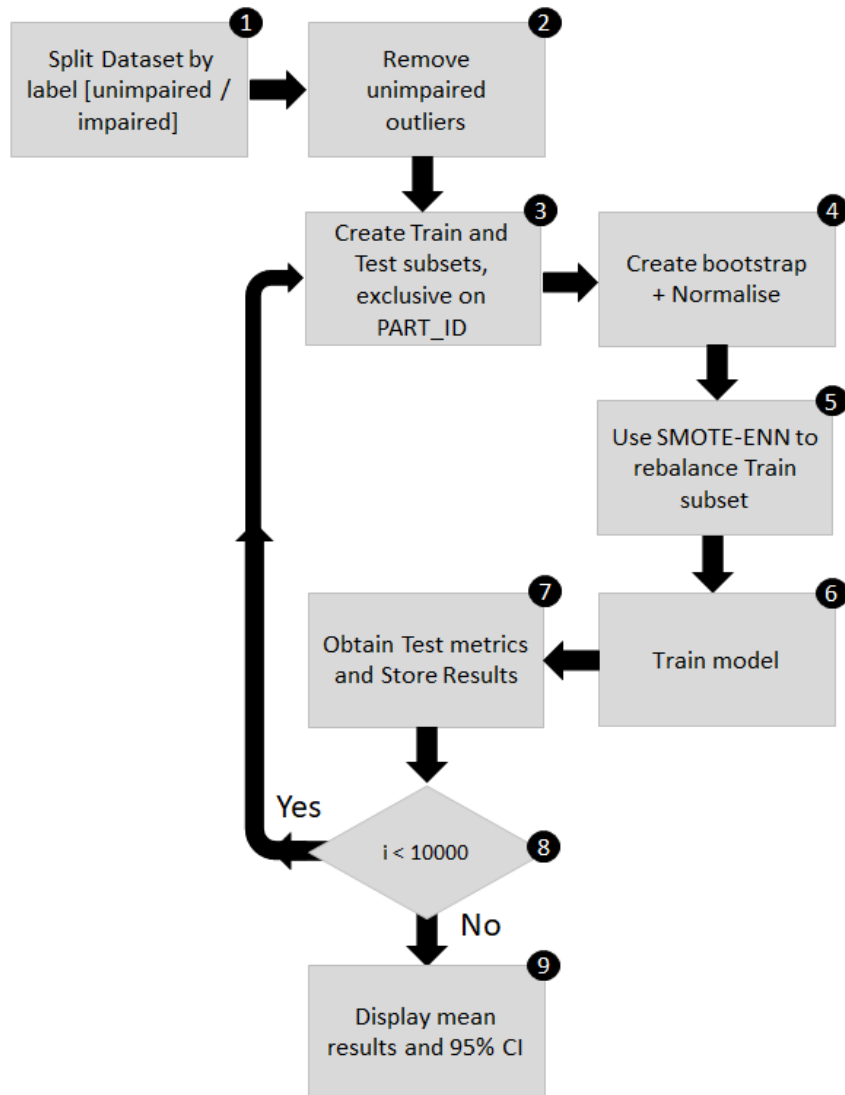


Figure 7.1: **A flowchart of the bootstrap process.** 1) The dataset was split into unimpaired and impaired groups; 2) Outliers in the unimpaired group were removed (using the same outlier detection method as used to identify candidate metrics); 3) Train and Test subsets were created, split on Participant ID (PART_ID) and records assigned to each subset randomly, such that in every iteration a new set is drawn, without replacement. However, no participant was present in both Train and Test subsets; 4) Random re-sampling with replacement was used to create bootstraps of the original data and normalised (using the normalize method of sci-kit learn [225]); 5) The bootstraps were rebalanced using SMOTE-ENN [126]; 6) The model was trained; 7) The test set was used to obtain result metrics, for that iteration and these results were stored; 8) This process continued for 10,000 iterations; and 9) At the end of 10,000 iterations, mean values for all results and 95% confidence intervals were displayed.

7.3.3 Experiments

In the first part of this investigation, two *falls-risk-biased metrics* were identified (MDIST and AREA_CE). There was significant different in the values of the *falls-risk-biased metrics*, between the two healthy groups (**Healthy-Adult** and **Non-Faller**) and the two groups which contain individuals with a high falls-risk (**Self-reported-Faller** and **Clinically-Impaired**). In the second part of this investigation, two subsequent experiments were performed to 1) compare the effectiveness of clinical labels vs self-reporting in identifying fallers, and 2) estimate the diagnostic accuracy of the best model, against a larger population.

To achieve this, a bootstrapping method, outlined in Figure 7.1, was used to find a suitable discriminator. The ability of several classification models (Logistic regression, Random Forest, Multilayer Perceptron (MLP) neural net, KNN classifier, SVM, and Gaussian Naive Bayes (GNB)) to identify fallers were assessed. The GNB, Logistic regression and MLP models gave equally good results. The results of the GNB model are shown below. Four models were trained covering the two labelling schemes (**Self-reported-Faller** and **Clinically-Impaired**) and the two fit groups (**Healthy-Adult** and **Self-reported-Faller**)

7.4 Results

Considering the confusion matrices in Figure 7.2 and the model results in Table 7.7, models trained with the Clinically impaired labels provided better Recall (the measure of how many impaired cases are correctly identified), also known as Sensitivity, and Specificity (the measure of how many unimpaired cases are correctly identified), when compared to models trained with the Self-reported-Fallers labels. Also, those trained using **Healthy-Adult** achieve better scores than those trained with **Non-Faller**.

Table 7.7: **The mean results after rounds of 10,000 bootstrapping:**. The results show the mean value and the 95% CI

	Self-reported-Fallers vs Non-Fallers	Clinically Impaired vs Non-Fallers	Self-reported-Fallers vs Healthy-Adult	Clinically Impaired vs Healthy-Adult
Mean Accuracy	0.54 ±0.18	0.70 ±0.21	0.64 ±0.17	0.76 ±0.18
Mean Specificity	0.56 ±0.34	0.70 ±0.30	0.71 ±0.24	0.78 ±0.23
Mean Recall	0.52 ±0.32	0.68 ±0.45	0.57 ±0.30	0.72 ±0.46
Mean ROC AUC	0.58 ±0.23	0.74 ±0.34	0.70 ±0.20	0.81 ±0.30

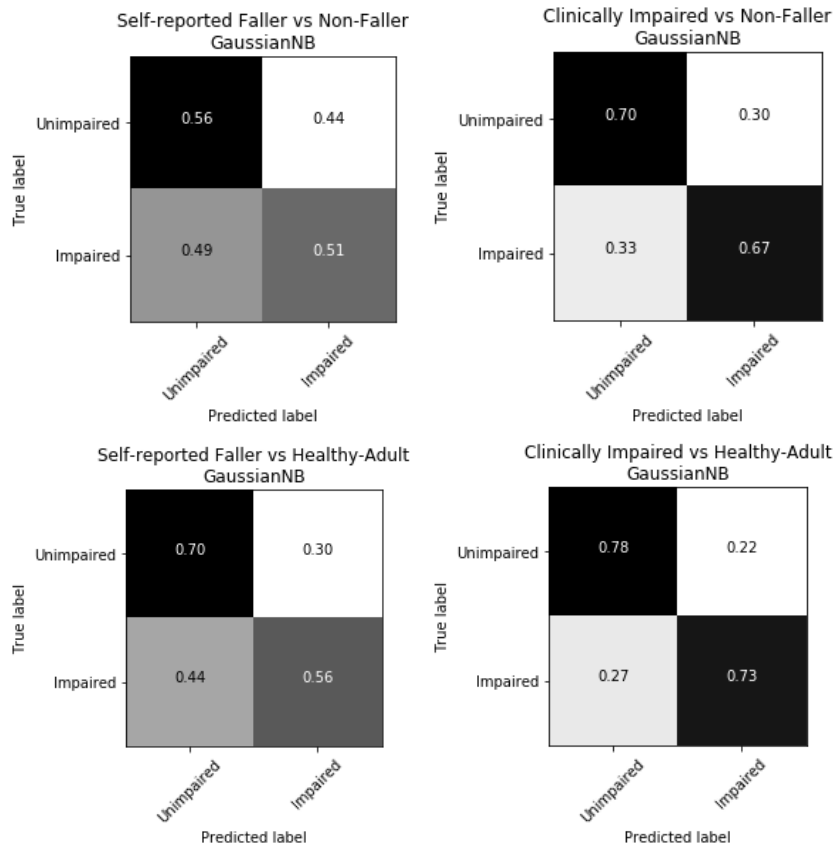


Figure 7.2: **Confusion matrices produced from training a Gaussian Naive Bayes Model:** The best separation is seen when using clinical labels. Confusion is seen in the models when using falls history as a label

As illustrated by the ROC curves, in Figure 7.3, it is clear that the clinical labels 6.4.3 (used to identify those in the **Clinically-Impaired** group) provide a better indication of true impairment, compared to self-reporting labels, used to identify members of the **Self-Reported-Faller** group). i.e. The models, trained using the clinical labels, outperformed those trained using the self-reporting labels. Using the scale outlined in [223], the model that compares **Healthy-Adults** to **Clinically-Impaired** (far right), would be regarded as having very good diagnostic accuracy when used to identify those at most risk of falls, i.e. those labelled here as **Clinically-Impaired**.

7.5 Discussion

This chapter examined the most universal of balance assessment stances, that of quiet standing, eyes open. Future studies may examine the predictive power

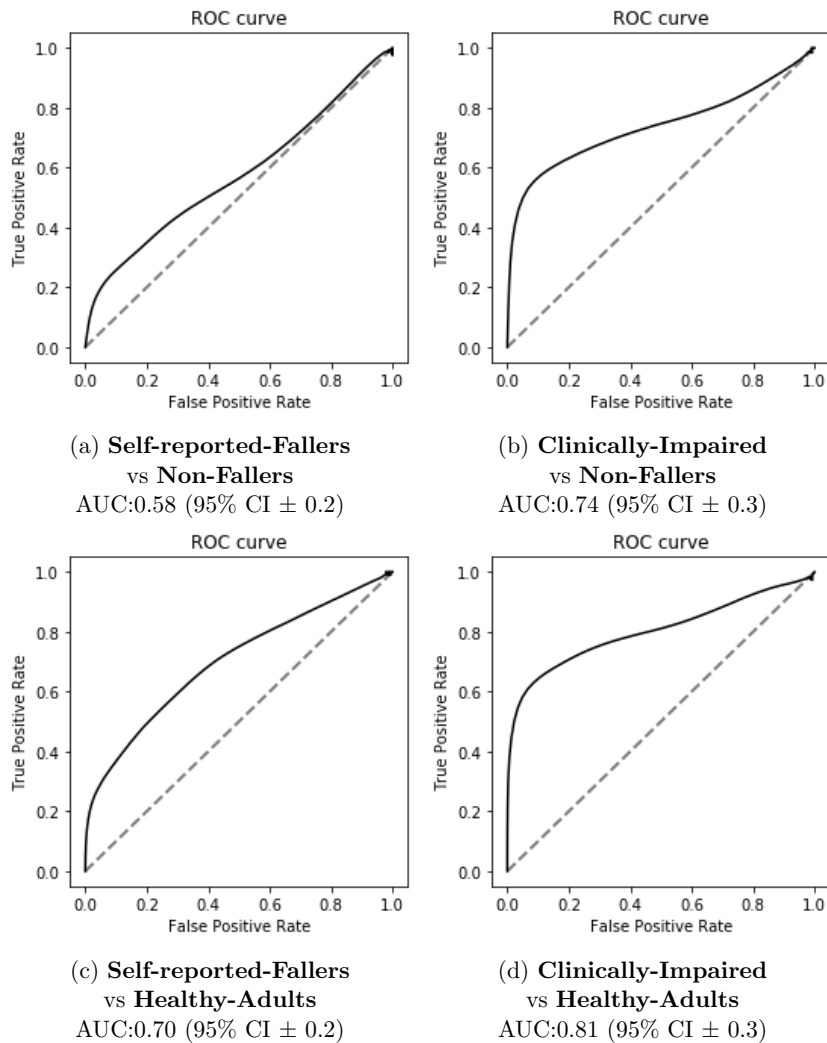


Figure 7.3: ROC curves for models. The AUC increases from top left to bottom right, the greatest overlap, seen between the those labelled clinically impaired vs Healthy-Adults

of other stances and movements, either alone or in combination.

Using the pre-calculated metrics of the KINECAL dataset, Frequency (MFREQ_AP), Velocity (MEVLO, MEVLO_AP), and Total excursion, also known as path length, (TOTEX, TOTEX_AP), were found to be biased towards age-related differences, summered in table 7.4. This is in line with previous studies. Prieto1996 et al. [189] point to age-related changes in frequency and velocity measures, and Hageman et al. [87] points to an association between increased path length and age.

Table 7.6 demonstrates that changes in these metrics could also be associated with impairment, but to a lesser degree. Piirtola and Pertti, in their

review paper [185] drew the connection between falls-risk and increased ML sway and sway area. The comparison of the **Healthy-Adult** group to the groups containing individuals with high falls-risk (the **Self-reported-Faller** and **Clinically-Impaired** groups) seemed to validate their findings. However, when the **Non-Faller** group was compared to the high falls-risk groups, a significant difference was not found for any of the ML metrics. Of the other metrics, only AREA_CE and MDIST show significant difference at the $p < 0.01$ level across all of the combinations shown in TABLE 7.6. These two metrics became the features used in the second part of this investigation.

To examine the effect that labelling has on predictive power, four Gaussian Naive Bayes models were built to classify those at risk of falls. Looking at the confusion matrices Figure 7.2 it is clear there is confusion in the model when trying to separate **Self-reported-Fallers** from **Non-Fallers**. This is a common issue with using self-report as an indication of impairment. This was the inspiration for providing labels of Clinical impairment in the KINECAL dataset. KINECAL uses the standard question used when labelling fallers, by falls history. However, this approach is prone to interpretation and could lead to an over or underestimation of the significance of a fall. i.e. mistaking a trip, or minor accident for a fall that relates to physical impairment. Or brushing off a fall that is related to impairment as "just an accident". This confusion is also present when considering **Self-reported-Fallers** vs **Healthy-Adults**, which may be an indication of the general overestimation of the significance of a single fall. Using clinical labels improves the separation between groups and so improves the models' ability to identify potential fallers. This finding points to AREA_CE and MDIST as having a bias towards being an indicator of impairment. However, these metrics must also change, to some extent, with age, seen as better Specificity and Recall, seen for models trained using the **Healthy-Adult** group. This points to the idea that while the identified metrics are good indicators of impairment, factors other than impairment, such as physical changes related to age, might be having an impact on these metrics. Hence, models trained using examples of **Non-Fallers** do not perform as well as those trained using examples of **Healthy-Adults**.

This investigation used a combination of statistics and machine models to examine both traditional sway metrics and the importance of labelling when considering falls-risk. The machine learning model, trained with the best combination of metrics (AREA_CE and MDIST) and labels (**Clinically impaired**

vs **Healthy Adult**), could potentially be developed into a primary screening tool for those who would be regarded as being having an elevated falls-risk, based on clinical test see section 6.4.3) for basis.

7.6 Conclusion

In this chapter, the question “are certain metrics more associated with impairment than with the process of ageing”, is considered. Two metrics, AREA_CE and MDIST, were identified as having a bias towards impairment. Using these metrics a machine model was developed, which could be used as a primary screen for impairment. In addition, the use of the clinical labels in the KINECAL was explored.

In this chapter, a binary classification model was used. This model attempts to find a threshold, under which someone could be regarded as impaired. Unless there is a clear margin between groups, it is very difficult for this type of model to achieve anything close to 100% accuracy. The results demonstrate that such a margin does not exist, when using traditional sway metrics. In fact, the opposite is true, there is a large area of overlap between older groups which are at normal and elevated risk of falls. This is not surprising as most physical impairments are on a continuum, and are not wholly correlated to postural sway. As such, one person may be able to compensate for a high level of sway and still be able to maintain balance in day-to-day activities while others with less sway may be prone to falls.

In the next chapter, A different approach is taken, that of using a distance metric to develop a scoring system, which can be used to assess falls-risk. This approach better fits the problem of impairment and frailty. Instead of postural sway, joint dis-coordination is considered, as a measure of impairment.

Chapter 8

Quantification of Falls-Risk, Based on a Representational Model

8.1 Introduction

As discussed in section 1.1, frailty is a common problem in people over the age of 65. Frailty has been defined separately by Walston [251], and Rockwood [202] but both point to Sarcopenia being a key factor, leading to reduced muscle power and coordination issues and the propensity to fall.

STS-5 test, is a well-established test for falls recurrence and frailty [23, 256, 141]. The sit to stand movement is an essential movement in many activities of daily living [112]. It also requires the coordination of many elements of the musculoskeletal system. In addition, by asking the participant to complete it as quickly as possible, the STS-5 test also provides an indication of muscle power. Therefore, a simple and easy to administer test provides the information necessary to assess falls-risk.

The time to complete the STS-5 provides a test for gross impairment. However, more informative data can be obtained by considering the coordination of joints needed to achieve this movement. Markerless motion capture provides a means of collecting this type of information away from the lab.

In this chapter, the STS-5 recording from the KINECAL dataset, was used to train an autoencoder neural network to model healthy patterns of coordination. Once trained, this model was used to identify pathological patterns,

which characterise those at risk of falling.

Using the raw skeletal data from the KINECAL, a multi-channel-time-series was created, which represents the planar angles (sagittal, frontal, transverse) of 5 key joints (knee, hip, spine mid, spine shoulder, neck). Examples of **Healthy-Adults** carrying out this movement were used to train the autoencoder. During the training process, the autoencoder learned to encode and then decode the healthy movements. In doing so, it built an internal representation of a healthy STS-5. Once trained, the autoencoder could recreate healthy movements with little error. However, the more the movement deviated from healthy, the more it struggled to recreate the input. By combining the reconstruction error with the variance between [repetitions \(reps\)](#), a scoring system was derived, which can quantify impairment.

8.2 Participants

In this chapter the **Healthy-Adult**, **Non-Faller Clinically-Impaired Self-reported-Faller_s** and **Self-reported-Faller_m** groups were used. Table 8.1 shows the makeup of each group. Some recordings of the STS-5 had to be removed as they were errors in recording, picked up in the segmentation process 8.3.3. The groups were filtered to ensure no participant appears in more than one group. When assigning participants to groups, groups further down the table took precedence over ones higher up.

Further groupings were made to aid the understanding of the results. These groupings were unique to this chapter. Those ≥ 65 years old were separated into **Impaired** and **Unimpaired** groups. i.e. The **Self-reported-Fallers_m** and the **Clinically-Impaired** were grouped together and marked as **Impaired**. Similarly the **Non-Fallers** and **Self-reported-Fallers_s** were grouped together and marked as **Unimpaired**.

The assumption used here is the same as that used to separate **Self-reported**, into **Self-reported-Faller_s** and **Self-reported-Faller_m** but it extends this idea to segregate all of the ≥ 65 -year-olds into two groups. i.e. that a single fall could be bad luck, whereas multiple falls are an indication of underlying issues

Table 8.1: **Participant Groups:** This table shows the split between the different groups used in this trial. The groups are exclusive and no participant belongs to more than one group

	Description	Age (\pm 95% CI)	Total Number	Male	Female
Healthy-Adult	< 65 years, no history of falls in the last 12 months	mean age 45.1 (\pm 23.8)	28	19	9
Non-Faller	≥ 65 years, no history of falls in the last 12 months	mean age 72.6 (\pm 9.9)	30	15	16
Self-reported-Faller_s	≥ 65 years, reported 1 fall, in the last 12 months	mean age 73.7(\pm 15.4)	10	5	5
Self-reported-Faller_m	≥ 65 years, reported >1 fall, in last 12 months	mean age 70.2 (\pm 9.6)	6	2	4
Clinically-Impaired	≥ 65 years identified as impaired by ≥ 2 clinical tests	mean age 78.0 (\pm 4.2)	5	0	5

8.3 Methods

8.3.1 Skeletal Preprocessing

Before the angles were calculated, the raw skeletal recordings were filtered and normalised, as discussed below.

Filtering

Filtering was achieved using a Butterworth fourth-order zero-lag filter. The low-pass cut-off frequency was established as described by Winter [263]. The frequency used to filter the data, used in this thesis, was 8 Hz.

Pose Normalisation

Pose Normalisation alters the coordinates system from a camera-centred system to a person-centred system. To achieve this, each skeleton frame was aligned to the first frame of the recording, making the *SPINE_BASE* joint of the first frame of each recording $[0_x, 0_y, 0_z]$, using equation 8.1. All subsequent movements were related to this initial position.

$$p_{n,i}(x, y, z)^* = P_{n,i}(x, y, z) - P_{0,SPINE_BASE}(x, y, z) \quad (8.1)$$

where $p_{n,i}(x, y, z)^*$ represents the normalised position of the x, y, z axis of joint i in frame n . $P_{0,SPINE_BASE}(x, y, z)$ represents the position of the *SPINE_BASE* joint in the first frame of the recording, and $P_{n,i}(x, y, z)$ represents the positions of joint i in frame n .

8.3.2 Calculation of Joint Angles

Joint angles were calculated, in each of the anatomical planes (sagittal, frontal and transverse), using equation 8.2. This provides 3 values for each joint. Figure 8.1 shows an example for the knee angle in the Sagittal plane.

Joint angles were estimated, by calculating the angle between two vectors which represent the limbs which meet at the joint, using the equation 8.2

$$\Theta = \arccos \left(\frac{a \cdot b}{\|a\| \|b\|} \right) \quad (8.2)$$

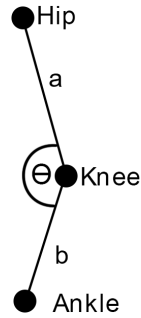


Figure 8.1: **Knee Angle:**Example of knee angle in the Sagittal plane. The angles in the other two planes are calculate in the same way.

8.3.3 Segmentation of Repetitions

A multi-step segmentation process was used to extract single repetitions for each recording of STS-5. The process was as follows: 1) Identify all of the valleys, using the `argrextrema` method of the `scipy.signal` python library [210]; 2) Walk the valleys clipping out proposed single reps, the end position of one valley, marks the end of that rep and the start of the next; 3) Compare the start and end values for the proposed reps, if the start and end are different by more than 30 degrees exclude that rep, (this captures odd start and end chunks where the recording captures movements other than the STS-5); and 4) A final visual inspection of each rep, to ensure it starts and ends correctly, and so captures a representative rep.

8.3.4 Resampling and Padding

The time to complete one rep of the STS-5 movement varied between individuals. Hence, so did the number of frames per rep. The smallest number of frames per rep was 54, and the largest 150 frames. The average for a member of the **Healthy-Adult** was 80 frames. To provide a standard basis for comparison, each rep was resampled to 80 frames. The resampling was achieved by Fourier transform resampling [94], implemented via the `signal.resample` method of the `scipy` python library [210]. This process also centred the movement.

Once centred, the repetition was padded with a 2 seconds buffer (60 frames) on either side of the main movement shown in Figure 8.2. The padding helps the autoencoder to learn by providing a lead-in before the movement.

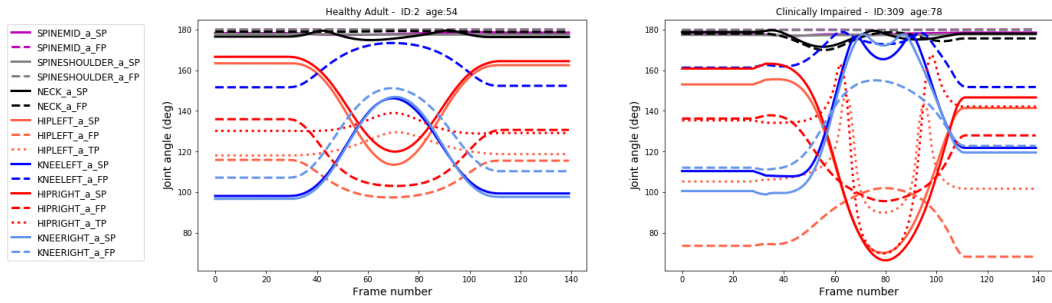


Figure 8.2: **Joint angle for a single rep:** Illustration of the changes in joint angles over a single rep for **Healthy-Adult** (left) and **Clinical-Impaired** (right).

Normalisation

Before training, the samples were normalised, using the normalization function from scikit-learn [225], to aid training.

8.3.5 Autoencoder

Autoencoders discussed in section 2.16.6 are trained in an unsupervised fashion. That is to say that, unlike the models used for classification, e.g. GNB models used in 7, training is achieved without labels. (see section 2.16.1 for more details on different types of learning).

This difference is the key to understanding how Autoencoders work and their application. In supervised learning, the model learns to map an input to a label, this type of model can address the question, given an input "which of the learned classes, is it most likely for the input to belong to?". This approach can work well when wide decision boundaries can be found between classes. However, this is not the case for falls-risk. Instead, falls-risk lies on a continuum. An alternative is to cast the problem of falls-risk as an anomaly detection problem. To implement this approach, the autoencoder was trained on a single class **Healthy-Adult**, in an unsupervised manner. Although no class labels were used, the back-propagation process still needs an error signal to allow for corrections during the backward pass through the network. When training in this way, the input is essentially used as the label. In this work, the error signal was provided by calculating the Mean Square Error (MSE), between the input and the output of the network.

As mentioned above, the job of an autoencoder is to recreate the input at the output layer. This might seem like a trivial task. However, the struc-

ture of autoencoders prevents the network from mapping an identity function. Figure 8.3 shows the structure of the autoencoder used in this work. Like all autoencoders, it contains two halves, the Encoder and the Decoder. The role of the Encoder is to compress the input into fewer and fewer neurons, or LSTM units, as used here. In the network used here, the last layer of the Encoder is just 4 units. The job of the Decoder is to take this compressed version and reconstruct the input over successive layers, reversing the encoding process.

Through successive rounds of training, the autoencoder learns to recreate the training data. In doing so, it is learning the distribution of the training data, and it will be able to recreate inputs drawn from the same distribution with ease. However, if challenged with an input from a different distribution, the autoencoder will struggle to recreate that input, as it has never “seen an input quite like this before”. The input is anomalous to the training data, and so the network will make errors in reconstruction. The degree to which the output differs from the input can be quantified by various means, e.g. by calculating the euclidean distance. The size of the error can be seen as a measure of how anomalous the input is. Hence the autoencoder can be used as an anomaly detector, and the degree of anomaly can be quantified and used as a measure of impairment. i.e. how far an input lies from the normal distribution. The details of the distance measure used in this work is discussed in section 8.3.6, below.

The autoencoder used in this work was constructed using the Keras framework. Its structure is shown in Figure 8.3. The numbers, shown in each layer refer to LSTM units. LSTM networks are well suited to extracting features from time series data, such as that presented in this chapter. The input and reconstructed output was a time series of 200 frames by 16 channels. The channels represent the following angles SPINE_MID, sagittal and frontal; SPINE_SHOULDER, sagittal and frontal; NECK sagittal and frontal; HIP_LEFT sagittal, frontal and transverse; HIP_RIGHT sagittal, frontal and transverse; KNEE_LEFT, sagittal and frontal; KNEE_RIGHT, sagittal and frontal.

8.3.6 Distance Metrics and Scoring

As discussed above, the degree of anomaly can be quantified using many metrics. In this work euclidean distance was used, as detailed in equation 8.4.

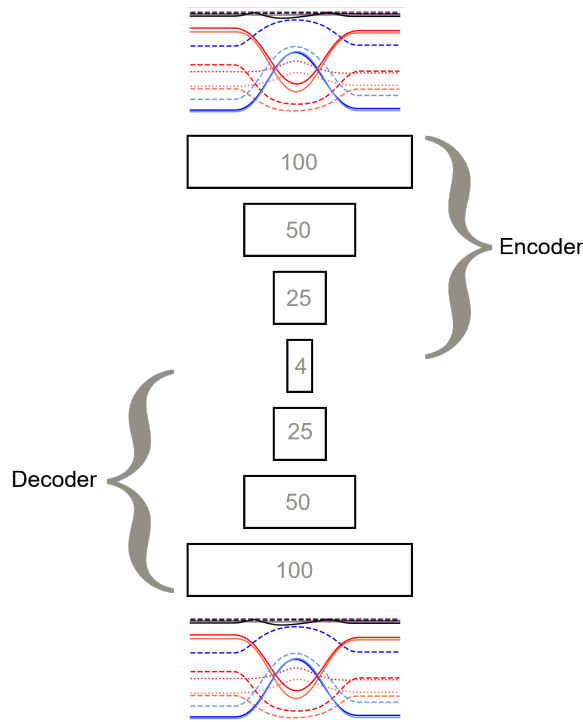
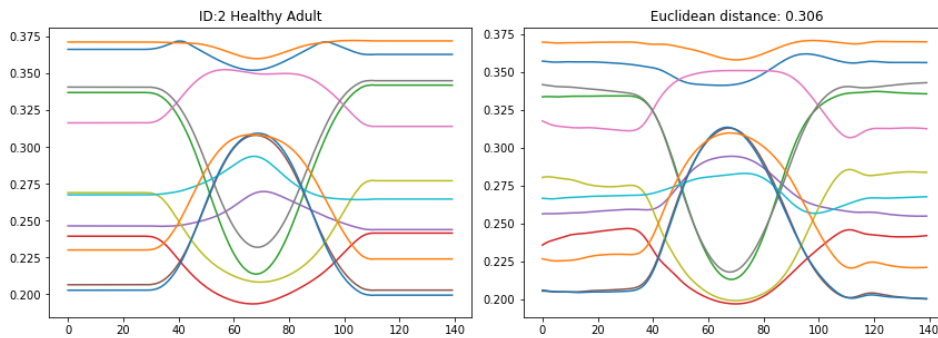


Figure 8.3: **Autoencoder**: representation of autoencoder architecture. It consists of a three layer encoding and a 3-layer decoder. The latent representation is 4 LSTM units. The input time series was 200 frames by 16 channels, this was also the demotions of the reconstructed output

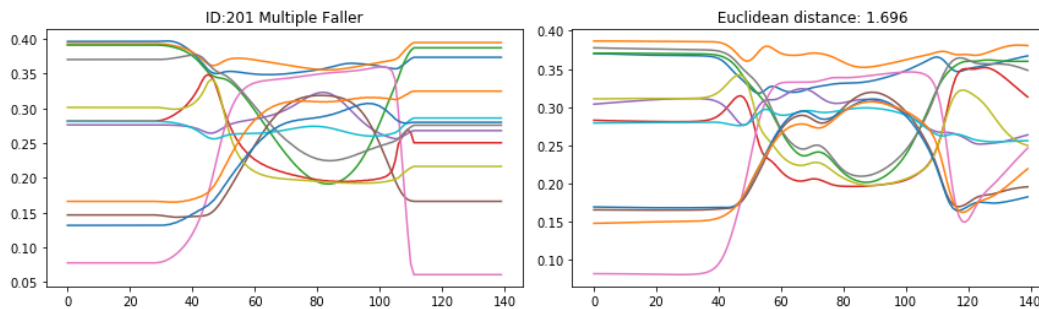
Once trained, the network was able to recreate movements similar to those found in the training data with a high degree of faithfulness. This was demonstrated by low euclidean distance. In other words, the movement lies close to the distribution learned in training. Physically impaired individuals have different patterns of activation and muscle contractions. Hence they produce different types of trace. Impaired movements lie further away from the training distribution. Hence, they have a higher euclidean distance.

Figure 8.4, show the input and the reconstructed time series for (a) an unseen **Healthy-Adult** movement, from the validation set (b) a **Clinically-Impaired** movement, from the test set (b). The reconstruction error for (b) is 5.5 times that of (a)

The distance metric alone was not consistent enough to separate the healthy from impaired individuals. Some repetitions of impaired individuals can be close to normal, while others lie far away. To refine the distance measure, a scoring schema is proposed, detailed in equation 8.3.



(a) Reconstruction of a member of the **Healthy-Adult** group



(b) Reconstruction of a member of the **Clinically-Impaired** group

Figure 8.4: **Reconstruction of STS-5 movement:** This figure shows the reconstruction of STS-5 movements carried out by (a) a member of the **Healthy-Adult** group and (b) a member of the **Clinically-Impaired** group. Movement (a) was part of the validation set, movement (b) was part of the test set. The Autoencoder is able to recreate movement (a) with high faithfulness, and so the reconstruction error, (expressed as Euclidean Distance) is low. The autoencoder struggles to recreate movement (b) because it comes from a different distribution, the reconstruction error is 5.5 times larger for this movement, indicating it lies far away from the training distribution. The time series, shown here have been normalised to aid recognition. *Note, the first 30 and last 30 frames, of the reconstructed time series, are clipped before the distance is calculated, these early frames often contain encoding errors and so do not truly reflect the reconstruction.*

The score multiplies the distance value by the variance, between distance values, calculated from the 5 reps of the STS-5 movement. Including the variance, reflects the fact that healthy individuals are more able to consistently carry out the movement. Subtracting this term from 1 makes 1 the maximum score achievable and impairment on a scale of < 1 . Finally the per-rep scores for each individual are averaged to give a final score. Using these scores, in place of the distance value, individuals can be more easily separated, and placed on a scale of impairment.

This scale must have a natural top and bottom, and future work will seek to expand the dataset to discover this scale. In the current work, the scale is arbitrary. The more negative the score, the further away an individual is from the **Healthy-Adult** group. When graphed, this score enables the placement of individuals relative to **Healthy-Adult** group, as seen in Figures 8.7 and 8.9. Furthermore, by calculating a threshold value, a one-class, classification system can be implemented, allowing for the calculation of metrics such as accuracy, specificity and sensitivity.

$$Score = \sum (1 - (ED * ED_var))/n \quad (8.3)$$

where ED is the Euclidean Distance measured in a pixel by pixel fashion, given by equation 8.4, and calculated using the `spatial.distance.euclidean` method of the `scipy.signal` python library [210]. ED_var is the unbiased variance between ED values, given by 8.5 and calculated using the `pandas.DataFrame.var` method of the `pandas` python library [180], n is the number of repetitions of the sit-to-stand movement.

$$ED = \sqrt{(i_1 - r_1)^2 + (i_2 - r_1)^2 + \dots + (i_i - r_i)^2} \quad (8.4)$$

where ED is the Euclidean distance, i is the linearised input, and r is the linearised reconstruction.

$$ED_var = \frac{\sum_{i=1}^n (ED_i - \bar{ED})^2}{n - 1} \quad (8.5)$$

where ED_var is the variance between euclidean distance values (ED) for the reconstructed repetitions of a sit-to-stand movement, \bar{ED} is the mean of the euclidean distance values for all reconstructed repetitions of a sit-to-stand movement.

8.3.7 Training and Cross-validation

The cross-validation process is shown in diagram form in Figure 8.6, the details of training are as follows:

The autoencoder was trained on a single class (**Healthy-Adults**) and then tested using all of the other classes [**Non-Faller**, **Self-reported-Faller_s**, **Self-reported-Faller_m** and **Clinically-Impaired**]. A K-fold (5-fold) cross-validation schema was used to quantify the bias within the training set. That is to say that 5 folds of the training set were prepared and separate models trained for each fold. In the test phase of the cross-validation, the same set of test data was used. In this way, the degree to which variations in the training data affect the ability to train an appropriate model was examined. The KFold method, from the sklearn python library[225], was used to prepare the folds. The splits were done at the level of individual participants, i.e. KFold returned an array of participant ids, which were used to select all the reps for a particular participant. Therefore reps from one participant were not allowed to leak between train and validation sets.

The model was trained using The Mean Square Error (MSE). the MSE loss of the validation set was used as a signal to an early stopping callback, which stopped training if the validation loss remained constant, or rose for 50 consecutive epochs. Together, these two measures helped to prevent overfitting and provided a train-time indication of the model's overall performance. Figure 8.5 demonstrates that the loss of the train and validation sets was very close throughout training.

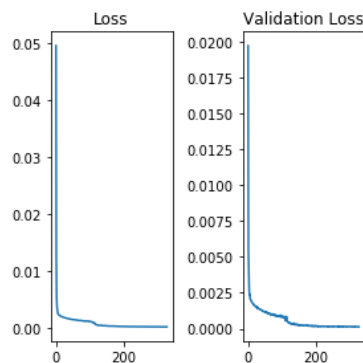


Figure 8.5: **Graph of Train vs Validation loss:** these graphs show how the validation set loss (to the right) matches the train set loss (to the left) in terms of MSE, very well throughout the training process. This demonstrates the similarity between the two set of healthy individuals.

All of the test set was processed through the trained model, and the reconstructions scored, as described in section 8.3.6. Using a threshold (described in section 8.3.6), the test set was classified, and metrics of accuracy, specificity and sensitivity calculated and stored. After all 5 folds had been processed, the scores were averaged and displayed.

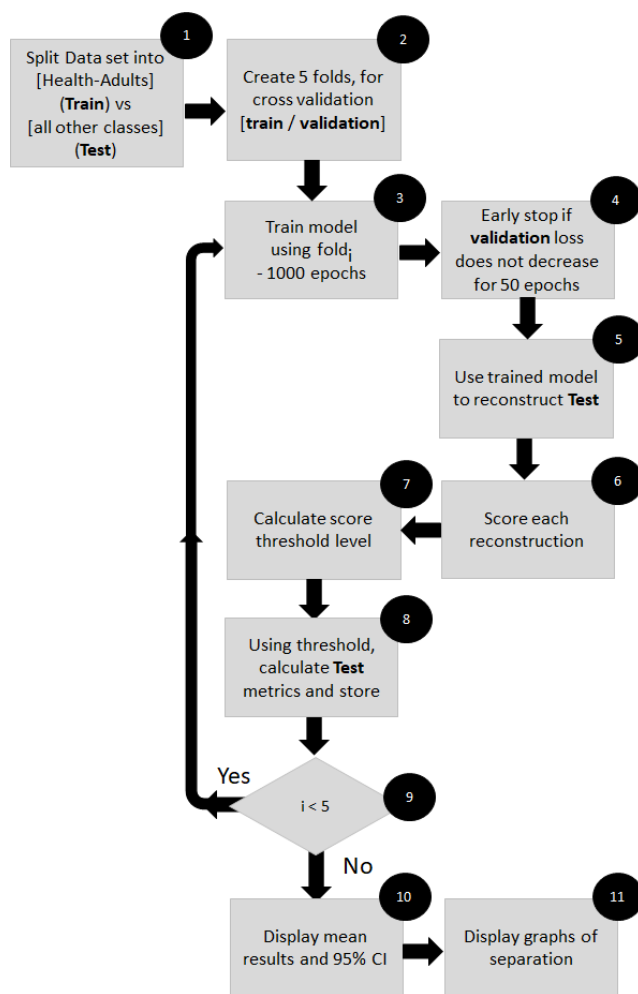


Figure 8.6: A flowchart of the cross validation process. 1) The dataset was split into **Train** and **Test** sets. The train being a single class **Healthy-Adults**; 2) 5 folds were created to for cross validation, each fold contained a **train** and **validation** set; 3) A model was trained, using the *i*th fold (nominally 1000 epocs); 4) Early sopping was used to prevent overfitting; 5) The trained model was used to reconstruct the movement from the **Test** set ; 6) Each member of the test set was scored; 7) The best threshold to identify impairment was calculated; 8) The metrics were calculated and stored; 9) the process continues for 5 iterations; 10) The mean metrics were calculated and scored; 11) The graph, showing separation were displayed

8.3.8 Calculation of Metrics

Accuracy, Specificity and Sensitivity scores were calculated for each fold, and then averaged to give an overall score.

All of these scores were based on the assumption of a binary split. While the method described here produces a distance measure, a threshold of impairment can be assumed. The calculation of the threshold is discussed in section [8.3.9](#).

Each participant was classified as being either **Impaired** falling below the threshold or **Unimpaired**, falling above the threshold. Each participant now had a true class (from the database) and a predicted class from the thresholding process. All of the values for the test set were collected together into an array and then passed to the Accuracy, Specificity and Sensitivity methods of the sklearn python library [\[225\]](#) to calculate the metrics.

8.3.9 Calculation of Threshold

The threshold, used to classify impairment was calculated using a Receiver Operating Characteristic (ROC) curve. The threshold provided the optimal binary split between labelled as **Unimpaired** and those labelled as **Impaired**. This threshold can be thought of as a threshold of normal.

The threshold was found by splitting the range of scores into 1000 segments and sweeping over this range to find the value which gave the best trade-off between a high true-positive rate and a low false-positive rate.

the true-positive rate and false-positive rate were calculated using the `confusion_matrix` method of the sklearn python library [\[225\]](#)

8.4 Results

Using the scoring system, the participants were separated from least to most impaired, shown graphically in Figure 8.7. The blue line indicates the threshold of normal.

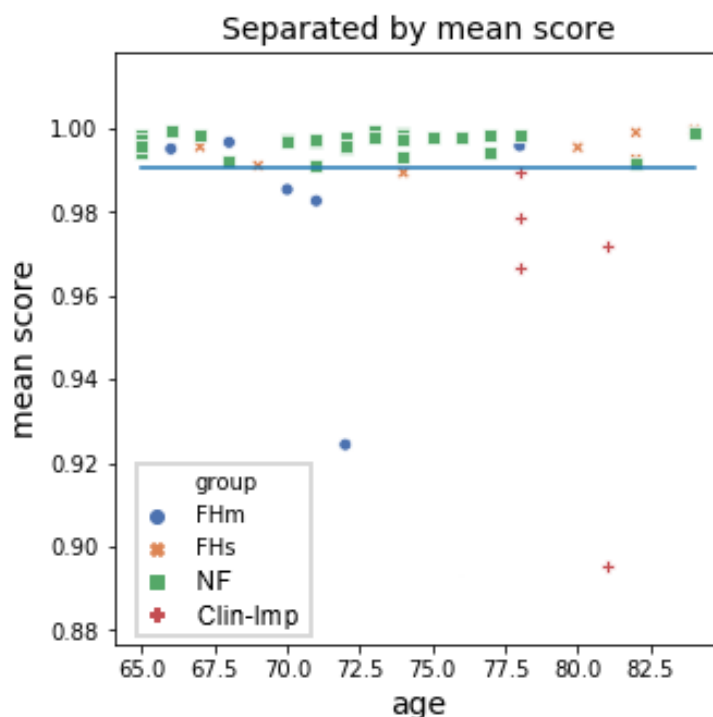


Figure 8.7: **Separation of individuals by impairment:** this graph represents the score derived from the autoencoder, One marker denotes a single participant. The most impaired are shown furthest away from the normal threshold. The normal threshold is indicated by the blue line. Key **NF**: Non-Fallers, **FHs**: Self-reported-Fallers.s, **FHm**: Self-reported-Fallers.m, **Clin-Imp**: Clinically-Impaired

The threshold was calculated using a Receiver Operating Characteristic (ROC) curve, shown in Figure 8.8. This ROC curve is the average result of 5 fold cross-validation. The best threshold was 0.991. This gave a Specificity of 0.88 with 95% CI (± 0.22) and a Sensitivity of 0.68 with 95 % CI (± 0.21). The metrics for each fold and the mean metrics are shown in Table 8.2

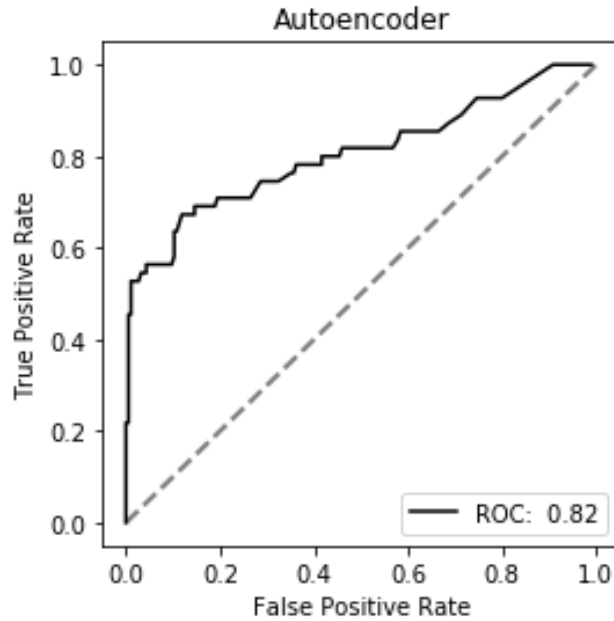


Figure 8.8: **ROC curve for the proposed model:** the ROC curve shows the trade of between different cut off levels for the threshold of normal. a score of 0.991 was found to give the best separation, with a Specificity of 0.88 95% CI (± 0.22) and a Sensitivity of 0.68 95% CI (± 0.21).

Table 8.2: **Table of metrics:** summation of 5-fold cross validation the mean values are shown with standard deviation in brackets and 95% confidence interval below.

	Accuracy	Specificity	Sensitivity
1	0.88	0.92	0.73
2	0.94	0.95	0.87
3	0.85	0.95	0.63
4	0.83	0.92	0.60
5	0.71	0.65	0.59
mean	0.84 (0.08)	0.88 (0.11)	0.68 (0.11)
	95%CI -/+0.15	95%CI -/+0.22	95%CI -/+0.21

Figure 8.9 shows a graph of scores vs age, stratified by impairment group. The pale-blue line shows close grouping of the **Unimpaired** group, across the whole range of ages, above the normal threshold line (mid-blue). The orange line shows the trend of increasing impairment with age for the **Impaired** group. The shaded orange area shows the 95% CI, with some appearing above the line, which places them alongside members of the **Unimpaired** group and others placed considerably below the line, making them very impaired.

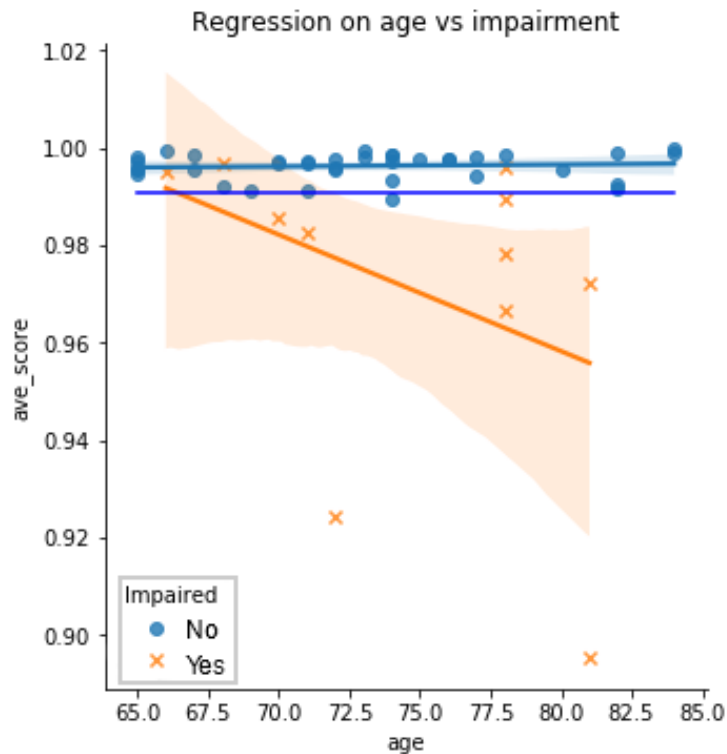


Figure 8.9: **Regression of age vs impairment:** this graph shows two distinct populations, Unimpaired (blue) and impaired (orange), One marker denotes a single participant. The Unimpaired group have scores that are similar to those found in the Healthy-Adult group, over a wide range of ages. The scores for the Impaired group decline with age. As the score goes down the falls-risk increases.

8.5 Discussion

In this chapter, quantifying impairment was recast as an anomaly detection problem. A deep autoencoder was trained to reconstruct graphs of joint angles as they change over time. Joint angles derived from **Healthy-Adults** carrying out the STS-5 test were used as input. During training, the autoencoder built an internal model of a **Healthy-Adults** carrying out 1 rep of the STS-5 test. A scoring system was developed, which can express the level of functional impairment relative to **Healthy-Adults** reps. Figure 8.7 demonstrates how more impaired individuals are placed further away from **Healthy-Adults** using this scoring system.

The trained autoencoder was able to reconstruct inputs from unseen **Healthy-Adults** with little error, demonstrated in Figure 8.4 a. During training, unseen **Healthy-Adults** were used as a validation set and a callback signal to prevent

overfitting. The autoencoder was trained using mean square error (MSE) as the back-propagation error signal. Euclidean Distance was used to quantify the reconstruction error, as this produced a greater range of normal values than MSE. This, in turn, aided the scoring of impaired individuals. Using Euclidean distance alone did not provide a strong enough signal to quantify impairment. Combining the distance measure with a measure of variability between reps, i.e. variance, gave a score that is able to quantify the level of impairment experienced by an individual. The intuition behind using variance is that healthy individuals are able to repeat movements many times, which are similar, while impaired individuals struggle to achieve consistency due to poor control of their musculoskeletal system. Figure 8.2 compares a single rep of the STS-5 movement, performed by a **Healthy-Adult** and a Clinically impaired individual. The graph on the left (**Healthy-Adult**) demonstrates smooth transitions in all joints, with the hip (red lines) and knee (blue lines) joints, viewed from each plane, following similar arcs. For the healthy adult, the joint angles are constrained by the bodies own systems and never reach their physical limits. The graph on the right (**Clinically-Impaired**), is much less well organised. There is not as much synchronicity in the hip and knee joints, and the joints experience a greater range of movement. The knee joint can be seen reaching their physical limits and then recoiling to recapture some needed degrees of freedom. This figure demonstrates dis-coordination and lack of control over movements for the impaired individual. As discussed in the introduction dis-coordination and a reduction in muscular control are a precursor to the development of frailty.

The STS-5 is an integral component of SPPB, it is included in the KINECAL dataset, and it is often used alone to identify those at risk of falling [23, 256, 141]. Ward et al. undertook a 4 year long, longitudinal study (N = 755, mean age 78.1 ± 5.4) that looked at SPPB as a predictor of injurious falls. They concluded that the STS-5 alone was all that is required to assess falls-risk. They suggested that a time to complete ≥ 16.7 seconds may be sufficient to identify those at risk of future falls. [239] also found that time taken to complete STS-5 was an excellent predictor of falls. They found that even a single sit-to-stand could provide a useful indication of falls-risk. Ejup et al., [61] used a Kinect camera to record community-dwelling older adults carrying out the 5x sit-to-stand test. They found that sit-to-stand velocity was a better discriminator of falls-risk than the time taken to complete the test. They note

that the sit-to-stand velocity provides a good estimate of muscle power, a key element of sarcopenia

Using Ward’s recommendation of 16.7 seconds to complete STS-5 [256] to identify members of the KINECAL dataset at risk of falls, it identified all of the **Clinically-Impaired** group, along with 6 **Self-reported-Faller_s**; 1 **Self-reported-Faller_m**, 11 **Non-fallers** and 2 **Healthy-Adult**. While this test did capture all of the **Clinically-Impaired** individuals, it failed to identify all of the **Self-reported-Faller_m** and categorised a lot of **Non-Fallers** as fallers. This points to the gross nature of this test. However, as shown in Figure 8.2, a Kinect camera can be used to extract biomechanical information, which can provide details of what is happening, bodily, during the movement. In the study published by Equip et al. [61], they used a Kinect camera but chose to track only a single joint (the head joint). They used the joint path to segment both the sit-to-stand and stand-to-sit phases of the trial and to estimate the velocity of each segment. This approach provides a single summative metric, much like tracking the Centre of Mass to assess postural sway. In this study, the dis-coordination of several joints is regarded as the hallmark of movement impairment, and ultimately frailty. The Kinect camera provides convenient way to track many joints at once.

A visual inspection of Figure 8.2 shows clear differences between the two individuals. Given enough time and lots of cross-checking, one could create a set of rules that relate the change in angle through the motion to impairment. This research seeks to automate that process and provide a useful measure of impairment.

By training the autoencoder to recreate the motions of a healthy adult it, necessarily, builds an internal spatio-temporal model of a healthy movement [207, 8]. When the autoencoder is asked to reconstruct the recording of someone with impairment, it will make errors in the reconstruction, some elements will resemble the healthy movement, and some will be very different. Therefore, the reconstruction error (euclidean distance in this study) can provide a measure of how different the movement is from a healthy exemplar. The reconstruction error was combined with the variance between reps, to produce a score of impairment.

A threshold was calculated below which individuals show signs of impairment. Although this should not be seen as a cliff-edge, and some individuals might be able to accommodate impairment better than others. This point up

the fact that systems, such as the one detailed here, should be an aid to a health professional and not a replacement for clinical judgement.

The majority of **Self-reported-Faller_s** are seen above the threshold line, mixed with the none-fallers. This is in line with other studies that suggest that **Self-reported-Faller_m** should be treated as true fallers, and a single fall could be due to bad luck [89]. The majority of those, categorised as impaired (**Self-reported-Faller_m** and **Clinically impaired**), can be seen ranged below the threshold line, ordered by the degree of impairment. Figure 8.9 show two distinct populations **Impaired** and **Unimpaired**. The **Unimpaired** group showing consistently low levels of impairment with age, The **Impaired** group showing increasing impairment with age. It should be noted that the proposed method is not truly a classification method and the decisions boundary used here is linear. Primarily this method provides a distance measure of how impaired an individual might be. Different applications of this approach might opt for different thresholds. Alternatively, the inclusion of a margin might prove useful in practical applications. The advantage of this approach, over a pure categorisation approach, is that it gives a score on a continuous scale which can not only be used to identify impaired individuals it also is useful in the tracking of improvements following interventions.

The use of a scoring system, which relates to an ideal form, has been used by several other studies. [5] used a distance measure derived from dynamic time warping (DTW) to assess if a particular exercise had been carried out to the required quality during rehabilitation. In a similar way, Gholami et al. [76] used DTW in the creation of a distance measure to quantify the degree of dissimilarity between the gait cycle of Multiple Sclerosis Patients and healthy patients of a similar age.

Houmanfar et al. [101] used a Hidden Markov Model (HMM) to model normal movement. The advantage of using a model approach is that the model can learn the essence of a movement through the training process. This achieves the dual-task of dimensionality reduction and defining a discriminative model. In [101], a distance metric was used to determine the relative quality of movements of people recovering from hip or knee replacements, with reference to healthy individuals. [33] demonstrated that a model-based approach outperformed DTW for monitoring rehabilitation.

Previous works have used LSTM autoencoders as a form of non-linear dimensionality reduction before using the latent representation with another

model. Vakanski et al. [1], used a mixture density network, Jun et al. [107] used a discriminative RNN, and Williams et al.[261] used a Gaussian Mixture Model (GMM) as the second model, trained on the output of the autoencoder.

In the current study, a unique scoring system was developed, which alone is enough to provide early warning of changes that could lead to frailty. In this way, the Autoencoder is used in a similar fashion as the HMM in [101], with the added advantage that an autoencoder is better able to model non-linear relationships.

Future developments of the pipeline outlined in this study, consisting of a portable depth camera, a machine model and scoring system could be used to create a device, which could sit in a doctors office and make the assessment of frailty as commonplace as taking someone's blood pressure. Potentially, the proposed method could provide an indication of physical impairment, giving the option of a referral on, to a falls clinic as a preventative measure.

8.6 Conclusion and Future Work

This study demonstrates the use of an autoencoder as an anomaly detector. When used together with the proposed scoring system, it can identify those at risk of future falls. This research opens the door to future devices which could provide a practical form of screening for those at risk of a fall currently absent in the UK.

Our proposed method provides not only a way of screening for future fallers, it also can be used in the rehabilitation process to demonstrate how interventions are moving the patient closer to normal. As well as being a useful aid to health professionals, this type of feedback can be a real spare to ensuring the recommended exercises are carried out on a regular basis, if people can see progress, they are more likely to continue.

This study demonstrates that an anomaly approach to falls-risk can work well. The data was gathered from willing volunteers in the local community. Inevitably, these people do not represent the most impaired of individuals. The model demonstrated that even in this groups, difference could be discovered. Future work will seek to validate this model on a wider range of participants. Although the Kinect camera used in this research is no longer manufactured, Microsoft has released its successor. Future work should consider this device.

Chapter 9

Conclusion

9.1 Introduction

An inexpensive method of providing objective measures of impairment could have a large impact on the lives of everyone at retirement age and older. Falls are a major risk for people over 65, and proven help is available to prevent future falls. However, access to this help is usually only granted after a fall has been reported. This is not done out of malice, rather the lack of a device that can provide evidence of future falls. This thesis looks at ways to move that option closer to reality.

However, we are not there yet, not even close. But this thesis has started the ball rolling, and sometimes that's the biggest sticking point. It would be a lie to say that there is a clear line from here to a practical product. This work needs to have collective effort applied to it. To open up the field to other researchers, this thesis has built the first dataset, designed to aid research into fall-risk assessment by markerless motion capture, KINECAL. KINECAL is designed to bridge the gap between lab-based test, which assess balance and motion, measured by a force plate or motion capture system and clinical test, which have a human observer score the movement base on a predefined scale. The dataset achieves this by having all three types of data per participant. The participants are also multiply labelled to allow many different questions to be addressed, relating to falls risk, ageing frailty, and balance. The use of these labels and the different modes of data were explored in chapters 7, and 8 which both demonstrated models able to identify those with high falls risk.

9.2 Summary of work

Table 9.1: **Table of objectives and outputs**

	Objective	Output
1	To develop a method to track CoM and calculate traditional postural sway metrics from the output of a Kinect and compare the proposed method and device used in clinical practice.	A new method of obtaining traditional sway metrics from a Kinect camera was developed. This method was then validated against The Balance Master
2	To create a new dataset of movements, widely used in clinical tests, using the proposed method.	The KINECAL dataset was created, designed to address the lack of data in this field of research
3	Disambiguate sway metrics associated with ageing vs those related to impairment.	We present an investigation into which of the traditional sway metric are more closely related to impairment vs ageing
4	To develop a method to quantify impairment using deep learning and the captured data.	By reframing the problem of identifying those at risk of falls as an anomaly detection problem, rather than one of classification. We were able to create a scale of impairment, based on a deep learning model.

Following the preliminary work, it became clear that distinguishing between young and older adults is an achievable task, using low-cost markerless motion capture. However, this approach was not able to identify those who are frail or at risk of falling. What follows details the journey, from having no appropriate data to a deep learning model which can achieve this goal, objective by objective as detailed in Table, [9.1](#)

The first objective was to prove that the output of a Kinect camera can produce traditional sway metrics that are equivalent to those produced by a force plate. This objective was selected because the vast majority of literature relating to instrumented balance assessment relates to metrics that are easily calculated from force plates. Chapter [5](#) details a method, that can achieve this. When these metrics were compared to those created from the Balance Master, good agreement was seen, as detailed in section [5.3](#). In addition, the combination of a low-cost depth camera and the proposed method can be used to collect sway metrics in situations impractical for the Balance Master, at a fraction of the cost.

Objective 2, was to create a dataset of movements widely used in clinical

tests. Clinical test being the de facto method of assessing falls-risk in practice. The output was the creation of the KINECAL dataset, detailed in chapter 6. Ultimately, the line of research detailed in this thesis aims to replace this type of test. Using the method from objective 1, 90 individuals were recorded, carrying out eleven movements which are used in a range of clinical tests. The participants were scored using four well recognised clinical scales. Those that were found to be clinically impaired on two out of the four scales were labelled as **Clinically Impaired**. This provided an alternative set of labels to falls history. This dataset is a unique resource that will be made available to fellow researchers.

Objective 3, was to disambiguate sway metrics associated with ageing vs those related to falls-risk. The underlying processes of ageing happens to everyone, and yet some people suffer falls, while others don't. In Chapter 7 an investigation was carried out to see if metrics could be identified, that are or related to falls-risk, rather than ageing. Velocity, total excursion and AP frequency were found to be more closely related to ageing while mean distance and area were more closely related to increased falls-risk. However, the distinction was not clear cut, and increased velocity is also indicative of impairment, to a lesser extent.

To investigate if area and distance metrics could be used to identify fallers and to explore the different labels in the KINECAL dataset, several GNB machine models were constructed. Examining the performance of the models provided evidence that the labels of clinical impairment are a useful addition and overcome the issues associated with falls history labelling. The best performing model achieved an AUC of 0.81, and could potentially be developed into a screening test for those who would be classified as impaired, using clinical tests.

Objective 4, was to develop a method to quantify impairment using deep learning and the captured data. From the study in chapter 7 sway metrics were examined, which provide a measure of balance. In chapter 8 features of human movement, which can give a better measure of a loss of coordination associated with falls-risk and frailty, were considered. The five times sit to stand test (5STS) is a well-validated test for falls-risk and balance impairment. As such, it is ideal for demonstrating how an alliance of low-cost motion capture and machine learning could lead to a useful alternative to both clinical test and existing equipment commonly used in clinical assessment. Through the

application of a representative model and the development of a unique scoring system, individuals can be placed on a continuum of impairment, which could find uses in rehabilitation as well as detection of falls-risk.

9.3 Limitations

While KINECAL is designed well and is the largest of its type, it still has relatively few participants. This raises the spectre of generalisation. The models detailed in this Thesis work for the KINECAL data, but it is unclear whether these models will generalise well to the larger population. To address this question, future work should seek to collaborate with clinicians to validate the models. This issue of generalisation can also be addressed by collecting more data and also encourage other researchers to help out with this task.

The work detailed in this thesis are retrospective studies, in which the fallers have been identified before the models have been developed. Future work should look at a prospective approach, where participants are recruited before they develop falls issues, then tracked over several years to see if the model can identify future fallers before their first fall.

There are lots more unexplored data in KINECAL. For example, the 3m walk and TUG movements from a gait point of view. As section 2.9 explains, variation in gait is a key indicator of falls-risk, and one that NICE [169] suggests warrants more investigation. However, Kinect V2 struggles to track ankle joints, Kinect V3 may be better suited to this task, and future work should explore this new device, along with competing devices. A new feature of Kinect V3 is the ability to use multiple cameras. This could address a big issue with using a single camera, that of occlusion. Although a single camera is the most simple to set up and the most compact, small arrays might provide a compromise between improved tracking and size constraints of doctors offices and care homes.

9.4 Future Work

The models developed in chapters 7 and 8 should be validated with unseen individuals, who are at both high and low falls-risk.

The KINECAL dataset provides a starting point for data that can be used in research towards a device that could be used to automatically assess balance

issues and frailty, but this is not the end. Our intention is to build a community to enable more research into this vital area. In addition, it is hoped that the community can help with the capturing of new data. In this way, a large dataset could be quickly created. The collection of new data has been severely hampered by the current pandemic. Through collaboration, new innovative and safe ways to collect new data may be found. To this end, the software used to record the raw Kinect data and then process it into the KINECAL dataset will be made available, open-source. The device used to record the dataset is no longer on sale. However, its successor, the Azure Kinect, is now available in the UK. Efforts will be made to update the code to support the new camera and provide options to port the existing data over to the new format.

Follow up. The labels of falls in the current dataset are historical. Future recordings should include follow up questionnaires to see if any of the participants have become fallers or suffered more falls, after the date of the recording.

In this thesis, much use was made of the skeletal data. However, the depth videos remain largely unexplored. There were some promising experiments using a CNN network to do some preliminary classification of young and old using this data. However, the computers available did not have enough memory on the GPU cards to fully explore this option. Future work should endeavour to reexamine depth data with more appropriate hardware.

In chapter 8 The human interpretation of time-series data is, briefly discussed. In this chapter, an automated approach is demonstrated. However, the time series traces alone or in combination with Electromyography (EMG) might aid physiologists to understand the underlying mechanisms driving impairment and frailty. One could also imagine a machine approach which once trained with both types of data, could estimate the EMG signal from the output of markerless motion capture.

This cross-training approach could also be an interesting line of investigation when it comes to the comparison between markerless motion capture and force plates data. In chapter 5 the best agreement was found for quiet standing eyes open. As the stance difficulty increased, the agreement lessened. To explain this, the fundamental difference between the way in which the Balance master estimates the position of CoM (from normative data and the inverted pendulum model) and the more direct means of estimated CoM, used by the proposed method was discussed. In the conclusion, of this chapter, future work

was suggested that should include a three-way comparison of metrics calculated using our proposed method, marker-based motion capture and a force plate, for both healthy and impaired individuals. Fundamentally force plates measure CoP. It would be interesting to see if a model can be built, which could better interpret the true CoM from, force-plate derived, CoP data.

9.5 Closing Comments

The work presented in this thesis, opens the door to the use of low-cost forms of markerless motion capture in the objective assessment of impairment, falls-risk and frailty. A much under research field, in comparison to other instrumented approaches, such as force plates. This thesis draws comparisons between approaches that use force plates and a proposed method of deriving the same metrics. It also demonstrates some issues with using a single point (CoM) to quantify the complexity of balance. Finally, it demonstrates how a combination of the more complete information, that can be obtained from depth cameras and machine learning, can provide a fresh approach to the quantification of impairment and falls-risk.

There is still much to do, but it is not hard to imagine a situation were a 70-year-old-man visits his GP, and she does not ask if “have you fallen recently?”. Instead, she asks “would you like to have your falls-risk assessed?”.

He says “Yes, why not!” and she pulls out a small portable depth camera plugged into a laptop from over on one side of the office, next to the height chart and the weighing scales.

After spending a minute to set-up the camera, a few meters from a chair, she asks him to “stand up and down 5 times, when she says go”. On go, he begins to stand, and she captures the movement. A second or two later, she has an estimate of his falls likelihood and based on the result. She can make an appropriate referral or tell him “everything is fine”.

Appendices

Appendix A

A.1 SPPB Scoring Sheet

Short Physical Performance Battery Protocol and Score Sheet

Participant Name: _____ Date: _____

All of the tests should be performed in the same order as they are presented in this protocol. Instructions to the participants are shown in bold italic and should be given exactly as they are written in this script.

1. BALANCE TESTS

The participant must be able to stand unassisted without the use of a cane or walker. You may help the participant to get up.

Now let's begin the evaluation. I would now like you to try to move your body in different movements. I will first describe and show each movement to you. Then I'd like you to try to do it, tell me and we'll move on to the next one. Let me emphasize that I do not want you to try to do any exercise that you feel might be unsafe.

do it. Ify

Do you have any questions before we begin?

A. Side-by-Side Stand

1. ***Now I will show you the first movement.***
2. (Demonstrate) ***I want you to try to stand with your feet together, side-by-side, for about 10 seconds.***
3. ***You may use your arms, bend your knees, or move your body to maintain your balance, but try not to move your feet. Try to hold this position until I tell you to stop.***
4. Stand next to the participant to help him/her into the side-by-side position.
5. Supply just enough support to the participant's arm to prevent loss of balance.
6. When the participant has his/her feet together, ask ***"Are you ready?"***
7. Then let go and begin timing as you say, ***"Ready, begin."***
8. Stop the stopwatch and say ***"Stop"*** after 10 seconds or when the participant steps out of position or grabs your arm.
9. If participant is unable to hold the position for 10 seconds, record result and go to the gait speed test.

B. Semi-Tandem Stand

1. ***Now I will show you the second movement.***
2. (Demonstrate) ***Now I want you to try to stand with the side of the heel of one foot touching the big toe of the other foot for about 10 seconds. You may put either foot in front, whichever is more comfortable for you.***
3. ***You may use your arms, bend your knees, or move your body to maintain your balance, but try not to move your feet. Try to hold this position until I tell you to stop.***
4. Stand next to the participant to help him/her into the semi-tandem position
5. Supply just enough support to the participant's arm to prevent loss of balance.
6. When the participant has his/her feet together, ask ***"Are you ready?"***
7. Then let go and begin timing as you say ***"Ready, begin."***
8. Stop the stopwatch and say ***"Stop"*** after 10 seconds or when the participant steps out of position or grabs your arm.
9. If participant is unable to hold the position for 10 seconds, record result and go to the gait speed test.

C. Tandem Stand

1. ***Now I will show you the third movement.***
2. (Demonstrate) ***Now I want you to try to stand with the heel of one foot in front of and touching the toes of the other foot for about 10 seconds. You may put either foot in front, whichever is more comfortable for you.***
3. ***You may use your arms, bend your knees, or move your body to maintain your balance, but try not to move your feet. Try to hold this position until I tell you to stop.***
4. Stand next to the participant to help him/her into the tandem position.
5. Supply just enough support to the participant's arm to prevent loss of balance.
6. When the participant has his/her feet together, ask ***"Are you ready?"***
7. Then let go and begin timing as you say, ***"Ready, begin."***
8. Stop the stopwatch and say ***"Stop"*** after 10 seconds or when the participant steps out of position or grabs your arm.

Short Physical Performance Battery Protocol and Score Sheet

SCORING:

A. Side-by-Side stand

- Held for 10 sec 1 point
- Not held for 10 sec 0 points
- Not attempted 0 points

If 0 points, end Balance Tests

Number of seconds held if less than 10 sec:
____.____ Sec

If participant did not attempt test or failed, circle why:

- Tried but unable 1
- Participant could not hold position unassisted 2
- Not attempted, you felt unsafe 3
- Not attempted, participant felt unsafe 4
- Participant unable to understand instructions 5
- Other (specify) 6
- Participant refused 7

B. Semi-Tandem Stand

- Held for 10 sec 1 point
- Not held for 10 sec 0 points
- Not attempted 0 points

(circle reason to the right)

If 0 points, end Balance Tests

Number of seconds held if less than 10 sec:
____.____ Sec

If participant did not attempt test or failed, circle why:

- Tried but unable 1
- Participant could not hold position unassisted 2
- Not attempted, you felt unsafe 3
- Not attempted, participant felt unsafe 4
- Participant unable to understand instructions 5
- Other (specify) 6
- Participant refused 7

C. Tandem Stand

- Held for 10 sec 2 point
- Held for 3 to 9.99 sec 1 points
- Held for < than 3 sec 0 points
- Not attempted 0 points

(circle reason above)

Number of seconds held if less than 10 sec:
____.____ Sec

If participant did not attempt test or failed, circle why:

- Tried but unable 1
- Participant could not hold position unassisted 2
- Not attempted, you felt unsafe 3
- Not attempted, participant felt unsafe 4
- Participant unable to understand instructions 5
- Other (specify) 6
- Participant refused 7

D. Total Balance Tests score _____ (sum points)

Comments: _____

2. GAIT SPEED TEST

Now I am going to observe how you normally walk. If you use a cane or other walking aid and you feel you need it to walk a short distance, then you may use it.

A. First Gait Speed Test

1. ***This is our walking course. I want you to walk to the other end of the course at your usual speed, just as if you were walking down the street to go to the store.***
2. Demonstrate the walk for the participant.
3. ***Walk all the way past the other end of the tape before you stop. I will walk with you. Do you feel this would be safe?***
4. Have the participant stand with both feet touching the starting line.
5. ***When I want you to start, I will say: "Ready, begin."*** When the participant acknowledges this instruction say: ***Ready, begin.***
6. Press the start/stop button to start the stopwatch as the participant begins walking.
7. Walk behind and to the side of the participant.
8. Stop timing when one of the participant's feet is completely across the end line.

B. Second Gait Speed Test

1. ***Now I want you to repeat the walk. Remember to walk at your usual pace, and go all the way past the other end of the course.***
2. Have the participant stand with both feet touching the starting line.
3. ***When I want you to start, I will say: "Ready, begin."*** When the participant acknowledges this instruction say: ***Ready, begin.***
4. Press the start/stop button to start the stopwatch as the participant begins walking.
5. Walk behind and to the side of the participant.
6. Stop timing when one of the participant's feet is completely across the end line.

Short Physical Performance Battery Protocol and Score Sheet

GAIT SPEED TEST SCORING:

Length of walk test course: Four meters Three meters

A. Time for First Gait Speed Test (sec)

1. Time for 3 or 4 meters _____.____ sec

2. If participant did not attempt test or failed, circle why:

- | | |
|---|---|
| Tried but unable | 1 |
| Participant could not walk unassisted | 2 |
| Not attempted, you felt unsafe | 3 |
| Not attempted, participant felt unsafe | 4 |
| Participant unable to understand instructions | 5 |
| Other (Specify) _____ | 6 |
| Participant refused | 7 |
- Complete score sheet and go to chair stand test

3. Aids for first walk..... None Cane Other

Comments: _____

B. Time for Second Gait Speed Test (sec)

1. Time for 3 or 4 meters _____.____ sec

2. If participant did not attempt test or failed, circle why:

- | | |
|---|---|
| Tried but unable | 1 |
| Participant could not walk unassisted | 2 |
| Not attempted, you felt unsafe | 3 |
| Not attempted, participant felt unsafe | 4 |
| Participant unable to understand instructions | 5 |
| Other (Specify) | 6 |
| Participant refused | 7 |

3. Aids for second walk..... None Cane Other

What is the time for the faster of the two walks?

Record the shorter of the two times _____.____ sec

[If only 1 walk done, record that time] _____.____ sec

If the participant was unable to do the walk: 0 points

Short Physical Performance Battery Protocol and Score Sheet

For 4-Meter Walk:		For 3-Meter Walk:	
If time is more than 8.70 sec:	<input type="checkbox"/> 1 point	If time is more than 6.52 sec:	<input type="checkbox"/> 1 point
If time is 6.21 to 8.70 sec:	<input type="checkbox"/> 2 points	If time is 4.66 to 6.52 sec:	<input type="checkbox"/> 2 points
If time is 4.82 to 6.20 sec:	<input type="checkbox"/> 3 points	If time is 3.62 to 4.65 sec:	<input type="checkbox"/> 3 points
If time is less than 4.82 sec:	<input type="checkbox"/> 4 points	If time is less than 3.62 sec:	<input type="checkbox"/> 4 points

3. CHAIR STAND TEST

Single Chair Stand

1. **Let's do the last movement test. Do you think it would be safe for you to try to stand up from a chair without using your arms?**
2. **The next test measures the strength in your legs.**
3. (Demonstrate and explain the procedure.) **First, fold your arms across your chest and sit so that your feet are on the floor; then stand up keeping your arms folded across your chest.**
4. Please stand up keeping your arms folded across your chest. (Record result).
5. If participant cannot rise without using arms, say "Okay, try to stand up using your arms." This is the end of their test. Record result and go to the scoring page.

Repeated Chair Stands

1. **Do you think it would be safe for you to try to stand up from a chair five times without using your arms?**
2. (Demonstrate and explain the procedure): **Please stand up straight as QUICKLY as you can five times, without stopping in between. After standing up each time, sit down and then stand up again. Keep your arms folded across your chest. I'll be timing you with a stopwatch.**
3. When the participant is properly seated, say: **"Ready? Stand"** and begin timing.
4. Count out loud as the participant arises each time, up to five times.
5. Stop if participant becomes tired or short of breath during repeated chair stands.
6. Stop the stopwatch when he/she has straightened up completely for the fifth time.
7. Also stop:
 - If participant uses his/her arms
 - After 1 minute, if participant has not completed rises
 - At your discretion, if concerned for participant's safety
8. If the participant stops and appears to be fatigued before completing the five stands, confirm this by asking **"Can you continue?"**
9. If participant says "Yes," continue timing. If participant says "No," stop and reset the stopwatch.

Short Physical Performance Battery Protocol and Score Sheet

SCORING

Single Chair Stand Test

- | | Yes | No |
|---|--------------------------|-----------------------------------|
| A. Safe to stand without help | <input type="checkbox"/> | <input type="checkbox"/> |
| B. Results: | | |
| Participant stood without using arms | <input type="checkbox"/> | → Go to Repeated Chair Stand Test |
| Participant used arms to stand | <input type="checkbox"/> | → End test; score as 0 points |
| Test not completed | <input type="checkbox"/> | → End test; score as 0 points |
| C. If participant did not attempt test or failed, circle why: | | |
| Tried but unable | 1 | |
| Participant could not stand unassisted | 2 | |
| Not attempted, you felt unsafe | 3 | |
| Not attempted, participant felt unsafe | 4 | |
| Participant unable to understand instructions | 5 | |
| Other (Specify) | 6 | |
| Participant refused | 7 | |

Repeated Chair Stand Test

- | | Yes | No |
|---|--------------------------|--------------------------|
| A. Safe to stand five times | <input type="checkbox"/> | <input type="checkbox"/> |
| B. If five stands done successfully, record time in seconds.
Time to complete five stands _____.____ sec | | |
| C. If participant did not attempt test or failed, circle why: | | |
| Tried but unable | 1 | |
| Participant could not stand unassisted | 2 | |
| Not attempted, you felt unsafe | 3 | |
| Not attempted, participant felt unsafe | 4 | |
| Participant unable to understand instructions | 5 | |
| Other (Specify) | 6 | |
| Participant refused | 7 | |

Scoring the Repeated Chair Test

- Participant unable to complete 5 chair stands or completes stands in >60 sec: 0 points
- If chair stand time is 16.70 sec or more: 1 points
- If chair stand time is 13.70 to 16.69 sec or more: 2 points
- If chair stand time is 11.20 to 13.69 sec: 3 points
- If chair stand time is 11.19 sec or less: 4 points

Short Physical Performance Battery Protocol and Score Sheet

Participant ID: _____ Date: _____ Tester Initials: _____

Scoring for Complete Short Physical Performance Battery

Test Scores

Total Balance Test score _____ points

Gait Speed Test score _____ points

Chair Stand Test score _____ points

Total Score _____ **points** (sum of points above)

Appendix B

B.1 Motor Unit Study Questionnaire: MMU

Motor Unit study questionnaire: MMU

(Version 2: 17/05/2017)

Please complete this questionnaire as thoroughly and as accurately as you can to help us with our research. All your answers will be treated as **strictly confidential** and will only be seen by the research team.

If you require this questionnaire in large print or have any difficulties with the questions, please contact the research team:

Email: j.s.mcphee@mmu.ac.uk , sean.maudsley-barton@mmu.ac.uk

Telephone: 0161 247 5675



Please use **black pen** and make sure you tick **inside** the boxes, not next to them. Thank you!

Please first complete:

Your name: _____

Your date of birth: / /

Today's date: / /

Study ID (office use only): MU

Your personal information

Please **tick one box** for the following questions



1.1 What is your current marital status?

- Single and never been married
- Married and living with husband/wife
- Married & separated from husband/wife
- Divorced
- Widowed
- Registered partnership
- Co-habiting

1.2 What was your maximum educational level attained by 26 years of age?

- CSE
- GCSE
- GCSE O level
- A/S level
- GCE A level (or S Level)
- Scottish School Certificate
- Higher School Certificate or Scottish School Qualification
- Diploma of Higher Education
- First degree (e.g. BA, BSc)
- Other degree level qualification
Such as graduate membership of professional institute
- Higher degree (e.g. PhD, MSc)
- Nursing or other para-medical qualification
- PGCE- Post-graduate Certificate of Education

- Other teaching qualification
- None of these

1.3 What is the full title of your main occupation during your working life? (*Please use precise terms, for example 'primary school teacher' rather than 'teacher'. For government or civil service, please provide grade. For armed forces, please provide rank.*)

1.4 If you have ever been a married woman, what is/was your husband's main occupation? (*Please leave blank if not applicable*)

1.5 What is your height?

_____ Metres OR

_____ Feet and _____ inches

1.6 How much do you currently weigh?

_____ Kilograms OR

_____ Stone and _____ pounds

Your health status

2.1 How would you describe your current health status?

Very good
 Good
 Fair
 Poor
 Very Poor

2.2 Do you **have** or **have you ever** had any of the following diseases?

Disease	Yes	No	If yes, please specify which disease or type
A. Chronic non-specific lung disease (asthma, chronic bronchitis or pulmonary emphysema)			
B. Cardio-vascular diseases			
C. Peripheral arterial disease			
D. Diabetes mellitus			
E. Stroke			
F. Cancer			
G. Osteoporosis			
H. Arthritis (Rheumatoid/Osteo)			
I. Chronic liver or kidney disease			
J. Anorexia nervosa			
K. Overactive thyroid/parathyroid gland			
L. Coeliac disease or Malabsorption			
M. Parkinson's disease			
N. Poor vision not corrected by glasses.			

2.3 Are you currently on any medication?

Yes No

2.3.1 If **yes**, please provide details:

	Name of medication <i>(Please copy name in full from container)</i>	Strength of dosage and how often <i>(please copy from container)</i>	Reason for taking
1			
2			
3			
4			
5			
6			
7			
8			
9			
10			
11			
12			

2.4 Are you a current smoker?

Yes No

2.4.1 If yes, how many cigarettes do you smoke in a normal day? *(If you smoke roll-ups, cigars or pipes, please give the equivalent number of cigarettes)*

1-5 5-10 10-20 >20

2.4.2 What age were you when you started smoking?

<16 16-25 26-35 36-45 46-55 >55

2.5 Have you **ever** smoked cigarettes regularly *(by which we mean at least one cigarette a day for 12 months or more)*

Yes No

2.5.1 If yes, how long ago did you give up smoking? *(fill in number of weeks or months or years below and circle as appropriate)*

_____ (weeks / months / years)

2.6 Have you drunk alcohol in the last year?

Yes No

2.7.1 If yes, In the last **7 days** have you had any of the following drinks? (*Do not count non-alcoholic drinks*)

A. Spirits or liqueurs (e.g. whisky, gin, brandy)

No
 Yes _____ measures

B. Wine, sherry, martini, or port

No
 Yes _____ Glasses

C. Beer, lager, cider, or stout

No
 Yes
_____ Pints
_____ ½ pints

2.7 In the last year, have you noticed loss of strength or weakness in your hands?

- Not at all or rarely
- A little or some of the time
- A moderate amount of time
- Most of the time

2.8 In the last year, have you lost more than 10 pounds in weight unintentionally?

Yes No

2.9 How often in the last week did the following apply?

“I felt that everything I did was an effort” or “I could not get going”

- Rarely or none of the time (<1 day)
- Some or a little of the time (1-2 days)
- A moderate amount of time (3-4 days)
- Most of the time (>4 days)

2.10 The following statements are about **feelings** and **thoughts**. Please circle one number per line that best describes your experience of each statement over the **last 2 weeks**.

Statements	<i>please circle one number per line</i>				
	None of the time	Rarely	Some of the time	Often	All of the time
I've been feeling optimistic about the future	1	2	3	4	5
I've been feeling useful	1	2	3	4	5
I've been feeling relaxed	1	2	3	4	5
I've been feeling interested in other people	1	2	3	4	5
I've had energy to spare	1	2	3	4	5
I've been dealing with problems well	1	2	3	4	5
I've been thinking clearly	1	2	3	4	5
I've been feeling good about myself	1	2	3	4	5
I've been feeling close to other people	1	2	3	4	5
I've been feeling confident	1	2	3	4	5
I've been able to make up my own mind about things	1	2	3	4	5

I've been feeling loved	1	2	3	4	5
I've been interested in new things	1	2	3	4	5
I've been feeling cheerful	1	2	3	4	5

3.1. Have you noticed that you've been getting tired in the past month

Yes No

3.1.1 If yes, on how many days have you felt tired in the past seven days?

1-3 4+

3.1.2 Have you felt so tired that you've had to push yourself to get things done in the past 7 days?

Yes No

3.1.3 Have you felt tired when doing things you enjoy in the past seven days?

Yes No I haven't done anything enjoyable in the past week

3.1.4 What do you think is the main reason for feeling tired?

Problems
with sleep

Physical illness

Tablets or
medication

Stress of
worry

My age

Working
too hard

Physical
exercise

If other, please specify

3.1.5 How long have you been feeling tired like this?

Less than
2 weeks

2 weeks - 6 months

6 months – 1 year

1-2 years

2+ years

For Female Participants only

4.1 Have you passed the menopause?

Yes No Current Don't know

6.1.1 If yes, at what age did your periods stop (approx)? _____

6.1.2 Did your periods stop naturally
because of an operation

4.2 Except for pregnancy, or the onset of menopause, have your periods ever stopped for more than 6 months?

Yes No

4.3 Have you had a hysterectomy?

Yes No

5.3.1 If yes, how old were you? _____

5.3.2 Were both ovaries removed?

Both One Neither Don't know

4.4 Have you ever used Hormone Replacement Therapy (HRT)? (this includes patches, tablets, implant)

Yes No

Your current physical activity

5.1 Do you make regular journeys every day or most days either walking or cycling?

- No I walk I cycle Both

5.2 How many times during a typical day do you walk up a flight of stairs (1 flight of stairs = 10 steps)?

- None 0-2 2-4 5-10 times More than 10 times

5.3 Which of the following best describes your walking speed?

-
- Unable to walk Very slow Stroll at an easy pace Normal speed Fairly brisk Fast

5.4 Over the past 7 days, have you taken part in any physical activity? Yes No

5.4.1 **If yes**, please tick one box for each activity that you have participated in during the last 7 days.

	0-1 hours	1-2 hours	2-4 hours	More than 4 hours
<i>Aerobics</i>				
<i>Aqua aerobics</i>				
<i>Badminton</i>				
<i>Bowls</i>				
<i>Cycling</i>				
<i>Dancing</i>				
<i>Football/hockey</i>				
<i>Gardening, light (e.g. pruning, watering)</i>				
<i>Gardening, heavy (e.g. digging, mowing)</i>				
<i>Golf</i>				
<i>Gym</i>				
<i>Hiking</i>				
<i>Housework</i>				
<i>Jogging/running</i>				
<i>Snow skiing</i>				
<i>Squash</i>				
<i>Swimming</i>				
<i>Tennis</i>				
<i>Tai Chi/ Yoga/ Pilates</i>				
<i>Walking</i>				
<i>Water sports (e.g. windsurfing)</i>				
<i>Other physical activity (please state)</i> _____				

5.4.2 You have just been asked about your physical activities in the past 7 days, were these 7 days normal as compared to the rest of the past year?

Yes

No, I did more because of:

The weather Holiday

Other.....

No, I did less because of:

The weather Holiday Illness

Other.....

Your past physical activity

6.1 How often did/do you take part in sports and leisure time exercise involving weight bearing activity, e.g. running, racquet sports, football, rugby, hockey, dancing and running, not including walking, cycling or swimming? (*Please tick your best approximation for each age category*)

	None	Occasionally (once a month)	Frequently (once a week)	Very frequently (more than once a week)
a) Up to age 18				
b) When you were aged 18-30				
c) When you were aged 30-50				
d) Since you have been 50				

6.2 Considering 20 minutes of brisk walking is about 1 mile, how many miles did/do you usually walk each day? (*Please tick appropriate answer for each age category*)

	Under 1 mile	1 to 2 miles	3 to 5 miles	Over 5 miles
a) Up to age 18				
b) When you were aged 18-30				
c) When you were aged 30-50				
d) Since you have been 50				

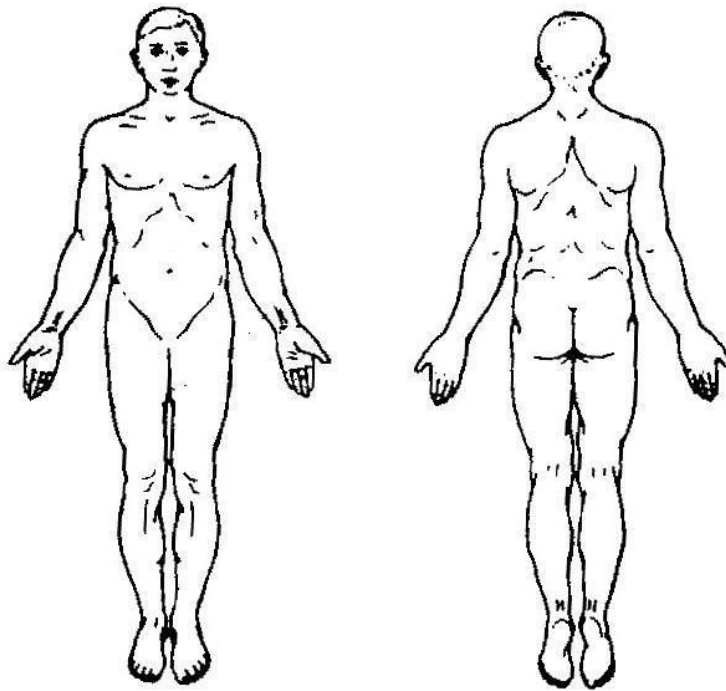
Your joints and bones

7.1 Has a doctor told you that you have broken, fractured or chipped any bones since the age of 45?

Yes

No

7.1.1 If yes, please mark on the drawing below the location of the broken bone(s)



7.1.2 Please provide details of the broken bone(s)

Name of bone	Age when fracture occurred	How did the fracture occur?

7.2 Have you had any fall including a slip or trip in which you lost your balance and landed on the floor or ground or lower level in the past 12 months?

None One Two Three Four or more

7.2.1 Did you seek medical attention for any of these falls?

Yes No Not applicable

7.2.2 Are you worried about falling again?

Yes No

7.2.2.1 If yes, do you limit or stop going out because of this?

Yes No

7.3 On a scale of 1 to 10, with **10 being very confident** and **1 being not confident** at all, how confident are you that you can do the following activities without falling?
(Please tick the relevant box to indicate your confidence for each activity)

Activity	1 Not confident	2	3	4	5	6	7	8	9	10 Very confident
Take a bath or shower										
Reach into cabinets or closets										
Walk around the house										
Prepare meals not requiring carrying heavy or hot objects										
Get in and out of bed										
Answer the door or telephone										
Getting in and out of a chair										
Getting dressed and undressed										
Personal grooming (i.e. washing your face)										
Getting on and off the toilet										
Total score <i>(office use)</i>										

7.4 Do you regularly use any of the following to help you get around? *(Please tick as many that apply)*

Walking stick Zimmer frame Trolley/frame Mobility scooter Wheelchair Not applicable

If other, please state

.....

7.5 Do you have a noticeable limp?

Yes No

7.6 Have you had a joint replacement?

Yes No

7.7 If yes, please tick the appropriate box(s) indicating which joint was replaced and how long ago.

Joint replaced	Time since replacement			
	<i>Less than 6 months</i>	<i>6-12 months</i>	<i>1-2 years</i>	<i>More than 2 years ago</i>
<i>a) Hip (right)</i>				
<i>b) Hip (left)</i>				
<i>c) Knee (right)</i>				
<i>d) Knee (left)</i>				

7.8 Is your ability to walk restricted due to pain?

Yes No

7.9 If yes, please tick the appropriate box(s) indicating where the pain occurs and the time walked before you have to stop as a result of the pain.

Joint where pain occurs	Time walked before being interrupted by pain				
	<i>Less than 1 minute</i>	<i>1-5 minutes</i>	<i>5-10 minutes</i>	<i>10-20 minutes</i>	<i>More than 20 minutes</i>
<i>a) Hip (right)</i>					
<i>b) Hip (left)</i>					
<i>c) Knee (right)</i>					
<i>d) Knee (left)</i>					
<i>e) Ankle (right)</i>					
<i>f) Ankle (left)</i>					
<i>g) Back</i>					

Physical Endurance

8.1. How frequently do you exercise?

Never

Less than
once a week

Once a
week

2-3 times a
week

Almost every
day

8.2. If you exercise as frequently as once or more times a week, how hard do you push yourself?

I take it easy
without
breaking a
sweat or
losing my
breath

I push myself
so hard that I
lose my
breath and
break into
sweat

I push
myself
near
exhaustion

8.3. How long does each session last?

Less than
15
minutes

15–29
minutes

30 minutes
to 1 hour

More than
1 hour

***Thank you for taking the time to complete this
questionnaire.***

Bibliography

- [1] Vakanski A, Ferguson JM, and Lee S. Mathematical Modeling and Evaluation of Human Motions in Physical Therapy Using Mixture Density Neural Networks. *Journal of Physiotherapy & Physical Rehabilitation*, 01(04):1–10, 2016.
- [2] Diana Abrahamova and Frantisek Hlavacka. Age-related changes of human balance during quiet stance. *Physiological Research*, 57(6):1–17, 2008.
- [3] Dimitrios Alexiadis, Petros Daras, Philip Kelly, Noel E O, Tamy Boubekeur, and Maher Ben Moussa. Evaluating a Dancer’s Performance using Kinect-based Skeleton Tracking. In *MM ’11 Proceedings of the 19th ACM international conference on Multimedia*, pages 659–662, 2011.
- [4] E. Anson, S. Studenski, P. J. Sparto, and Y. Agrawal. Community-dwelling adults with a history of falling report lower perceived postural stability during a foam eyes closed test than non-fallers. *Experimental Brain Research*, 237(3):769–776, 3 2019.
- [5] D. Antón, A. Goñi, and A. Illarramendi. Exercise Recognition for Kinect-based Telerehabilitation. *Methods of Information in Medicine*, 54(02):145–155, 1 2015.
- [6] Geraldine Aubert and Peter M Lansdorp. Telomeres and Aging. *Physiological Reviews*, 88(2):557–579, 4 2008.
- [7] Bernard Auvinet, Gilles Berrut, Claude Touzard, Laurent Moutel, Nadine Collet, Denis Chaleil, and Eric Barrey. Gait Abnormalities in Elderly Fallers. *Journal of Aging and Physical Activity*, 11(1):40–52, 1 2003.

- [8] Pierre Baldi. Autoencoders, Unsupervised Learning, and Deep Architectures. *ICML Unsupervised and Transfer Learning*, pages 37–50, 2012.
- [9] Leonard E Baum and Ted Petrie. Statistical Inference for Probabilistic Functions of Finite State Markov Chains. *The Annals of Mathematical Statistics*, 37(6):1554–1563, 12 1966.
- [10] Mr. Bayes and Mr. Price. LII. An essay towards solving a problem in the doctrine of chances. By the late Rev. Mr. Bayes, F. R. S. communicated by Mr. Price, in a letter to John Canton, A. M. F. R. S. *Philosophical Transactions of the Royal Society of London*, 53:370–418, 12 1763.
- [11] Brian J. Benda, Patrick O. Riley, and David E. Krebs. Biomechanical Relationship Between Center of Gravity and Center of Pressure During Standing. *IEEE Transactions on Rehabilitation Engineering*, 2(1):3–10, 3 1994.
- [12] Y. Bengio, Patrice Simard, and Paolo Frasconi. Learning long-term dependencies with gradient descent is difficult. *IEEE Transactions on Neural Networks*, 5(2):157–166, 3 1994.
- [13] Yoshua Bengio, Pascal Lamblin, Dan Popovici, and Hugo Larochelle. Greedy layer-wise training of deep networks. In *Advances in Neural Information Processing Systems*, pages 153–160, 2007.
- [14] Katherine O. Berg, Brian E. Maki, Jack I. Williams, Pamela J. Holliday, and Sharon L. Wood-Dauphinee. Clinical and laboratory measures of postural balance in an elderly population. *Archives of Physical Medicine and Rehabilitation*, 73(11):1073–1080, 1992.
- [15] Alexandre Bernardino, Christian Vismara, Sergi Bermudez i Badia, Elvio Gouveia, Fatima Baptista, Filomena Carnide, Simao Oom, and Hugo Gamboa. A dataset for the automatic assessment of functional senior fitness tests using kinect and physiological sensors. In *2016 1st International Conference on Technology and Innovation in Sports, Health and Wellbeing (TISHW)*, pages 1–6. IEEE, 12 2016.
- [16] Nikolai Bernstein and Aleksandrovich. *The Coordination and Regulation of Movements*. Pergarmon Press: Oxford, UK, 1967.

- [17] A. Amini Maghsoud Bigy, K. Banitsas, A Badii, and J Cosmas. Recognition of Postures and Freezing of Gait in Parkinson’s Disease Patients Using Microsoft Kinect Sensor. *7th Annual International IEEE EMBS Conference on Neural Engineering*, pages 731–734, 2015.
- [18] F. Owen Black, Conrad Wall, Howard E. Rockette, and Russell Kitch. Normal subject postural sway during the romberg test. *American Journal of Otolaryngology*, 3(5):309–318, 9 1982.
- [19] J Martin Bland and Douglas G Altman. STATISTICAL METHODS FOR ASSESSING AGREEMENT BETWEEN TWO METHODS OF CLINICAL MEASUREMENT. *Lancet*, 327(8476):307–310, 1986.
- [20] Séverine Bleuse, François Cassim, Jean-Louis Blatt, Etienne Labyt, Philippe Derambure, Jean-Daniel Guieu, and Luc Defebvre. Effect of age on anticipatory postural adjustments in unilateral arm movement. *Gait & Posture*, 24(2):203–210, 10 2006.
- [21] An Bogaerts, Sabine Verschueren, Christophe Delecluse, Albrecht L Claessens, and Steven Boonen. Effects of whole body vibration training on postural control in older individuals: A 1 year randomized controlled trial. *Gait & Posture*, 26(2):309–316, 2007.
- [22] Richard W. Bohanno. Test-retest reliability of the five-repetition sit-to-stand test: A systematic review of the literature involving adults. *Journal of Strength and Conditioning Research*, 25(11):3205–3207, 2011.
- [23] Richard W. Bohannon. Reference Values for the Five-Repetition Sit-to-Stand Test: A Descriptive Meta-Analysis of Data from Elders. *Perceptual and Motor Skills*, 103(1):215–222, 8 2006.
- [24] Richard W Bohannon, Patricia A Larkin, Amy C Cook, James Gear, and Julio Singer. Decrease in timed balance test scores with aging. *Physical therapy*, 64(7):1067–70, 7 1984.
- [25] Bernhard E Boser, Isabelle M Guyon, and Vladimir N Vapnik. A training algorithm for optimal margin classifiers. In *Proceedings of the fifth annual workshop on Computational learning theory - COLT ’92*, pages 144–152, 1992.

- [26] H. Bourlard and Y. Kamp. Auto-association by multilayer perceptrons and singular value decomposition. *Biological Cybernetics*, 59(4-5):291–294, 9 1988.
- [27] Séverine Buatois, René Gueguen, Gérome C. Gauchard, Athanase Benetos, and Philippe P. Perrin. Posturography and risk of recurrent falls in healthy non-institutionalized persons aged over 65. *Gerontology*, 52(6):345–352, 2006.
- [28] Elizabeth R. Burns, Judy A. Stevens, and Robin Lee. The direct costs of fatal and non-fatal falls among older adults — United States. *Journal of Safety Research*, 58:99–103, 9 2016.
- [29] Judith Butepage, Michael J Black, Danica Kragic, and Hedvig Kjellstrom. Deep Representation Learning for Human Motion Prediction and Classification. In *2017 IEEE Conference on Computer Vision and Pattern Recognition (CVPR)*, volume 2017-Janua, pages 1591–1599. IEEE, 7 2017.
- [30] Michele L. Callisaya, Leigh Blizzard, Michael D. Schmidt, Kara L. Martin, Jennifer L. McGinley, Lauren M. Sanders, and Velandai K. Srikanth. Gait, gait variability and the risk of multiple incident falls in older people: a population-based study. *Age and Ageing*, 40(4):481–487, 7 2011.
- [31] Judith Campisi. Cellular senescence and apoptosis: how cellular responses might influence aging phenotypes. *Experimental Gerontology*, 38(1-2):5–11, 1 2003.
- [32] M. Capecci, M. G. Ceravolo, F. Ferracuti, S. Iarlori, S. Longhi, L. Romeo, S. N. Russi, and F. Verdini. Accuracy evaluation of the Kinect v2 sensor during dynamic movements in a rehabilitation scenario. In *2016 38th Annual International Conference of the IEEE Engineering in Medicine and Biology Society (EMBC)*, pages 5409–5412. IEEE, 8 2016.
- [33] Marianna Capecci, Maria Gabriella Ceravolo, Francesco Ferracuti, Sabrina Iarlori, Ville Kyrki, Andrea Monteriù, Luca Romeo, and Federica Verdini. A Hidden Semi-Markov Model based approach for rehabilitation exercise assessment. *Journal of Biomedical Informatics*, 78(July 2017):1–11, 2 2018.

- [34] Marianna Capecci, Maria Gabriella Ceravolo, Francesco Ferracuti, Sabrina Iarlori, Andrea Monteriu, Luca Romeo, and Federica Verdini. The KIMORE Dataset: KInematic Assessment of MOvement and Clinical Scores for Remote Monitoring of Physical REhabilitation. *IEEE Transactions on Neural Systems and Rehabilitation Engineering*, 27(7):1436–1448, 7 2019.
- [35] Wayne E. Carlson. *Computer Graphics and Computer Animation: A Retrospective Overview*. Th Ohio State University, 2017.
- [36] Olivier Caron, T. Gelat, Patrice Rougier, and J. P. Blanchi. A comparative analysis of the center of gravity and center of pressure trajectory path lengths in standing posture: An estimation of active stiffness. *Journal of Applied Biomechanics*, 16(3):234–247, 2000.
- [37] Yao-Jen Jen Chang, Shu-Fang Fang Chen, and Jun-Da Da Huang. A Kinect-based system for physical rehabilitation: A pilot study for young adults with motor disabilities. *Research in Developmental Disabilities*, 32(6):2566–2570, 2011.
- [38] N. V. Chawla, K. W. Bowyer, L. O. Hall, and W. P. Kegelmeyer. SMOTE: Synthetic Minority Over-sampling Technique. *Journal of Artificial Intelligence Research*, 16(Sept. 28):321–357, 6 2002.
- [39] Heeryon Cho and Sang Min Yoon. Divide and conquer-based 1D CNN human activity recognition using test data sharpening. *Sensors (Switzerland)*, 18(4):16–18, 2018.
- [40] Kyunghyun Cho, Bart van Merriënboer, Caglar Gulcehre, Dzmitry Bahdanau, Fethi Bougares, Holger Schwenk, and Yoshua Bengio. Learning Phrase Representations using RNN Encoder-Decoder for Statistical Machine Translation. *arXiv*, pages 1724–1734, 2014.
- [41] Ross A. Clark, Yong-Hao Hao Pua, Karine Fortin, Callan Ritchie, Kate E. Webster, Linda Denehy, and Adam L. Bryant. Validity of the Microsoft Kinect for assessment of postural control. *Gait & Posture*, 36(3):372–377, 7 2012.
- [42] Ross A. Clark, Yong-Hao Hao Pua, Cristino C. Oliveira, Kelly J. Bower, Shamala Thilarajah, Rebekah McGaw, Ksaniel Hasanki, and

- Benjamin F. Mentiplay. Reliability and concurrent validity of the Microsoft Xbox One Kinect for assessment of standing balance and postural control. *Gait & Posture*, 42(2):210–213, 2015.
- [43] Helen Cohen. Modified Clinical Test of Sensory Interaction in Balance, 1993.
- [44] International Conference, Information Sciences, Signal Processing, and Main Tracks. MULTIPLE DEPTH CAMERAS CALIBRATION AND BODY VOLUME RECONSTRUCTION FOR GAIT ANALYSIS. In *Conference on Information Sciences, Signal Processing and their Applications*, pages 478–483. IEEE, 2012.
- [45] Corinna Cortes and Vladimir Vapnik. Support-vector networks. *Machine Learning*, 20(3):273–297, 9 1995.
- [46] D R Cox. The Regression Analysis of Binary Sequences. *Journal of the Royal Statistical Society: Series B (Methodological)*, 21(1):238–238, 1 1958.
- [47] C.E. E. Craig, D.J. J. Goble, and M. Dumas. Proprioceptive acuity predicts muscle co-contraction of the tibialis anterior and gastrocnemius medialis in older adults’ dynamic postural control. *Neuroscience*, 322:251–261, 5 2016.
- [48] A Crétual. Which biomechanical models are currently used in standing posture analysis? *Neurophysiologie Clinique*, 45(4-5):285–295, 2015.
- [49] Ramon Cuevas-Trisan. Balance Problems and Fall Risks in the Elderly. *Clinics in Geriatric Medicine*, 35(2):173–183, 5 2019.
- [50] D’Agostino R. B. DAgostino et al - normality tests, 1990.
- [51] Rina Dechter. Learning While Searching in Constraint-Satisfaction-Problems. *AAAI*, pages 178–185, 1986.
- [52] Hans Degens, Thomas Mark Maden-Wilkinson, Alex Ireland, Marko T. Korhonen, Harri Suominen, Ari Heinonen, Zsolt Radak, Jamie S. McPhee, and Jörn Rittweger. Relationship between ventilatory function and age in master athletes and a sedentary reference population. *AGE*, 35(3):1007–1015, 6 2013.

- [53] Persi Diaconis and Bradley Efron. Computer-Intensive Methods in Statistics. *Scientific American*, 248(5):116–130, 5 1983.
- [54] Timothy J. Doherty, Anthony A. Vandervoort, and William F. Brown. Effects of Ageing on the Motor Unit: A Brief Review. *Canadian Journal of Applied Physiology*, 18(4):331–358, 12 1993.
- [55] Elham Dolatabadi, Babak Taati, Gemma S Parra-Dominguez, and Alex Mihailidis. A MARKERLESS MOTION TRACKING APPROACH TO UNDERSTAND CHANGES IN GAIT AND BALANCE : A CASE STUDY. *ehabilitation Engineering and Assistive Technology Society of North America*, 2013.
- [56] Yong Du, Yun Fu, and Liang Wang. Skeleton Based Action Recognition using Convolutional Neural Network. In *ACPR*, 2015.
- [57] Yong Du, Wei Wang, and Liang Wang. Hierarchical recurrent neural network for skeleton based action recognition. *Proceedings of the IEEE Computer Society Conference on Computer Vision and Pattern Recognition*, 07-12-June:1110–1118, 2015.
- [58] Marcos Duarte and Dagmar Sternad. Complexity of human postural control in young and older adults during prolonged standing. *Experimental Brain Research*, 191(3):265–276, 11 2008.
- [59] Amandine Dubois and Francois Charpillet. Human activities recognition with RGB-Depth camera using HMM. In *2013 35th Annual International Conference of the IEEE Engineering in Medicine and Biology Society (EMBC)*, pages 4666–4669. IEEE, 7 2013.
- [60] Amandine Dubois and Francois Charpillet. A gait analysis method based on a depth camera for fall prevention. *2014 36th Annual International Conference of the IEEE Engineering in Medicine and Biology Society, EMBC 2014*, pages 4515–4518, 2014.
- [61] Andreas Ejupi, Matthew Brodie, Yves J. Gschwind, Stephen R. Lord, Wolfgang L. Zagler, and Kim Delbaere. Kinect-Based Five-Times-Sit-to-Stand Test for Clinical and In-Home Assessment of Fall Risk in Older People. *Gerontology*, 62(1):118–124, 2015.

- [62] Fabienne El-Khoury, Bernard Cassou, Marie-Aline Charles, and Patricia Dargent-Molina. The effect of fall prevention exercise programmes on fall induced injuries in community dwelling older adults:. *British Journal of Sports Medicine*, 49(20):1348–1348, 10 2013.
- [63] Moataz Eltoukhy, Christopher Kuenze, Jeonghoon Oh, and Joseph Signorile. Validation of Static and Dynamic Balance Assessment using Microsoft Kinect for Young and Elderly Populations. *IEEE Journal of Biomedical and Health Informatics*, 2194(c):1–7, 2017.
- [64] Moataz Eltoukhy, Jeonghoon Oh, Christopher Kuenze, and Joseph Signorile. Improved kinect-based spatiotemporal and kinematic treadmill gait assessment. *Gait & Posture*, 51:77–83, 1 2017.
- [65] Ana Ferlinc, Ester Fabiani, Tomaz Velnar, and Lidija Gradisnik. The Importance and Role of Proprioception in the Elderly: a Short Review. *Materia Socio Medica*, 31(3):219, 2019.
- [66] Michael Firman. RGBD Datasets: Past, Present and Future. In *Computer Vision and Pattern Recognition Workshop*, pages 19–31, 2016.
- [67] E Fix and JL Hodges. Nonparametric discrimination: consistency properties. Technical Report Feb, University of California, 1951.
- [68] Leila Floriani, Michela Spagnuolo, Thomas Giacomo, HyungSeok Kim, Laurent Moccozet, and Nadia Magnenat-Thalmann. *Shape Analysis and Structuring*. Mathematics and Visualization. Springer Berlin Heidelberg, Berlin, Heidelberg, 2008.
- [69] E.W. Forgy. Cluster Analysis of Multivariate Data: Efficiency versus Interpretability of Classifications. *Biometrics*, 21:768–769, 1965.
- [70] Moshe Gabel, Ran Gilad-Bachrach, Erin Renshaw, and Assaf Schuster. Full Body Gait Analysis with Kinect *. In *Annual International Conference of the IEEE*. IEEE, pages 1964–1967, 2012.
- [71] Brook Galna, Gillian Barry, Dan Jackson, Dadirayi Mhiripiri, Patrick Olivier, and Lynn Rochester. Accuracy of the Microsoft Kinect sensor for measuring movement in people with Parkinson’s disease. *Gait & Posture*, 39(4):1062–1068, 4 2014.

- [72] B Ganse, H Degans, M Drey, J Korhonen, Jamie Mcphee, K Muller, B.W Jonannes, and J Rittweger. Impact of age, performance and athletic event on injury rates in master athletics – First results from an ongoing prospective study. *J Musculoskelet Neuronal Interact*, 14(2):148–154, 2014.
- [73] Jaime A Garcia, Yusuf Pisan, Chek Tien Tan, and Karla Felix Navarro. Assessing the kinect’s capabilities to perform a time-based clinical test for fall risk assessment in older people. *Lecture Notes in Computer Science (including subseries Lecture Notes in Artificial Intelligence and Lecture Notes in Bioinformatics)*, 8770:100–107, 2014.
- [74] Daphne J. Geerse, Bert H. Coolen, and Melvyn Roerdink. Kinematic validation of a multi-Kinect v2 instrumented 10-meter walkway for quantitative gait assessments. *PLoS ONE*, 10(10), 2015.
- [75] G Gehlsen and M H Whaley. Falls in the elderly: Part II, Balance, strength, and flexibility. *Archives of physical medicine and rehabilitation*, 71 10:739–741, 1990.
- [76] Farnood Gholami, Daria A. Trojan, Jozsef Kovecses, Wassim M. Haddad, and Behnood Gholami. A Microsoft Kinect-Based Point-of-Care Gait Assessment Framework for Multiple Sclerosis Patients. *IEEE Journal of Biomedical and Health Informatics*, 21(5):1376–1385, 2017.
- [77] Elena Gianaria and Marco Grangetto. Kinect-Based Gait Analysis for Automatic Frailty Syndrome Assessment. In *IEEE International Conference on Image Processing (ICIP)*, 2016.
- [78] Iván Gómez-Conde, David Olivieri, Xosé Antón Vila, and Stella Orozco-Ochoa. Simple Human Gesture Detection and Recognition Using a Feature Vector and a Real-Time Histogram Based Algorithm. *Journal of Signal and Information Processing*, 02(04):279–286, 2011.
- [79] D. González-Ortega, F.J. Díaz-Pernas, M. Martínez-Zarzuela, and M. Antón-Rodríguez. A Kinect-based system for cognitive rehabilitation exercises monitoring. *Computer Methods and Programs in Biomedicine*, 113(2):620–631, 2014.

- [80] Ian J Goodfellow, Yaroslav Bulatov, Julian Ibarz, Sacha Arnoud, and Vinay Shet. Multi-digit Number Recognition from Street View Imagery using Deep Convolutional Neural Networks. *2nd International Conference on Learning Representations, ICLR 2014 - Conference Track Proceedings*, 12 2013.
- [81] Urs Granacher, Albert Gollhofer, Tibor Hortobágyi, Reto W. Kressig, and Thomas Muehlbauer. The Importance of Trunk Muscle Strength for Balance, Functional Performance, and Fall Prevention in Seniors: A Systematic Review. *Sports Medicine*, 43(7):627–641, 7 2013.
- [82] Sherry A Greenberg. Analysis of Measurement Tools of Fear of Falling for High-Risk, Community-Dwelling Older Adults. *Clinical Nursing Research*, 21(1):113–130, 2 2012.
- [83] Jack M. Guralnik, Luigi Ferrucci, Eleanor M. Simonsick, Marcel E. Salive, and Robert B. Wallace. Lower-extremity function in persons over the age of 70 years as a predictor of subsequent disability. *New England Journal of Medicine*, 332(9):556–562, 3 1995.
- [84] Jack M. Guralnik, Eleanor M. Simonsick, Luigi Ferrucci, Robert J Glynn, Lisa F Berkman, Dan G Blazer, Paul A Scherr, and Robert B. Wallace. A Short Physical Performance Battery Assessing Lower Extremity Function. *Journal of Gerontology*, 49(2):M85–M94, 1994.
- [85] Jack M. Guralnik, Eleanor M. Simonsick, Luigi Ferrucci, Robert J Glynn, Lisa F Berkman, Dan G Blazer, Paul A Scherr, Robert B. Wallace, Guralnik, Ferrucci, Simonsick, Salive, and Wallace. A short physical performance battery assessing lower extremity function: association with self-reported disability and prediction of mortality and nursing home admission. *Journal of gerontology*, 49(2):M85–M94, 3 1994.
- [86] Jack M. Guralnik, Eleanor M. Simonsick, Luigi Ferrucci, Robert J Glynn, Lisa F Berkman, Dan G Blazer, Paul A Scherr, Robert B. Wallace, Guralnik, Ferrucci, Simonsick, Salive, and Wallace. Short physical performance battery protocol and score sheet. *Center for Successful Aging*, 49(2):1–8, 1994.

- [87] Patricia A Hageman, J Michael Leibowitz, and Daniel Blanke. Age and gender effects on postural control measures. *Archives of physical medicine and rehabilitation*, 76(October):961–965, 1995.
- [88] Barbara Hammer. On the approximation capability of recurrent neural networks. *Neurocomputing*, 31(1-4):107–123, 3 2000.
- [89] Adam W Harley. *Advances in Visual Computing*, 2013.
- [90] Lee Harrison. Page 93-Black overlay.
- [91] Asma Hassani, Alexandre Kubicki, Vincent Brost, and Fan Yang. Real-Time 3D TUG Test Movement Analysis for Balance Assessment Using Microsoft Kinect. In *Symposium on Artificial Intelligence, Workshop on Artificial Intelligence for Ambient Assisted Living*, Pisa, 2014.
- [92] B. R. Hasselkus and G. M. Shambes. Aging and postural sway in women. *Journals of Gerontology*, 30(6):661–667, 11 1975.
- [93] Jeffrey M. Hausdorff, Dean A. Rios, and Helen K. Edelberg. Gait variability and fall risk in community-living older adults: A 1-year prospective study. *Archives of Physical Medicine and Rehabilitation*, 82(8):1050–1056, 8 2001.
- [94] W.G. Hawkins. Fourier transform resampling: theory and application. In *1996 IEEE Nuclear Science Symposium. Conference Record*, volume 3, pages 1491–1495. IEEE, 1996.
- [95] Geoffrey E. Hinton, Simon Osindero, and Yee Whye Teh. A fast learning algorithm for deep belief nets. *Neural computation*, 18(7):1527–54, 7 2006.
- [96] Sepp Hochreiter. The Vanishing Gradient Problem During Learning Recurrent Neural Nets and Problem Solutions. *International Journal of Uncertainty, Fuzziness and Knowledge-Based Systems*, 06(02):107–116, 4 1998.
- [97] Sepp; Hochreiter, J Urgan Schmidhuber, and J Schmidhuber. Long Short-term Memory. *Neural Computation*, 9(8):1735–80, 11 1997.

- [98] Arthur E. Hoerl and Robert W. Kennard. Ridge Regression: Biased Estimation for Nonorthogonal Problems. *Technometrics*, 12(1):55–67, 2 1970.
- [99] J Holviala, W. J. Kraemer, E. Sillanpää, H. Karppinen, J. Avela, A. Kauhanen, A. Häkkinen, and K. Häkkinen. Effects of strength, endurance and combined training on muscle strength, walking speed and dynamic balance in aging men. *European Journal of Applied Physiology*, 112(4):1335–1347, 4 2012.
- [100] Kurt Hornik, Maxwell Stinchcombe, and Halbert White. Multilayer feedforward networks are universal approximators. *Neural Networks*, 2(5):359–366, 1989.
- [101] Roshanak Houmanfar, Michelle Karg, and Dana Kulic. Movement Analysis of Rehabilitation Exercises: Distance Metrics for Measuring Patient Progress. *IEEE Systems Journal*, 10(3):1014–1025, 9 2016.
- [102] Gonul Babayigit Irez, Recep Ali Ozdemir, Ruya Evin, Salih Gokhan Irez, and Feza Korkusuz. Integrating pilates exercise into an exercise program for 65+ year-old women to reduce falls. *Journal of sports science & medicine*, 10(1):105–11, 2011.
- [103] Y P Ivanenko, R E Poppele, and F Lacquaniti. Five basic muscle activation patterns account for muscle activity during human locomotion. *The Journal of Physiology*, 556(1):267–282, 4 2004.
- [104] Imen Jegham, Anouar Ben, Ihsen Alouani, and Mohamed Ali. Forensic Science International : Digital Investigation Vision-based human action recognition : An overview and real world challenges. *Forensic Science International: Digital Investigation*, 32:200901, 2020.
- [105] Gunnar Johansson. Visual perception of biological motion and a model for its analysis. *Perception & Psychophysics*, 14(2):201–211, 6 1973.
- [106] Hochreiter Josef. *dynamischen neuronalen netzen*. PhD thesis, Josef Hochreiter Institut für Informatik Technische Universität München, 12 1991.
- [107] Kooksung Jun, Deok Won Lee, Kyoobin Lee, Sanghyub Lee, and Mun Sang Kim. Feature Extraction Using an RNN Autoencoder for

- Skeleton-Based Abnormal Gait Recognition. *IEEE Access*, 8:19196–19207, 2020.
- [108] Tharushi Kalinga, Chapa Sirithunge, A.G. Buddhika, P. Jayasekara, and Indika Perera. A Fall Detection and Emergency Notification System for Elderly. In *International Conference on Control, Automation and Robotics (ICCAR)*, pages 706–712. IEEE, 4 2020.
- [109] Neeta Kanekar and Alexander S Aruin. The effect of aging on anticipatory postural control. *Experimental Brain Research*, 232(4):1127–1136, 4 2014.
- [110] T S Kapteyn, W Bles, C J Njiokiktjien, L Kodde, C H Massen, and J M Mol. Standardization in platform stabilometry being a part of posturography. *Agressologie: revue internationale de physio-biologie et de pharmacologie appliquees aux effets de l'agression*, 24(7):321–326, 1983.
- [111] B. Amir H. Kargar, Ali Mollahosseini, Taylor Struempf, Wilson Pace, Rodney D Nielsen, and Mohammad H Mahoor. Automatic measurement of physical mobility in Get-Up-and-Go Test using kinect sensor. In *2014 36th Annual International Conference of the IEEE Engineering in Medicine and Biology Society*, volume Nov, pages 3492–3495. IEEE, 8 2014.
- [112] SIDNEY KATZ. Assessing Self-maintenance: Activities of Daily Living, Mobility, and Instrumental Activities of Daily Living. *Journal of the American Geriatrics Society*, 31(12):721–727, 12 1983.
- [113] Qiuhong Ke, Mohammed Bennamoun, Senjian An, Ferdous Sohel, and Farid Boussaid. Learning Clip Representations for Skeleton-Based 3D Action Recognition. *IEEE Transactions on Image Processing*, 27(6):2842–2855, 2018.
- [114] Ji-Won Kim, Gwang-Moon Eom, Chul-Seung Kim, Da-Hye Kim, Jae-Ho Lee, Byung Kyu Park, and Junghwa Hong. Sex differences in the postural sway characteristics of young and elderly subjects during quiet natural standing. *Geriatrics & Gerontology International*, 10(2):191–198, 2 2010.

- [115] Donald Knuth. *The Art of Computer Programming*. Addison-Wesley, 1973.
- [116] Alex Krizhevsky, Ilya Sutskever, and Geoffrey E Hinton. ImageNet Classification with Deep Convolutional Neural Networks. In F Pereira, C J C Burges, L Bottou, and K Q Weinberger, editors, *Advances in Neural Information Processing Systems 25*, pages 1097–1105. Curran Associates, Inc., 2012.
- [117] Max J. Kurz and Nicholas Stergiou. The aging humans neuromuscular system expresses less certainty for selecting joint kinematics during gait. *Neuroscience Letters*, 348(3):155–158, 9 2003.
- [118] D Lafond, M Duarte, and F Prince. Comparison of three methods to estimate the center of mass during balance assessment. *Journal of Biomechanics*, 37(9):1421–1426, 9 2004.
- [119] Sara Nicole Lawson, Neal Zaluski, Amanda Petrie, Cathy Arnold, Jenny Basran, and Vanina Dal Bello-Haas. Validation of the Saskatoon Falls Prevention Consortium’s Falls Screening and Referral Algorithm. *Physiotherapy Canada*, 65(1):31–39, 1 2013.
- [120] Yann Le Cun. Learning Process in an Asymmetric Threshold Network. In *Disordered Systems and Biological Organization*, pages 233–240. Springer Berlin Heidelberg, Berlin, Heidelberg, 1986.
- [121] Yann LeCun, Léon Bottou, Yoshua Bengio, and Patrick Haffner. Gradient-based learning applied to document recognition. *Proceedings of the IEEE*, 86(11):2278–2323, 1998.
- [122] Hsin-Chieh Lee, Chia-Lin Huang, Sui-Hua Ho, and Wen-Hsu Sung. The Effect of a Virtual Reality Game Intervention on Balance for Patients with Stroke: A Randomized Controlled Trial. *Games for Health Journal*, 6(5), 10 2017.
- [123] A M Legendre. *Nouvelles méthodes pour la détermination des orbites des comètes*. Nineteenth Century Collections Online (NCCO): Science, Technology, and Medicine: 1780-1925. F. Didot, 1805.

- [124] Daniel Leightley, Jamie McPhee, and Moi Hoon Yap. Automated Analysis and Quantification of Human Mobility using a Depth Sensor. *IEEE Journal of Biomedical and Health Informatics*, 21(4):939–948, 2017.
- [125] Daniel Leightley, Moi Hoon Yap, Jessica Coulson, Yoann Barnouin, Jamie S. McPhee, Y Barnouin J. Coulson, Jamie S. McPhee, Jessica Coulson, Yoann Barnouin, and Jamie S. McPhee. Benchmarking human motion analysis using kinect one: An open source dataset. In *Asia-Pacific Signal and Information Processing Association Annual Summit and Conference (APSIPA)*, pages 1–7. IEEE, 12 2015.
- [126] Guillaume Lemaitre, Fernando Nogueira, and Christos K Aridas. Imbalanced-learn: A Python Toolbox to Tackle the Curse of Imbalanced Datasets in Machine Learning. *Journal of Machine Learning Research*, 18(17):1–5, 2017.
- [127] Moshe Leshno, Vladimir Ya Lin, Allan Pinkus, and Shimon Schocken. Multilayer feedforward networks with a nonpolynomial activation function can approximate any function. *Neural Networks*, 6(6):861–867, 1 1993.
- [128] Mindy F Levin, Jeffrey A Kleim, and Steven L Wolf. What Do Motor “Recovery” and “Compensation” Mean in Patients Following Stroke? *Neurorehabilitation and Neural Repair*, 23(4):313–319, 5 2009.
- [129] Carole Lewis and Keiba Shaw. One-Legged (Single Limb) Stance Test, 2006.
- [130] Jan E. Lexell and David Y. Downham. How to assess the reliability of measurements in rehabilitation. *American Journal of Physical Medicine and Rehabilitation*, 84(9):719–723, 2005.
- [131] C. Leys, C. Ley, O. Klein, P. Bernard, and L. Licata. Journal of Experimental Social Psychology Detecting outliers : Do not use standard deviation around the mean, use absolute deviation around the median. *Experimental Social Psychology*, pages 4–6, 2013.
- [132] Chao Li, Qiaoyong Zhong, Di Xie, and Shiliang Pu. Co-occurrence Feature Learning from Skeleton Data for Action Recognition and Detection with Hierarchical Aggregation. *arXiv*, 2018.

- [133] Ting-Yang Lin, Chung-Hung Hsieh, and Jiann-Der Lee. A kinect-based system for physical rehabilitation: Utilizing tai chi exercises to improve movement disorders in patients with balance ability. In *2013 7th Asia Modelling Symposium*, pages 149–153. IEEE, 2013.
- [134] Rebecca A.L. Liston and Brenda J Brouwer. Reliability and validity of measures obtained from stroke patients using the balance master. *Archives of Physical Medicine and Rehabilitation*, 77(5):425–430, 5 1996.
- [135] Jun Liu, Amir Shahroudy, Mauricio Lisboa Perez, Gang Wang, Ling-Yu Duan, and Alex Kot Chichung. NTU RGB+D 120: A Large-Scale Benchmark for 3D Human Activity Understanding. *IEEE Transactions on Pattern Analysis and Machine Intelligence*, 8828(c):1–1, 2019.
- [136] Stuart P. Lloyd. Least Squares Quantization in PCM. *IEEE Transactions on Information Theory*, 28(2):129–137, 1982.
- [137] S. R. Lord, R. D. Clark, and I. W. Webster. Postural stability and associated physiological factors in a population of aged persons. *Journals of Gerontology*, 46(3):69–76, 5 1991.
- [138] Stephen R Lord, John A Ward, Philippa Williams, and Kaarinj Anstey. Physiological Factors Associated with Falls in Older Community-dwelling Women. *J Am Geriatr Soc*, 42:1110–1117, 1994.
- [139] Laura Luna-Oliva, Rosa María Ortiz-Gutiérrez, Roberto Cano-de la Cuerda, Rosa Martínez Piédrola, Isabel M. Alguacil-Diego, Carlos Sánchez-Camarero, and María del Carmen Martínez Culebras. Kinect Xbox 360 as a therapeutic modality for children with cerebral palsy in a school environment: A preliminary study. *NeuroRehabilitation*, 33(4):513–521, 2013.
- [140] Lillemor Lundin-Olsson, Lars Nyberg, and Yngve Gustafson. “Stops walking when talking” as a predictor of falls in elderly people. *The Lancet*, 349(9052):617, 3 1997.
- [141] Michelle M. Lusardi, Stacy Fritz, Addie Middleton, Leslie Allison, Mariana Wingood, Emma Phillips, Michelle Criss, Sangita Verma, Jackie Osborne, and Kevin K. Chui. Determining Risk of Falls in Community Dwelling Older Adults - A Systematic Review and Meta-analysis Using

- Posttest Probability. *Journal of Geriatric Physical Therapy*, 40(1):1–36, 2017.
- [142] Michelle M. Lusardi, Geraldine L. Pellecchia, and Marjorie Schulman. Functional Performance in Community Living Older Adults. *Journal of Geriatric Physical Therapy*, 26(3):14–22, 2003.
- [143] J MacQueen. Some methods for classification and analysis of multivariate observations. In *Proceedings of the 5th Berkeley Symposium on Mathematical Statistics and Probability*, volume 1, pages 281–296, 1967.
- [144] Priscilla Gilliam MacRae, Michael Lacourse, and Ron Moldavon. Physical Performance Measures That Predict Faller Status in Community-Dwelling Older Adults. *Journal of Orthopaedic & Sports Physical Therapy*, 16(3):123–128, 9 1992.
- [145] A A Markov. An Example of Statistical Investigation of the Text Eugene Onegin Concerning the Connection of Samples in Chains. *Science in Context*, 19(4):591–600, 12 2006.
- [146] Georgios Mastorakis and Dimitrios Makris. Fall detection system using Kinect’s infrared sensor. *Journal of Real-Time Image Processing*, 9(4):635–646, 12 2012.
- [147] S. Mathias, U. S.L. Nayak, and B. Isaacs. Balance in elderly patients: the ”get-up and go” test. *Archives of physical medicine and rehabilitation*, 67(6):387–9, 6 1986.
- [148] Denise McGrath, Emer P. Doheny, Lorcan Walsh, David McKeown, Clodagh Cunningham, Lisa Crosby, Rose Anne Kenny, Nicholas Stergiou, Brian Caulfield, and Barry R. Greene. Taking balance measurement out of the laboratory and into the home: Discriminatory capability of novel centre of pressure measurement in fallers and non-fallers. *Proceedings of the Annual International Conference of the IEEE Engineering in Medicine and Biology Society, EMBS*, 8:3296–3299, 2012.
- [149] McKinly Laboratory. Timed Up and Go (TUG). Technical report, Physical therapy university of delaware, 2010.

- [150] Jamie S. McPhee, David P. French, Dean Jackson, James Nazroo, Neil Pendleton, and Hans Degens. Physical activity in older age: perspectives for healthy ageing and frailty. *Biogerontology*, 17(3):567–580, 6 2016.
- [151] I. Melzer. Postural stability in the elderly: a comparison between fallers and non-fallers. *Age and Ageing*, 33(6):602–607, 9 2004.
- [152] Benjamin F. Mentiplay, Luke G. Perraton, Kelly J. Bower, Yong Hao Pua, Rebekah McGaw, Sophie Heywood, and Ross A. Clark. Gait assessment using the Microsoft Xbox One Kinect: Concurrent validity and inter-day reliability of spatiotemporal and kinematic variables. *Journal of Biomechanics*, 2015.
- [153] Yvonne L Michael, Evelyn P Whitlock, Jennifer S Lin, Rongwei Fu, Elizabeth A. O’Connor, and Rachel Gold. Primary Care–Relevant Interventions to Prevent Falling in Older Adults: A Systematic Evidence Review for the U.S. Preventive Services Task Force. *Annals of Internal Medicine*, 153(12):815–825, 12 2010.
- [154] Ingo Michaelis, A. Kwiet, U. Gast, A. Boshof, T. Antvorskov, T. Jung, J. Rittweger, and D. Felsenberg. Decline of specific peak jumping power with age in master runners. *Journal of musculoskeletal & neuronal interactions*, 8(1):64–70, 2008.
- [155] Marvin Minsky and Seymour Papert. *Perceptrons: an introduction to computational geometry*. The MIT Press, 1969.
- [156] Leandro Miranda, Thales Vieira, Dimas Martinez, Thomas Lewiner, Antonio W. Vieira, and Mario F.M. Campos. Real-time gesture recognition from depth data through key poses learning and decision forests. *Brazilian Symposium of Computer Graphic and Image Processing*, pages 268–275, 2012.
- [157] E. M. Monsell, J. M. Furman, S. J. Herdman, H. R. Konrad, and N. T. Shepard. Computerized dynamic platform posturography. *Otolaryngology - Head and Neck Surgery*, 117(4):394–398, 1997.
- [158] Pietro G Morasso, Gino Spada, and Roberto Capra. Computing the COM from the COP in postural sway movements. *Human Movement Science*, 18(6):759–767, 1999.

- [159] Charlotte Le Mouel. Anticipatory coadaptation of ankle stiffness and neural feedback for standing balance. *bioRxiv*, 2018.
- [160] Jesse W. Muir, Douglas P. Kiel, Marian Hannan, Jay Magaziner, and Clinton T. Rubin. Dynamic Parameters of Balance Which Correlate to Elderly Persons with a History of Falls. *PLoS ONE*, 8(8):70566, 8 2013.
- [161] S.W. Muir-Hunter and J.E. Wittwer. Dual-task testing to predict falls in community-dwelling older adults: a systematic review. *Physiotherapy*, 102(1):29–40, 3 2016.
- [162] Banu Müjdeci, Songul Aksoy, and Ahmet Atas. Evaluation of balance in fallers and non-fallers elderly. *Brazilian Journal of Otorhinolaryngology*, 78(5):104–109, 9 2012.
- [163] Björn Müller, Winfried Ilg, Martin A. Giese, and Nicolas Ludolph. Validation of enhanced kinect sensor based motion capturing for gait assessment. *PLoS ONE*, 12(4):13–18, 4 2017.
- [164] Alessandro Napoli, Stephen Glass, Christian Ward, Carole Tucker, and Iyad Obeid. Performance analysis of a generalized motion capture system using microsoft kinect 2.0. *Biomedical Signal Processing and Control*, 38:265–280, 9 2017.
- [165] A. Nardone and M. Schieppati. The role of instrumental assessment of balance in clinical decision making. *European journal of physical and rehabilitation medicine*, 46(2):221–37, 6 2010.
- [166] Antonio Nardone, Margherita Grasso, Jessica Tarantola, Stefano Corna, and Marco Schieppati. Postural coordination in elderly subjects standing on a periodically moving platform. *Archives of Physical Medicine and Rehabilitation*, 81(9):1217–1223, 2000.
- [167] Lewis M Nashner, F O Black, and Conrad Wall. Adaptation to altered support and visual conditions during stance: patients with vestibular deficits. *The Journal of neuroscience : the official journal of the Society for Neuroscience*, 2(5):536–44, 1982.
- [168] National Institute for Care Excellence, NICE, and Wendy Barker. Assessment and prevention of falls in older people. *Nursing Older People*, 26(6):18–24, 2013.

- [169] National Institute for Health and Care Excellence. 2019 surveillance of falls in older people : assessing risk and prevention (NICE guideline CG161). Technical Report May, NICE, 2019.
- [170] Michael C Nevitt and R Steven. Risk Factors for Recurrent Nonsyncopal Falls Prospective Study. *Journal of american medical association*, 261:2663–8, 1989.
- [171] Karl M Newell. *Motor Development in Children: Aspects of Coordination and Control*. Martinus Nijhoff, 1986.
- [172] Isaac Newton. *Newton’s Principia: The Mathematical Principles of Natural Philosophy — 1687*. Benjamin Motte, 1846.
- [173] Christopher Olah. Understanding LSTM Networks – colah’s blog, 2015.
- [174] Marcio R. Oliveira, Edgar R. Vieira, André W.O. Gil, Karen B.P. Fernandes, Denilson C. Teixeira, Cesar F. Amorim, and Rubens A. Da Silva. One-legged stance sway of older adults with and without falls. *PLoS ONE*, 13(9):e0203887, 9 2018.
- [175] ONS. 2011 Census - Office for National Statistics, 2011.
- [176] Rosa Ortiz-Gutiérrez, Roberto Cano-de-la Cuerda, Fernando Galán-del Río, Isabel Alguacil-Diego, Domingo Palacios-Ceña, and Juan Miangolarra-Page. A Telerehabilitation Program Improves Postural Control in Multiple Sclerosis Patients: A Spanish Preliminary Study. *International Journal of Environmental Research and Public Health*, 10(11):5697–5710, 10 2013.
- [177] Maura O’sullivan, Catherine Blake, Conal Cunningham, Gerard Boyle, and Ciarán Finucane. Correlation of accelerometry with clinical balance tests in older fallers and non-fallers. *Age and Ageing*, 38(3):308–313, 2009.
- [178] Karen Otte, Bastian Kayser, Sebastian Mansow-Model, Julius Verrel, Friedemann Paul, Alexander U. Brandt, and Tanja Schmitz-Hübsch. Accuracy and Reliability of the Kinect Version 2 for Clinical Measurement of Motor Function, 11 2016.

- [179] Marco The LIFE Study Investigators Pahor. Effects of a Physical Activity Intervention on Measures of Physical Performance. *The Journals of Gerontology: Series A: Biological Sciences and Medical Sciences*, 61A(11):1157–1165, 2006.
- [180] Pandas. pandas documentation — pandas 1.1.1 - pandas.pydata.org, 2020.
- [181] Maxime R. Paquette, Jason R. Fuller, Allan L. Adkin, and Lori Ann Vallis. Age-related modifications in steering behaviour: effects of base-of-support constraints at the turn point. *Experimental Brain Research*, 190(1):1–9, 9 2008.
- [182] Judea Pearl. Bayesian networks: A model of self-activated memory for evidential reasoning. In *Proceedings of the 7th Conference of the Cognitive Science Society*, 1985.
- [183] S. Pekár. Effect of selective insecticides on the beneficial spider community of a pear orchard in the Czech Republic. ... of the 17th European colloquium of ... , 27(1):337–342, 1998.
- [184] Antoine Piau, Nora Mattek, Rachel Crissey, Zachary Beattie, Hiroko Dodge, and Jeffrey Kaye. When Will My Patient Fall? Sensor-Based In-Home Walking Speed Identifies Future Falls in Older Adults. *The Journals of Gerontology: Series A*, 75(5):968–973, 4 2020.
- [185] Maarit Piirtola and Pertti Era. Force Platform Measurements as Predictors of Falls among Older People – A Review. *Gerontology*, 52(1):1–16, 2006.
- [186] L. Pizzigalli, M. Micheletti Cremasco, A. Mulasso, and A. Rainoldi. The contribution of postural balance analysis in older adult fallers: A narrative review. *Journal of Bodywork and Movement Therapies*, 20(2):409–417, 4 2016.
- [187] Diane Podsiadlo and Sandra Richardson. The Timed “Up & Go”: A Test of Basic Functional Mobility for Frail Elderly Persons. *Journal of the American Geriatrics Society*, 39(2):142–148, 2 1991.
- [188] Janet S. Pohl, Barbara B. Cochrane, Karen G. Schepp, and Nancy F. Woods. Falls and Social Isolation of Older Adults in the National Health

- and Aging Trends Study. *Research in Gerontological Nursing*, 11(2):61–70, 3 2018.
- [189] Thomas E. Prieto, Joel B. Myklebust, Raymond G. Hoffmann, and Eric G. Lovett. Measures of postural steadiness: Differences between healthy young and elderly adults. *IEEE Transactions on Biomedical Engineering*, 43(9):956–966, 1996.
- [190] Thomas E. Prieto, Joel B. Myklebust, and Barbara M. Myklebust. Characterization and Modeling of Postural Steadiness in the Elderly: A Review. *IEEE Transactions on Rehabilitation Engineering*, 1(1):26–34, 3 1993.
- [191] Aleš Procházka, Oldřich Vyšata, Martin Vališ, Ondřej Āupa, Martin Schätz, and Vladimír Mařík. Bayesian classification and analysis of gait disorders using image and depth sensors of Microsoft Kinect. *Digital Signal Processing*, 47:169–177, 12 2015.
- [192] Hai Qiu, Rana Zia Ur Rehman, Xiaoqun Yu, and Shuping Xiong. Application of Wearable Inertial Sensors and A New Test Battery for Distinguishing Retrospective Fallers from Non-fallers among Community-dwelling Older People. *Scientific Reports*, 8(1):1–10, 2018.
- [193] Lien Quach, Andrew M Galica, Richard N Jones, Elizabeth Procter-Gray, Brad Manor, Marian T Hannan, and Lewis A Lipsitz. The Non-linear Relationship Between Gait Speed and Falls: The Maintenance of Balance, Independent Living, Intellect, and Zest in the Elderly of Boston Study. *Journal of the American Geriatrics Society*, 59(6):1069–1073, 6 2011.
- [194] J R Quinlan. Induction of Decision Trees. *Machine Learning*, 1(1):81–106, 1986.
- [195] J Ross Quinlan. *Machine Learning Vol. 1, No. 1*. 1975.
- [196] J Ross Quinlan. C4. 5: Programming for machine learning. *Morgan Kauffmann*, 38, 1993.
- [197] Michalis Raptis, Darko Kirovski, and Hugues Hoppe. Real-Time Classification of Dance Gestures from Skeleton Animation. In *SCA '11 Pro-*

- ceedings of the 2011 ACM SIGGRAPH/Eurographics Symposium*, pages 147–156, 2011.
- [198] Juan Felipe Reyes, James Steven Montealegre, Yor Jaggy Castano, Christian Urcuqui, and Andres Navarro. LSTM and Convolution Networks exploration for Parkinson’s Diagnosis. *2019 IEEE Colombian Conference on Communications and Computing, COLCOM 2019 - Proceedings*, pages 19–22, 2019.
- [199] Natalia Aquaroni Ricci, Daniele de Faria Figueiredo Gonçalves, Arlete Maria Valente Coimbra, and Ibsen Bellini Coimbra. Sensory interaction on static balance: A comparison concerning the history of falls of community-dwelling elderly. *Geriatrics and Gerontology International*, 9(2):165–171, 2009.
- [200] Massimo W. Rivolta, Md Aktaruzzaman, Giovanna Rizzo, Claudio L. Lafortuna, Maurizio Ferrarin, Gabriele Bovi, Daniela R. Bonardi, Andrea Caspani, and Roberto Sassi. Evaluation of the Tinetti score and fall risk assessment via accelerometry-based movement analysis. *Artificial Intelligence in Medicine*, 95:38–47, 4 2019.
- [201] Laura Rocchi, Lorenzo Chiari, Angelo Cappello, and Fay B Horak. Identification of distinct characteristics of postural sway in Parkinson’s disease: A feature selection procedure based on principal component analysis. *Neuroscience Letters*, 394(2):140–145, 2006.
- [202] Kenneth Rockwood. A global clinical measure of fitness and frailty in elderly people. *Canadian Medical Association Journal*, 173(5):489–495, 8 2005.
- [203] MARC A. ROGERS and WILLIAM J. EVANS. Changes in Skeletal Muscle with Aging. *Exercise and Sport Sciences Reviews*, 21(1):65–102, 1 1993.
- [204] Margaret Roller, Tom Boismier, and Joe Krzak. Balance Manager Clinical Interpretation Guide, 2009.
- [205] F. Rosenblatt. The perceptron: A probabilistic model for information storage and organization in the brain. *Psychological Review*, 65(6):386–408, 1958.

- [206] P Rosenrot. The relationship between velocity, stride time, support time, and swing time during normal walking. *J Hum Mov.*, 6:323–335, 1980.
- [207] David E. Rumelhart, Geoffrey E. Hinton, and Ronald J. Williams. Learning representations by back-propagating errors. *Nature*, 323(6088):533–536, 10 1986.
- [208] Karolina A. Rygiel, Martin Picard, and Doug M. Turnbull. The ageing neuromuscular system and sarcopenia: a mitochondrial perspective. *The Journal of Physiology*, 594(16):4499–4512, 8 2016.
- [209] Carsten Schelp. An Alternative Way to Plot the Covariance Ellipse — CarstenSchelp.github.io, 2018.
- [210] SciPy. SciPy.org - 1.5.2 - www.scipy.org, 2019.
- [211] Amir Shahroudy, Jun Liu, Tian-Tsong Ng, and Gang Wang. NTU RGB+D: A Large Scale Dataset for 3D Human Activity Analysis. *IEEE Conference on Computer Vision and Pattern Recognition*, pages 1010–1019, 4 2016.
- [212] Amir Shahroudy, Tian-Tsong Ng, Yihong Gong, and Gang Wang. Deep Multimodal Feature Analysis for Action Recognition in RGB+D Videos. *Transactions on Pattern Analysis and Machine Intelligence*, 2016.
- [213] Jun Shao. Linear model selection by cross-validation. *Journal of the American Statistical Association*, 88(422):486–494, 1993.
- [214] Catherine Sherrington, Julie C. Whitney, Stephen R. Lord, Robert D. Herbert, Robert G. Cumming, and Jacqueline C.T. T. Close. Effective Exercise for the Prevention of Falls: A Systematic Review and Meta-Analysis. *Journal of the American Geriatrics Society*, 56(12):2234–2243, 12 2008.
- [215] Meng Che Shih, Ray Yau Wang, Shih Jung Cheng, and Yea Ru Yang. Effects of a balance-based exergaming intervention using the Kinect sensor on posture stability in individuals with Parkinson’s disease: A single-blinded randomized controlled trial. *Journal of NeuroEngineering and Rehabilitation*, 13(1), 2016.

- [216] Jamie Shotton, Andrew Fitzgibbon, Mat Cook, Toby Sharp, Mark Finocchio, Richard Moore, Alex Kipman, Andrew Blake, Andrew Fitzgibbon, Mark Finocchio, Andrew Blake, Mat Cook, Richard Moore, Toby Sharp, Mark Finocchio, Richard Moore, Alex Kipman, Andrew Blake, Maoying Qiao, Jamie Shotton, Andrew Fitzgibbon, Mat Cook, Toby Sharp, Mark Finocchio, Richard Moore, Alex Kipman, Andrew Blake, Maoying Qiao, Jamie Shotton, Andrew Fitzgibbon, Mat Cook, Toby Sharp, Mark Finocchio, Richard Moore, Alex Kipman, Andrew Blake, and Maoying Qiao. Real-time human pose recognition in parts from single depth images. *Compute*, 411(1):1297–1304, 1 2011.
- [217] A. Shumway-Cook and F. B. Horak. Assessing the influence of sensory interaction on balance. Suggestion from the field. *Physical Therapy*, 66(10):1548–1550, 1986.
- [218] A Shumway-Cook and M H Woollacott. *Motor Control: Translating Research Into Clinical Practice*. Lippincott Williams & Wilkins, 2007.
- [219] Anne Shumway-Cook, Sandy Brauer, and Marjorie Woollacott. Predicting the Probability for Falls in Community-Dwelling Older Adults Using the Timed Up Go Test. *Physical Therapy*, 80(9):896–903, 9 2000.
- [220] Anne Shumway-Cook, Marjorie Woollacott, Kimberly A. Kerns, and Margaret Baldwin. The effects of two types of cognitive tasks on postural stability in older adults with and without a history of falls. *The Journals of Gerontology Series A: Biological Sciences and Medical Sciences*, 52A(4):M232–M240, 7 1997.
- [221] Kathryn M. Sibley, Sharon E. Straus, Elizabeth L. Inness, Nancy M. Salbach, and Susan B. Jaglal. Clinical balance assessment: perceptions of commonly-used standardized measures and current practices among physiotherapists in Ontario, Canada. *Implementation Science*, 8(1):33, 12 2013.
- [222] Stephen Simmons, Rachel McCrindle, Malcolm Sperrin, and Andy Smith. Prescription Software for Recovery and Rehabilitation Using Microsoft Kinect. In *Proceedings of the ICTs for improving Patients Rehabilitation Research Techniques*, 2013.

- [223] Ana-Maria Simundic. Measures of Diagnostic Accuracy. In *Measures of Diagnostic Accuracy*, pages 13–55. Wiley, 4 2011.
- [224] David Sinclair. Is DNA cut out for a long life? *Science of aging knowledge environment : SAGE KE*, 2003(16):1–6, 4 2003.
- [225] sklearn. sklearn.preprocessing.normalize — scikit-learn 0.23.2 - scikit-learn.org.
- [226] Helen Snooks, Wai Yee Cheung, Stella May Gwini, Ioan Humphreys, Antonio Sánchez, and Niroshan Siriwardena. 09 Can older people who fall be identified in the ambulance call centre to enable alternative responses or care pathways? *Emergency Medicine Journal*, 28(3):e1–e1, 2011.
- [227] Sijie Song, Cuiling Lan, Junliang Xing, Wenjun Zeng, and Jiaying Liu. An End-to-End Spatio-Temporal Attention Model for Human Action Recognition from Skeleton Data. In *AAAI Conference on Artificial Intelligence*, 2016.
- [228] Staford. multiclass svm, 2015.
- [229] J. A. Stevens and E. D. Sogolow. Gender differences for non-fatal unintentional fall related injuries among older adults. *Injury Prevention*, 11(2):115–119, 4 2005.
- [230] Stephen M. Stigler. Gergonne’s 1815 paper on the design and analysis of polynomial regression experiments. *Historia Mathematica*, 1(4):431–439, 11 1974.
- [231] Tino Stöckel, Robert Jacksteit, Martin Behrens, Ralf Skripitz, Rainer Bader, and Anett Mau-Moeller. The mental representation of the human gait in young and older adults. *Frontiers in Psychology*, 6(June), 7 2015.
- [232] E. E. Stone and M. Skubic. Passive in-home measurement of stride-to-stride gait variability comparing vision and Kinect sensing. In *2011 Annual International Conference of the IEEE Engineering in Medicine and Biology Society*, pages 6491–6494. IEEE, 8 2011.
- [233] Erik Stone and Marjorie Skubic. Capturing Habitual, In-Home Gait Parameter Trends Using an Inexpensive Depth Camera. In *Engineering in Medicine and Biology Society*, 2012.

- [234] Erik E. Stone and Marjorie Skubic. Fall Detection in Homes of Older Adults Using the Microsoft Kinect. *IEEE Journal of Biomedical and Health Informatics*, 19(1):290–301, 1 2015.
- [235] Chuan-Jun Su, Chang-Yu Chiang, and Jing-Yan Huang. Kinect-enabled home-based rehabilitation system using Dynamic Time Warping and fuzzy logic. *Applied Soft Computing*, 22(November 2010):652–666, 2014.
- [236] H. Tannous, D. Istrate, M.C. Ho Ba Tho, and T.T. Dao. Feasibility study of a serious game based on Kinect system for functional rehabilitation of the lower limbs. *European Research in Telemedicine / La Recherche Européenne en Télémedecine*, 5(3):97–104, 9 2016.
- [237] Robert L Thorndike. Who belongs in the family? *Psychometrika*, 18(4):267–276, 12 1953.
- [238] Yang Tian, James Thompson, David Buck, and Lara Sonola. Exploring the system-wide costs of falls in older people in Torbay. Technical report, The Kings Fund, 2013.
- [239] Anne Tiedemann, Hiroyuki Shimada, Catherine Sherrington, Susan Murray, and Stephen Lord. The comparative ability of eight functional mobility tests for predicting falls in community-dwelling older people. *Age and Ageing*, 37(4):430–435, 7 2008.
- [240] Tin Kam Ho. Random decision forests. In *Proceedings of 3rd International Conference on Document Analysis and Recognition*, volume 1, pages 278–282, 1995.
- [241] Mary E. Tinetti. Predictors and Prognosis of Inability to Get Up After Falls Among Elderly Persons. *JAMA: The Journal of the American Medical Association*, 269(1):65, 1 1993.
- [242] Chris Todd and Dawn Skelton. What are the main risk factors for falls amongst older people and what are the most effective interventions to prevent these falls ? Technical Report March, WHO, 2004.
- [243] R. Tuma. The Two Faces of Oxygen. *Science of Aging Knowledge Environment*, 2001(1):5oa–5, 10 2001.

- [244] Sarinnapha Vasunilashorn, Antonia K. Coppin, Kushang V. Patel, Fulvio Lauretani, Luigi Ferrucci, Stefania Bandinelli, and Jack M. Guralnik. Use of the short physical performance battery score to predict loss of ability to walk 400 meters: Analysis from the InCHIANTI study. *Journals of Gerontology - Series A Biological Sciences and Medical Sciences*, 64(2):223–229, 2 2009.
- [245] BRUNO J. VELLAS, SHARON J. WAYNE, LINDA J. ROMERO, RICHARD N. BAUMGARTNER, and PHILIP J. GARRY. Fear of falling and restriction of mobility in elderly fallers. *Age and Ageing*, 26(3):189–193, 1997.
- [246] Raviteja Vemulapalli, Felipe Arrate, and Rama Chellappa. Human action recognition by representing 3D skeletons as points in a lie group. *Proceedings of the IEEE Computer Society Conference on Computer Vision and Pattern Recognition*, pages 588–595, 2014.
- [247] Joe Verghese, Roe Holtzer, Richard B. Lipton, and Cuiling Wang. Quantitative Gait Markers and Incident Fall Risk in Older Adults. *The Journals of Gerontology Series A: Biological Sciences and Medical Sciences*, 64A(8):896–901, 8 2009.
- [248] Jasper E. Visser, Mark G. Carpenter, Herman Van Der Kooij, Bastiaan R. Bloem, Herman van der Kooij, and Bastiaan R. Bloem. The clinical utility of posturography, 11 2008.
- [249] Jan P. Vox and Frank Wallhoff. Preprocessing and normalization of 3d-skeleton-data for human motion recognition. *2018 IEEE Life Sciences Conference, LSC 2018*, pages 279–282, 2018.
- [250] Harvey Wallmann. Comparison of Elderly Nonfallers and Fallers on Performance Measures of Functional Reach, Sensory Organization, and Limits of Stability. *Journal of gerontology: MEDICAL SCIENCES*, 56(9):580–583, 2001.
- [251] Jeremy Walston. Frailty—the search for underlying causes. *Science of aging knowledge environment : SAGE KE*, 2004(4):1–5, 1 2004.
- [252] Jeremy Walston, Evan C. Hadley, Luigi Ferrucci, Jack M. Guralnik, Anne B. Newman, Stephanie A. Studenski, William B. Ershler, Tamara

- Harris, and Linda P. Fried. Research Agenda for Frailty in Older Adults: Toward a Better Understanding of Physiology and Etiology: Summary from the American Geriatrics Society/National Institute on Aging Research Conference on Frailty in Older Adults. *Journal of the American Geriatrics Society*, 54(6):991–1001, 6 2006.
- [253] Jiang Wang, Zicheng Liu, Ying Wu, and Junsong Yuan. Mining actionlet ensemble for action recognition with depth cameras. In *Proceedings of the IEEE Computer Society Conference on Computer Vision and Pattern Recognition*, pages 1290–1297, 2012.
- [254] Pichao Wang, Wanqing Li, Philip Ogunbona, Jun Wan, and Sergio Escalera. RGB-D-based human motion recognition with deep learning: A survey. *Computer Vision and Image Understanding*, 171:118–139, 2018.
- [255] Qifei Wang, Qifei Wang, Gregorij Kurillo, Ferda Ofli, and Ruzena Bajcsy. Evaluation of Pose Tracking Accuracy in the First and Second Generations of Microsoft Kinect Evaluation of Pose Tracking Accuracy in the First and Second Generations of Microsoft Kinect. *arXiv*, 2015.
- [256] Rachel E. Ward, Suzanne G. Leveille, Marla K. Beauchamp, Thomas Trivison, Neil Alexander, Alan M. Jette, and Jonathan F. Bean. Functional performance as a predictor of injurious falls in older adults. *Journal of the American Geriatrics Society*, 63(2):315–320, 2 2015.
- [257] Geoffrey I Webb. Not So Naive Bayes: Aggregating One-Dependence Estimators. *Not So Naive Bayes: Aggregating One-Dependence Estimators*, 58(5-24):5–24, 2005.
- [258] WHO. Falls, 2018.
- [259] Wikipedia. Locating the center of mass - https://en.wikipedia.org/wiki/Locating_the_center_of_mass.
- [260] P Wilder. Seniors to seniors exercise program: a cost effective way to prevent falls in the frail elderly living at home. *Journal of Geriatric Physical Therapy*, 24(3):13, 2001.
- [261] Christian Williams, Aleksandar Vakanski, Stephen Lee, and David Paul. Assessment of physical rehabilitation movements through dimensional-

- ity reduction and statistical modeling. *Medical Engineering & Physics*, 74:13–22, 12 2019.
- [262] Dennis L. Wilson. Asymptotic Properties of Nearest Neighbor Rules Using Edited Data. *IEEE Transactions on Systems, Man, and Cybernetics*, SMC-2(3):408–421, 7 1972.
- [263] David A Winter. *Biomechanics and Motor Control of Human Movement*. John Wiley & Sons, Inc., Hoboken, NJ, USA, 9 2009.
- [264] David A. Winter, Aftab E. Patla, Francois Prince, Milad Ishac, and Krystyna Gielo-Perczak. Stiffness Control of Balance in Quiet Standing. *Journal of Neurophysiology*, 80(3):1211–1221, 9 1998.
- [265] David A Winter and A.D. Winter. Human balance and posture control during standing and walking. *Gait and Posture*, 3(4):193–214, 1995.
- [266] MARJORIE WOOLLACOTT, BARBARA INGLIN, and DIANE MANCHESTER. Response Preparation and Posture Control Neuromuscular Changes in the Older Adult. *Annals of the New York Academy of Sciences*, 515(1 Central Deter):42–53, 1 1988.
- [267] Xiaodong Yang and Ying Li Tian. EigenJoints-based Action Recognition Using Naïve-Bayes-Nearest-Neighbor. In *Workshops on IEEE Conf. on Comput. Vis. and Pattern Recog*, 2012.
- [268] Yang Yang, Fang Pu, Yan Li, Shuyu Li, Yubo Fan, and Deyu Li. Reliability and Validity of Kinect RGB - D Sensor for Assessing Standing Balance. *IEEE SENSORS JOURNAL*, 14(5):1633–1638, 5 2014.
- [269] L. F. Yeung, Kenneth C. Cheng, C. H. Fong, Winson C.C. Lee, and Kai Yu Tong. Evaluation of the Microsoft Kinect as a clinical assessment tool of body sway. *Gait and Posture*, 40(4):532–538, 2014.
- [270] Vladimir M. Zatsiorsky and Deborah L. King. An algorithm for determining gravity line location from posturographic recordings. *Journal of Biomechanics*, 31(2):161–164, 5 1997.
- [271] Yu Zhong and Mark Stevens. Action recognition in spatiotemporal volume. In *2010 IEEE Computer Society Conference on Computer Vision and Pattern Recognition - Workshops*, pages 25–30. IEEE, 6 2010.

- [272] Wentao Zhu, Cuiling Lan, Junliang Xing, Wenjun Zeng, Yanghao Li, Li Shen, and Xiaohui Xie. Co-occurrence Feature Learning for Skeleton based Action Recognition using Regularized Deep LSTM Networks. In *30th AAAI Conference on Artificial Intelligence, AAAI 2016*, pages 3697–3703, 3 2016.
- [273] Ondřej Ťupa, Aleš Procházka, Oldřich Vyšata, Martin Schätz, Jan Mareš, Martin Vališ, and Vladimír Mařík. Motion tracking and gait feature estimation for recognising Parkinson’s disease using MS Kinect. *Biomedical engineering online*, 14(1):97, 2015.